5. PRODUCT EVALUATION

Since the primary purpose of the ISV process is to stabilize and immobilize nuclear and toxic waste components, the chemical morphology and release characteristics of ISV waste forms must be known to provide for an accurate performance assessment. Full characterization of ISV waste forms from laboratory, engineering, intermediate field, and large field tests is needed to establish the adequacy of the ISV process as a buried waste treatment option.

The properties of ISV waste forms are directly related to the composition of the waste, composition of surrounding soil, and the thermal history of materials reacted during vitrification and cooling. The application of the ISV process to buried waste and soil at the INEL presents unique conditions compared to the homogeneous soil/waste conditions previously tested at Hanford and Oak Ridge National Laboratory (ORNL). Since the INEL soil and buried waste differ from previous soil and waste of ISV tests, a detailed characterization of the INEL ISV waste forms was performed.

Evaluation of the ISV waste form was divided into three general categories: (a) sampling and bulk description, (b) chemical and physical properties, and (c) durability testing. This is outlined in detail in the ISV product evaluation strategy.[9]

The objective of the sampling and bulk description activity was to provide representative samples to generate a general description of the ISV monolith and a gross identification of the different bulk phases. This megascopic description of the monolith was necessary before other characterization techniques could be detailed.

The purpose of the chemical and physical evaluation was to determine the elemental composition of the waste form. Because of the many elemental components in an ISV waste form, the slow thermal diffusion of the glass, and the long cooling times of the monolith, some glass will devitrify to crystalline material. The structure and elemental composition of each

crystalline phase will reveal if any waste components have segregated into a less durable phase.

Durability testing is divided into three types of leaching tests. The first, the Environment Protection Agency's Toxicity Characteristic Leach Procedure (TCLP),[10,11] meets the minimum regulatory testing requirements established for landfill disposal. However, the TCLP does not address radioactive waste components, provide a technical basis for assessing long-term durability, provide a basis for a comparison to highly durable waste forms or natural analogs, or provide an assessment of the source term release of the waste component for risk assessment models. To provide this information, additional durability tests must be conducted. These additional tests fall into two categories: comparative testing (comparing ISV waste forms to similar waste forms and natural analogs) and testing to determine the intrinsic rate (fastest) of waste form dissolution (k_+).

5.1 Excavation, Sampling, and Bulk Description

The two ISV blocks were allowed to cool prior to excavation. Although no cooldown data on the blocks were recorded, it appeared that both blocks had cooled to ambient conditions at the time of excavation, which began on September 10, 1990.

A careful and systematic excavation of the ISV processed pits was conducted in order to obtain physical descriptions of the waste pit morphology, the processed waste, and the vitrified product. Additionally, samples were collected for chemical and physical analysis. Direct observation of the product, achievable only through excavation, provided data directly applicable to such issues as the probability of underground fires due to ISV processing, thermal gradients adjacent to the melt front, correlation of ISV processing events with features exhibited by waste pit morphology, physical and chemical properties of the product, as well as other features that would provide insight into the dynamics of the ISV process. The materials

collected during the excavation of the test pits were analyzed to determine the bulk composition, the mineralogy, the tracer rare-earth element distribution, the density, the chemical and mechanical durability, and the micro-structure of the vitrified product. The chemical and physical characterization provided information about melt properties during the ISV processing and subsequent cool-down period, melt mixing and homogeneity, and the representativeness of "melt samples" taken from the molten waste form.

It should be noted that much of the following description involves unvitrified or partially vitrified waste at the edge of the vitrified block. Although much useful information is derived from these observations, it should be emphasized that these edge effects are inherent to single melts such as these test melts. For production-scale application of ISV to a large buried waste site, the edges would be fused together in larger contiguous blocks in multiple melts. Further testing will provide insight into operational and engineering considerations for processing adjacent areas.

5.1.1 Excavation/Sampling Methods

Many tools and techniques were used during the excavation process. A front loader and backhoe were used for major excavation activities. The backhoe was the primary excavation tool and was used to trench each side of the pit areas to a depth of about 0.91 m (3 ft). The front loader was not generally useful for direct excavation of the test pits because the force required for scooping dirt severely disturbed the pit and fractured the waste form. When necessary to preserve delicate features, the walls of the trench were then carefully collapsed by hand using shovels and a 5 in. masonry trowel. Dislodged soil and fused product, as well as unaffected simulated waste, were described, photographed, and then removed from the trench with the backhoe as the trench wall removal progressed. The trenching/caving process was repeated as necessary until the product had been completely exposed and/or

removed. Figure 82 shows Test Pit 1 excavated to a depth of approximately 1.2 m (4 ft) and illustrates the general shape of the pit area during the excavation process. All features of interest were described in the field notebook and photographed using a 35 mm single-lens reflex camera equipped with a 55 mm, 2.5f, macro lens.

Each film roll was identified by photographing a page from the field notebook showing the roll number, date, film type, camera and lens used, and other information. The film roll identifying frame was usually the first frame in the roll. Additional photographs were taken by personnel from the EG&G Idaho photography laboratory; however, detailed records were not maintained for these photographs in the field notebook. Direction, distance, and depth measurements were made with a transit, measuring tape, and 12-ft stadia rod. Each day the transit was set up in the same position by locating the transit over a steel rod driven permanently into the ground for reference. The location of the transit was verified by measuring the height and bearing of two to three reference points in the area. Samples were taken as appropriate and included soil, crystalline and vitrified product, and simulated waste in several stages of thermal alteration. Samples were placed in appropriate containers (e.g., new heavy-duty polyethylene trash bags for coherent materials and new 400 mL plastic bottles with tight screw lids for loose soils). Samples were labeled, and sampling information was recorded in the sample logbook.

Cores were drilled into the glassy waste form, or monolith, that pooled in the bottom of each pit. The drilling was carried out using a trailer-mounted rig with an air-cooled 10.2 cm (4 in.) diamond drill bit having a Hastalloy matrix. A 1.8-m (6-ft) steel "clam shell" type core-barrel was used. Four cores were drilled into the Test Pit 2 monolith and two cores were taken from the Test Pit 1 monolith. The cores were stored in 10.2-cm (4-in.) diameter Lexan tubes and were described in the sample notebook, bagged, and labeled, as were all the other coherent samples. Most cores were broken into

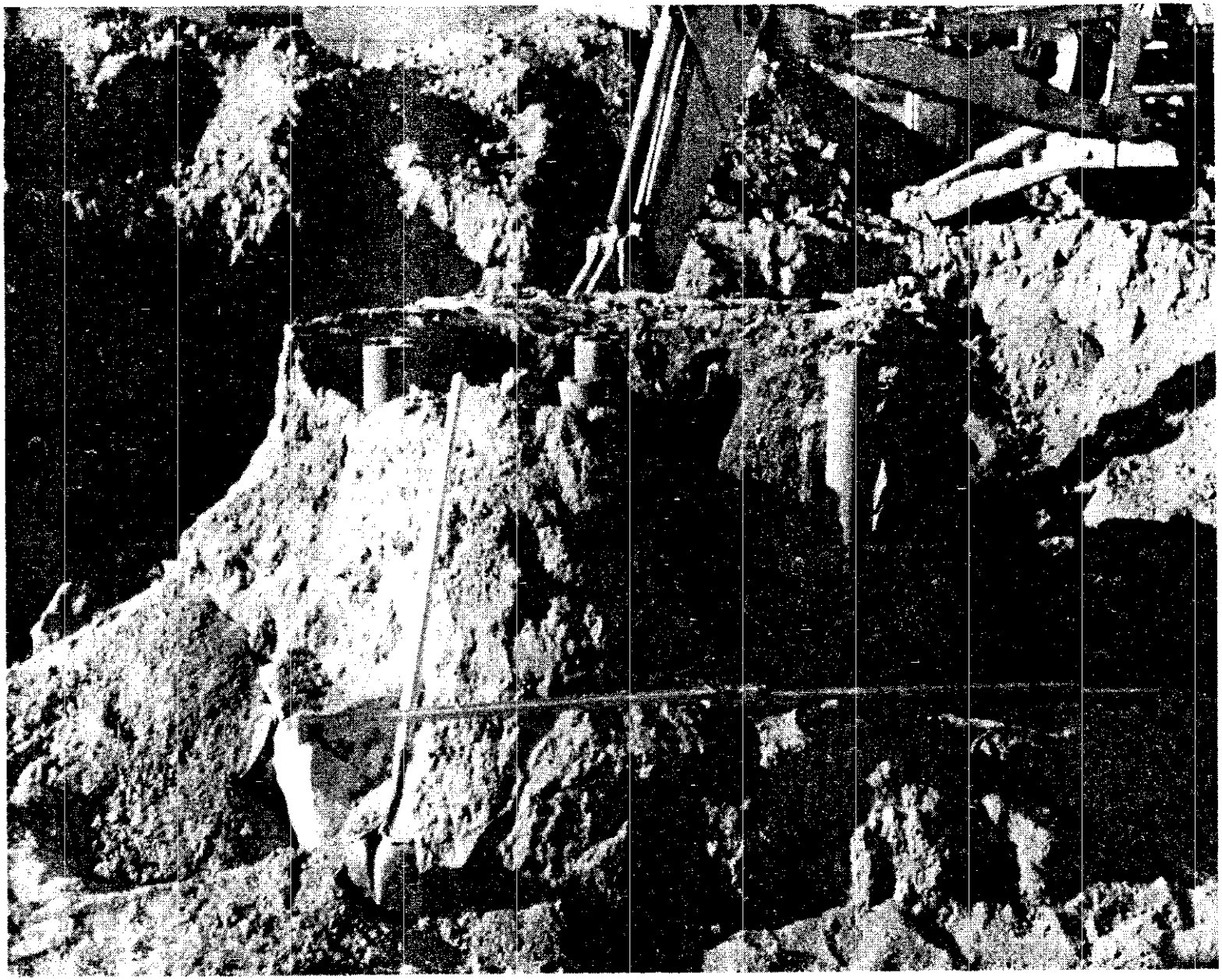

Figure 82. Test Pit 1 partially excavated.

small (approximately 5.1 to 10.2 cm [2 to 4 in.] on a side) fragments during the drilling process; therefore, the original location of each piece is probably known within a precision of ± 5 cm (2 in.).

5.1.2 Bulk Description

5.1.2.1 Processed Waste Test Pit 1. The general shape of Test Pit 1 after ISV processing was a square shaft with rounded corners, as shown in Figure 83. The depth from ground surface to the uppermost glassy material in the pit bottom, as measured directly from ground level, was about 1.5 m (5 ft). Depth from ground surface to the monolith (i.e., dense, well-defined glassy material in a contiguous mass), centered among the four electrodes, was approximately 1.9 m (6.1 ft) when measured during excavation. The monolith was approximately oval and about 1.5 x 1.8 m (5 x 6 ft) with the long axis under diagonal electrodes (SW to NE). The thickness of the monolith was about 0.55 to 0.61 m (1.8 to 2.0 ft) and was measured as the length of each of the cores taken from Test Pit 1. Figure 84 shows a schematic cross section of Test Pit 1 after ISV processing. Significant amounts of glassy material were found outside the cylindrical pit walls but within the simulated waste. This material was in the form of glassy fillings in cardboard boxes. The original shape of the boxes was preserved. A typical example of a "glassy box" is shown in Figure 85. In some cases, the boxes were completely filled with a mixture of glass and scrap metal. In other cases, the glassy boxes were empty and had a wall thickness as small as 0.64 cm (0.25 in.). Scrap metal was the only waste material found in the glassy boxes. An explanation for the "empty" glassy boxes suggests that the boxes originally contained nonmetal substances such as concrete and scrap glass. This material probably dissolved into the melt and/or was carried out of the box as the melt level in the pit dropped below the level of the box and as the molten material in the box drained back into the pit. Both glassy boxes and unaffected boxes were found at all levels in the pit. Glassy boxes were laterally distributed the full width, 3.05 m (10 ft), of the test pit. The total amount of processed waste recovered was 8267 kg (18,225 lb).

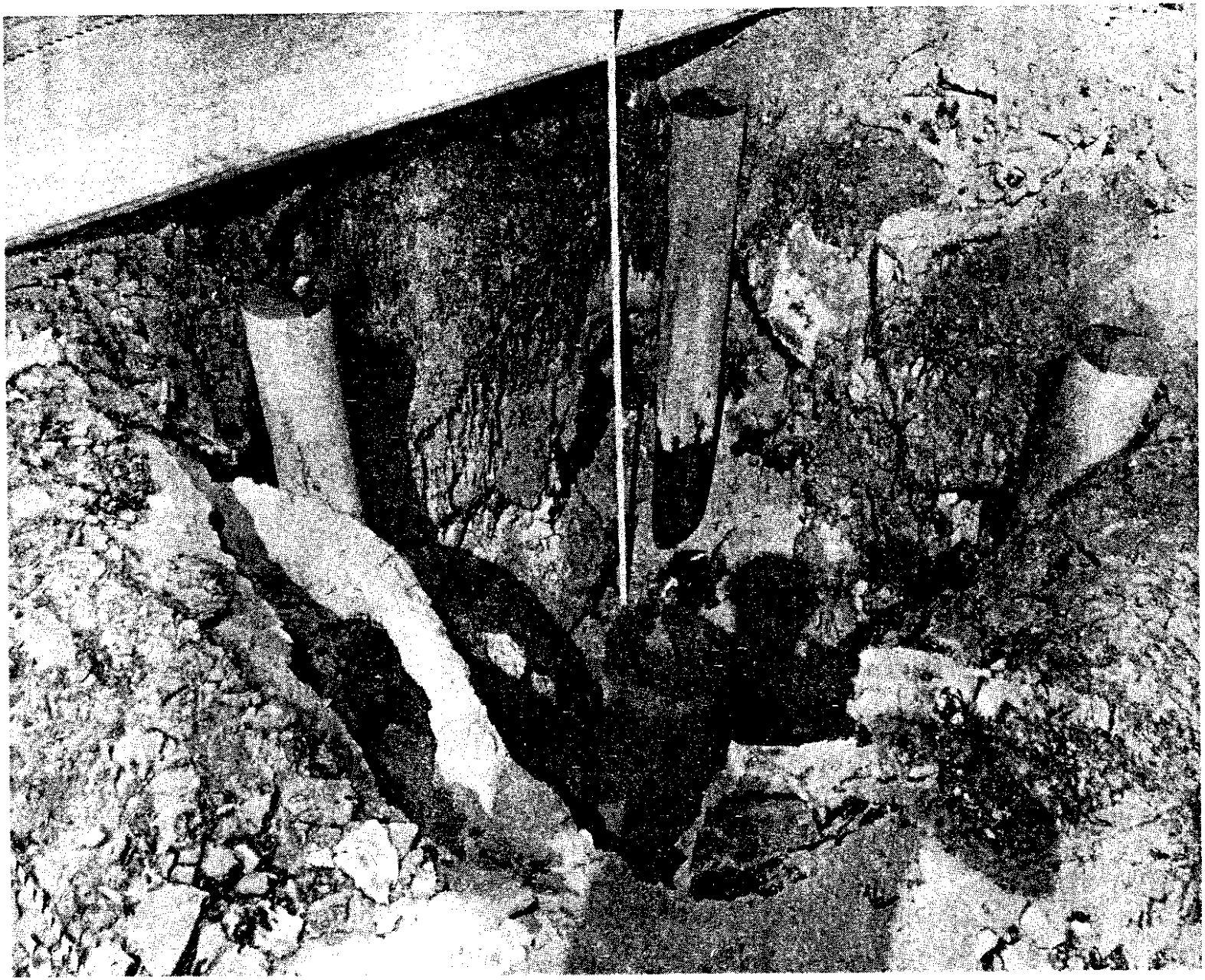

Figure 83. Test Pit 1 after ISV processing.

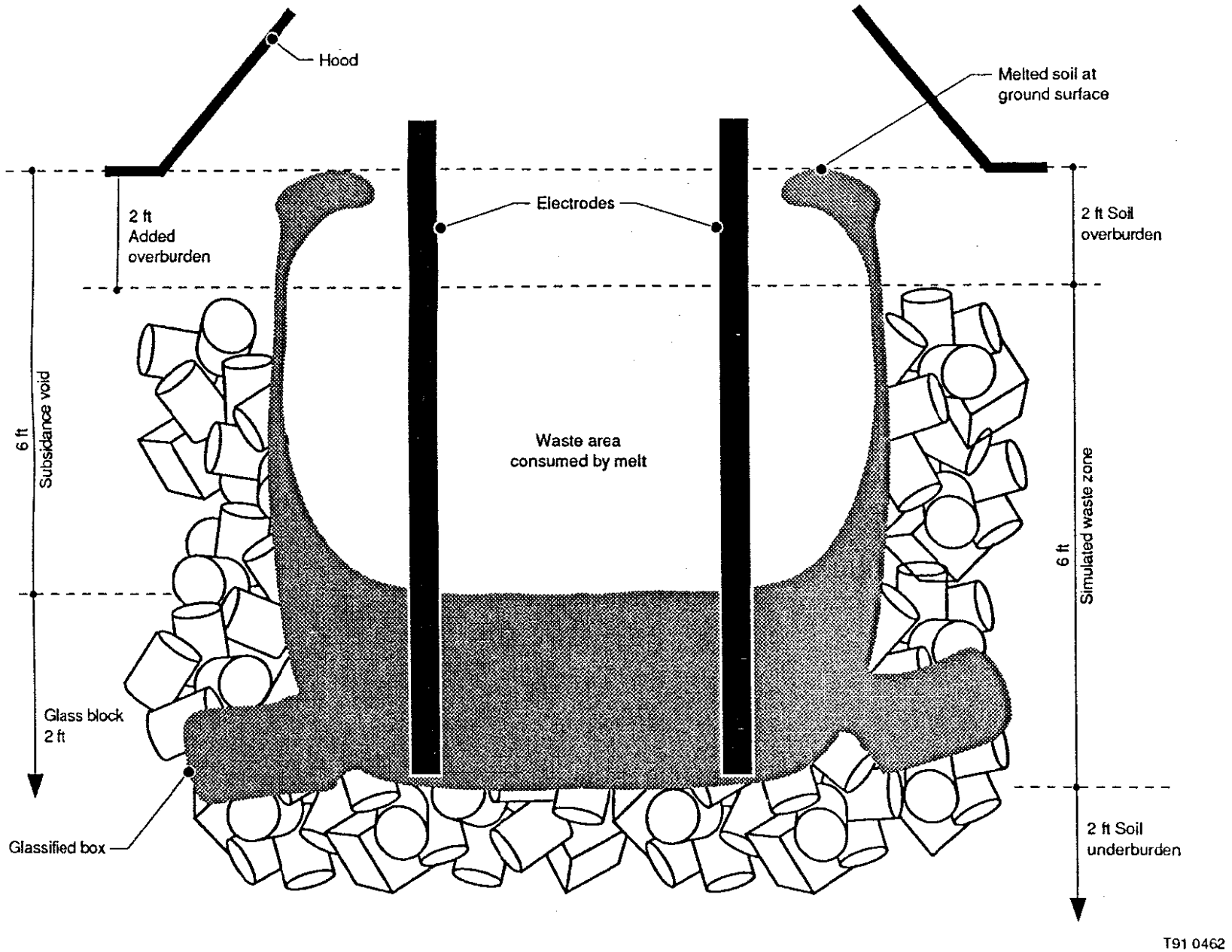

Figure 84. Schematic cross section of Test Pit 1 after ISV processing.

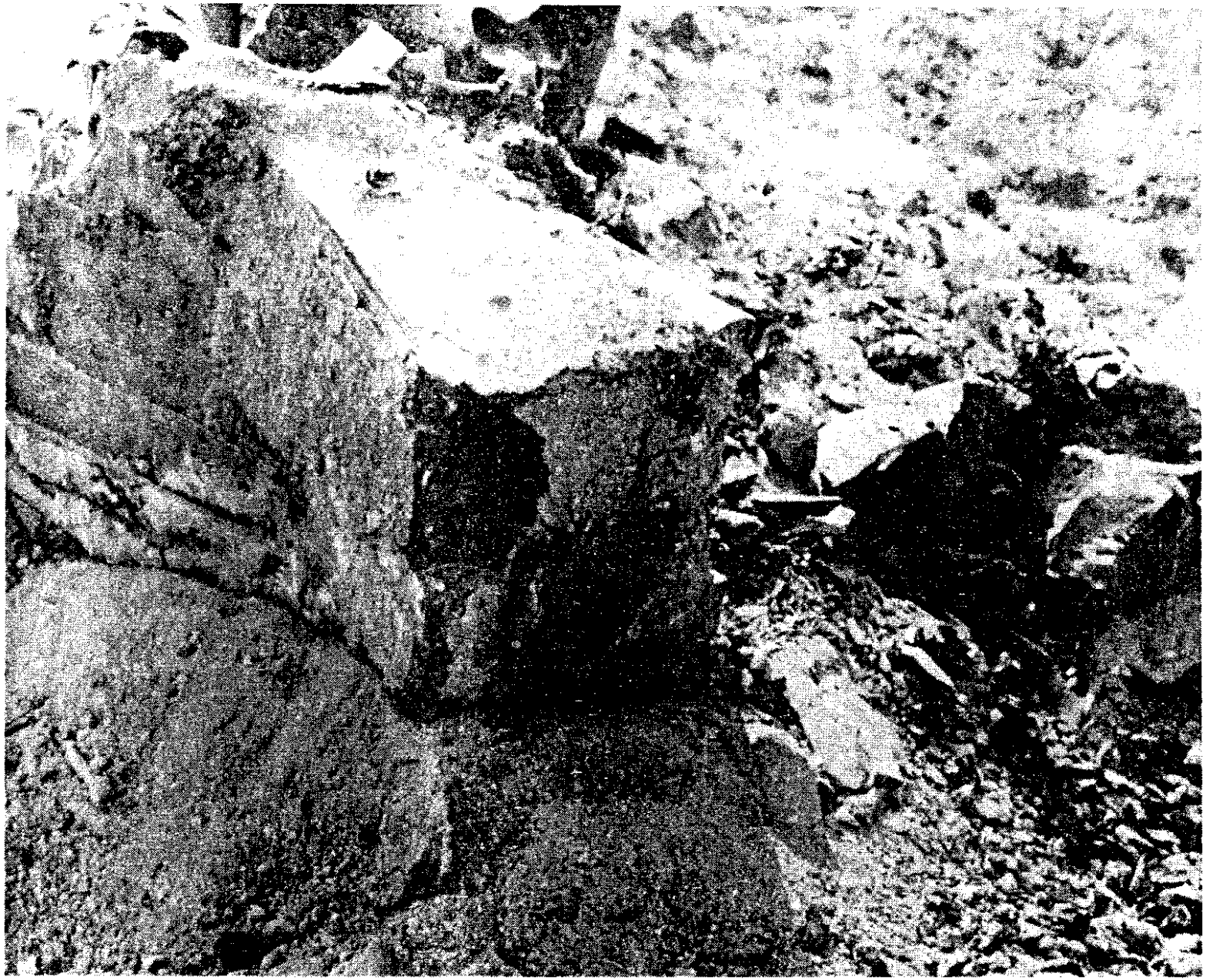

Figure 85. Test Pit 1 "glassy box."

5.1.2.2 Processed Waste Test Pit 2. The general shape of Test Pit 2 resembled a funnel on a box and is shown in cross section in Figure 86. The shaded cans shown in this figure are depicted for illustrative purposes; these cans were processed and incorporated into the melt. At the end of the test, a subsidence hole existed down to the top of the melt. Depth from ground surface to the monolith upper surface ranged from about 2.2 to about 2.3 m (7.2 to about 7.5 ft), with the monolith being about 0.98 m (3.2 ft) in thickness. (Note that "ground surface" was 0.6 m [2 ft] higher than Test Pit 1 and that the maximum thickness of the monolith was 1.14 m [3.75 ft] along the south edge of the block to 2.75 ft along the north side.) The maximum diameter of the funnel was 3.35 m (11 ft) at a depth about 0.46 m (1.5 ft) below ground surface. The funnel pinched inward to a diameter of about 1.5 m (5 ft) near the monolith upper surface. The funnel walls are shown in Figure 87. The thickness of the funnel wall was about 10.2 cm (4 in.).

The upper lip of the funnel was a rim of glass, roughly oval in cross section, at ground level with a diameter of 0.46 to 0.61 m (1.5 to 2 ft). The shape of the monolith was a rough rectangle with rounded corners. The maximum dimension was 3.35 m (11 ft) (N-S) and minimum was 2.90 m (9.5 ft) (E-W) measured from exposed coherent glass to exposed coherent glass on opposite sides of the monolith. Figure 88 shows the shape of the monolith together with the exposed scrap metal on the unlithified corners of the monolith. The simulated waste in Test Pit 2 was arranged with layers of cans on cardboard boxes. The melt filled and obliterated virtually all of the boxes, which measured 3.05 x 3.05 m (10 x 10 ft) total, except at the pit corners and, in a few cases, the very outermost surfaces of the boxes. The three sets of outermost cans, directly above the boxes, were affected much less extensively and are shown in Figure 89. Note that the cans in the third set were in contact with the glass of the funnel wall directly above the monolith. The weight of the monolith was 13,109 kg (28,900 lb), and the total amount of vitrified waste recovered from Test Pit 2 was 17,430 kg (38,425 lb).

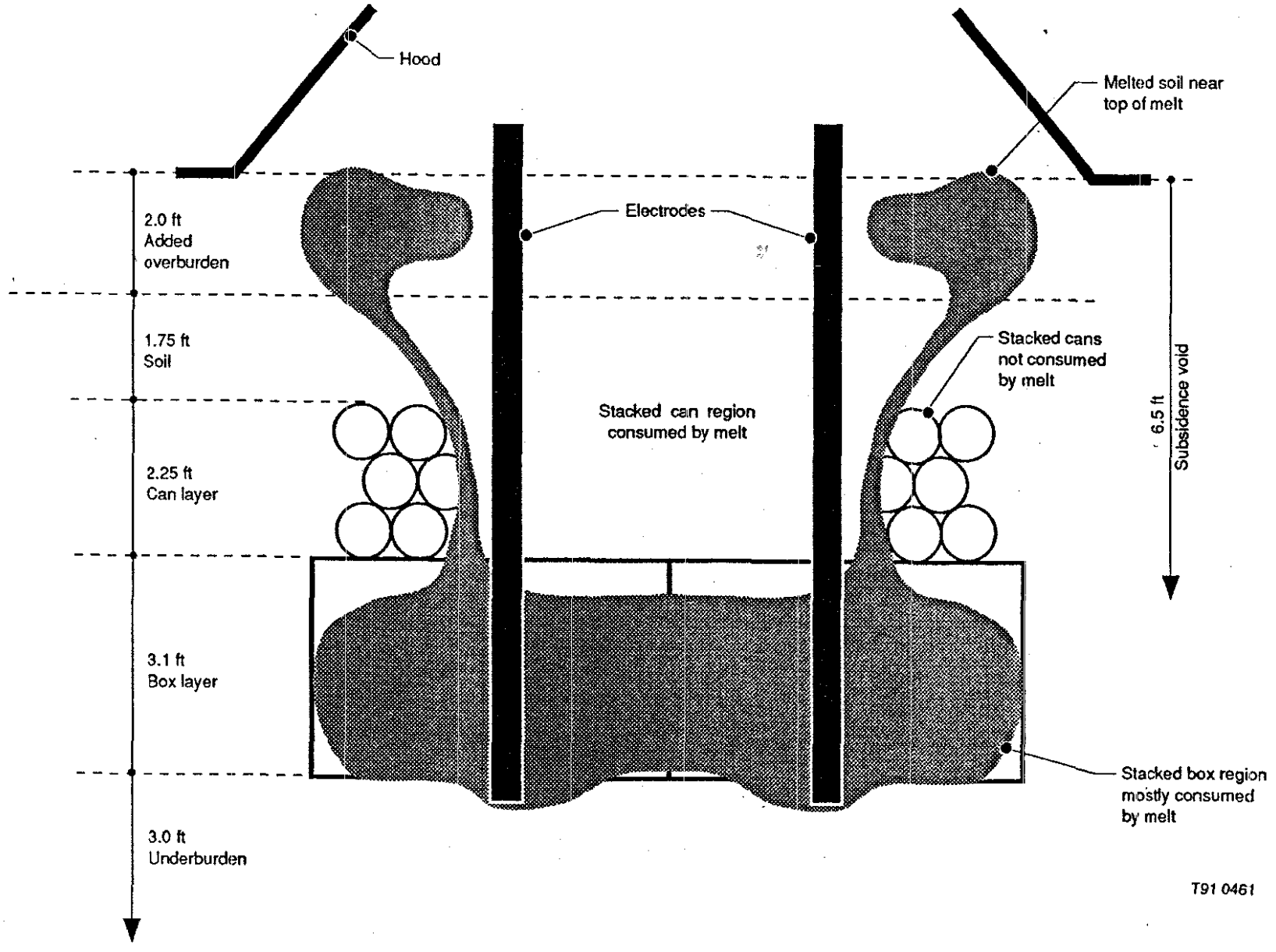

Figure 86. Schematic cross section of Test Pit 2 after ISV processing.

Figure 87. Test Pit 2 funnel walls.

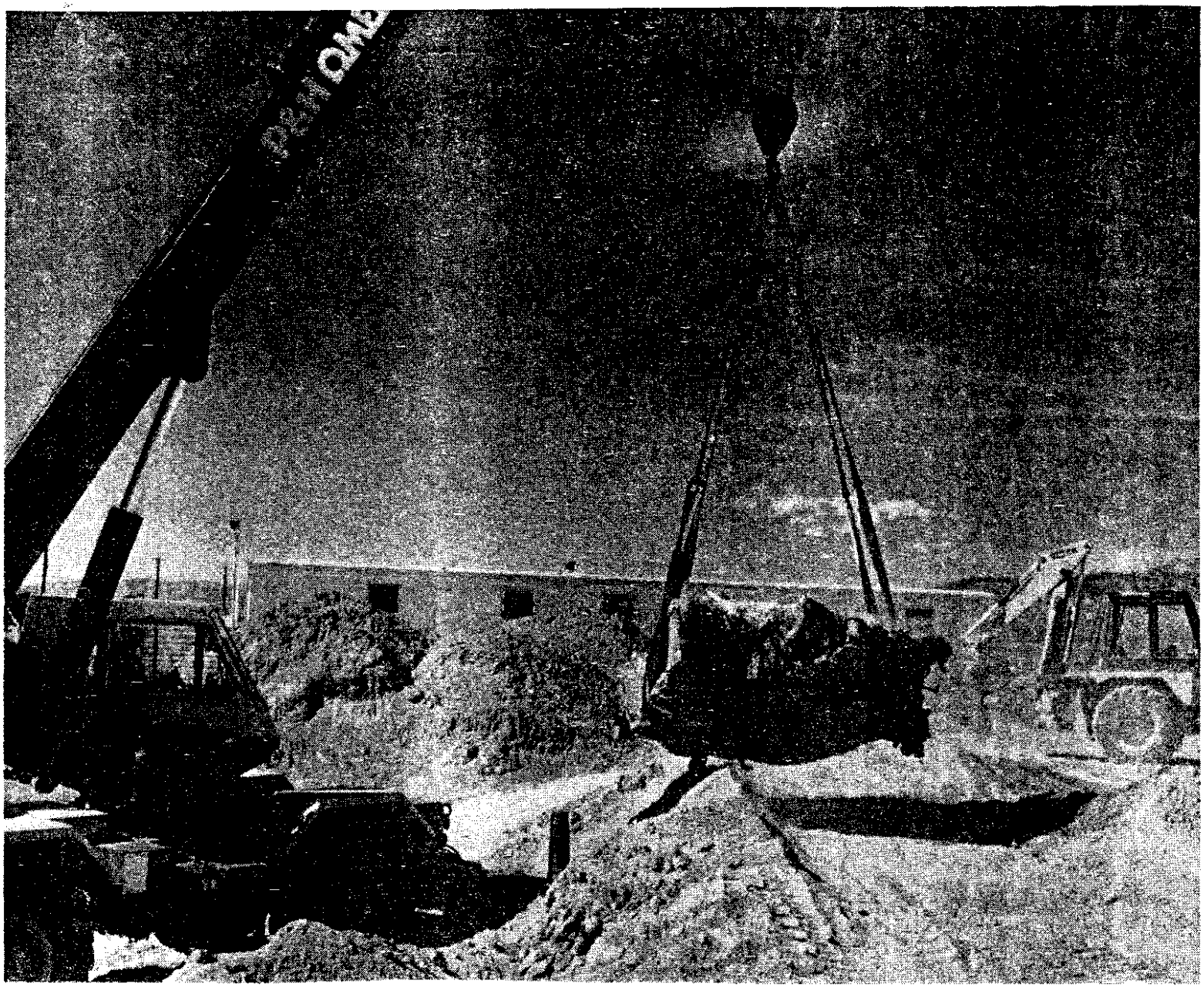

Figure 88. Test Pit 2 monolith.

Figure 89. Edge effects on cans in Test Pit 2.

5.2 Chemical and Physical Properties

5.2.1 Methods

Nearly one hundred samples were taken as appropriate and included soil, crystalized and vitrified product, and simulated waste in several stages of thermal alteration. Samples were placed in appropriate containers (e.g., new heavy-duty polyethylene trash bags for coherent materials and new 400 mL plastic bottles with tight screw lids for loose soils). Samples were labeled, and sampling information was recorded in the sample logbook. Cores were obtained as described alone in Section 5.1.1.

Twenty eight samples, including cores, from both test pits were selected for detailed study. In general, samples were taken systematically from each core at about 30 cm intervals and included both glassy and metallic materials. Additional core samples were collected so that all megascopically observable variations of the material were represented in the sample collection. Similarly, the remainder of the samples were selected so that representatives of all megascopically observable variants in the vitrified product were present in the data set. Sample descriptions are given in Tables 14 and 15 and sample locations within the test pits are shown on Figures 90 and 91. All samples were submitted for analysis under chain of custody. No special preservation or storage of the samples was required.

The major element bulk chemical analyses reported were carried out at three laboratories using two different analytical methods. The Separations and Analysis Unit of EG&G Idaho performed bulk chemical analysis by inductively coupled plasma atomic emissions spectroscopy (ICP-AES) using an ARL 3410 instrument. The preparation of glass samples involved first crushing, then dissolution using HF and nanopure water, followed by additions of HNO_3 and nanopure water. The metallic samples were prepared using the described HF dissolution on metal shavings. The ICP analyses were carried out using standard techniques. A multipoint calibration with replicate standards

Table 14. Sample descriptions Test Pit 1

Sample	Block Location	Description
IC013C90IW	1	Green glass, top of pit rim and edge, which contains ≈50% gas bubbles (diameter up to ≈1.3 cm) and traces of brown inclusions which are probably soil
IC044B90IW	2	Green glass from the top the central core (#5) The glass contains up to 20% bubbles (diameter up to 15 mm)
IC044D90IW	3	Dark green glass with 20% grey spherulites (≈2 mm diameter) trace of gas bubbles, core (#5) center 28 cm below IC044B90IW
IC044H90IW	4	Dark green glass with 2% grey spherulites (≈2 mm diameter) core (#5) bottom, 56 cm below IC044B90IW
IC048B90IW	5	Dark green glass, top of core#6, 76 cm NNW of core #5 (IC044B90IW), ≈30% gas bubbles ≈1 cm diameter
IC048C90IW	6	Dark green glass with 50% grey spherulites ≈1 mm in diameter and trace of gas bubbles, core #6, 30 cm below IC048B90IW
IC048H90IW	7	Dark green glass with about 60% spherulites ≈1 mm diameter and trace of gas bubbles, core bottom, 56 cm below IC048B90IW
IH061D90IW	8	Nodular aggregate of grey metal pooled beneath center of Test Pit 1 monolith, contains trace amounts of green glass

Table 15. Sample descriptions Test Pit 2

Sample	Block location	Description
IC006C90IE	1	Dark green glass with up to 30% gas bubbles, located ≈46 cm from pit top on the interior of the pit
IC007C90IE	2	Dark green glass with trace amounts of very small bubbles, collected from the lower "funnel" ≈1.5 m below ground surface
IC026D90IE	3	Green glass with a blue-grey cast, contains 25% gas bubbles and about 5% grey spherulites, top of central monolith core (#1)
IC026F90IE	4	Grey porcelinous material with ≈7% gas bubbles (diameter < 7 mm), 6.3 cm below IC026D90IE core #1
IC026I90IE	5	Aphanitic and spherulitic material (diameter up to 8 mm) with traces of gas bubbles, located ≈28 cm below IC026D90IE, core #1
IC026M90IE	6	Green glass and grey spherulitic material (diameter up to 7 mm) ≈54 cm below IC026D90IE, core #1
IC027D90IE	7	Green glass with 7% gas bubbles (diameter up to 7 mm), top of core #2, 43 cm due south of core #1 (IC026D90IE)
IC027B90IE	8	Aphanitic and 3 to 5 mm diameter spherulitic material, located 27 cm below IC027D90IE, core #2
IC037D90IE	9	Grey spherulitic material (3 to 5 mm in diameter) with traces of gas bubbles, core #2, ≈38 cm below IC027D90IE
IC037F90IE	10	Grey devitrified glass, core #2, 27 cm below IC037D90IE

Table 15. (continued)

Sample	Block Location	Description
IH037J90IE	11	Massive metal and traces of glass 10 cm thick located at the bottom of core #2,
IC038B90IE	12	Dark green glass with bubbles, top core #3, 46 cm NE of core #1
IC038C90IE	13	Grey green devitrified glass with traces of grey spherulites up to about 2 mm in diameter, located ≈7 cm below IC038C90IE, core #3
IC038D90IE	14	Green glass and grey spherulites up to 1 cm in diameter, located 46 cm below IC038B90IE, core #3
IC043D90IE	15	Dark green glass with 60% gas bubbles up to 2 cm in diameter, top of core #4, 1.3 m NE core #1, inline with cores #1 & 3
IC043F90IE	16	Green glass, grey devitrified material and grey spherulites ≈3 mm in diameter, core #4, located 34 cm below IC043D90IE
IC043J90IE	17	Aphanitic grey material with traces of spherulites (1 mm diameter) and gas bubbles, located at the bottom of core #4, ≈63 cm below top of core
IH074D90IE	18	Grey nodular metal from the bottom of Pit 2 monolith, 1 m toward monolith center from the NE corner
IC086C90IE	--	Dark green glass with traces of gas bubbles, sample of melt taken while ISV waste form was molten

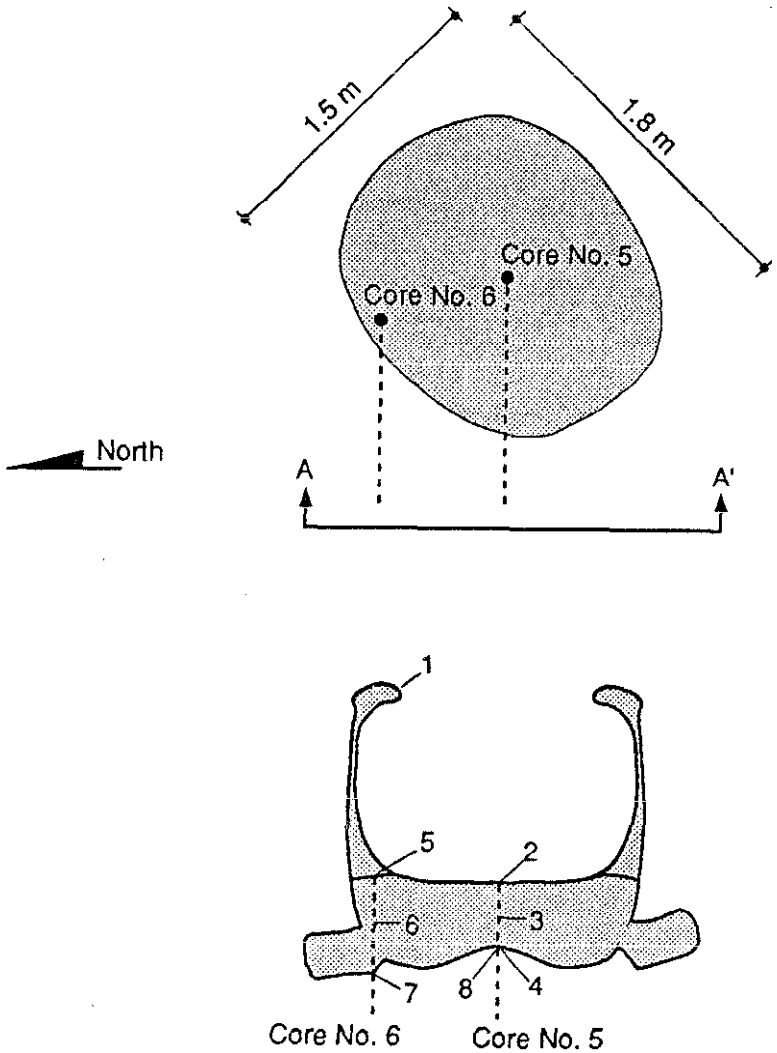

Figure 90. Product sample locations for Test Pit 1.

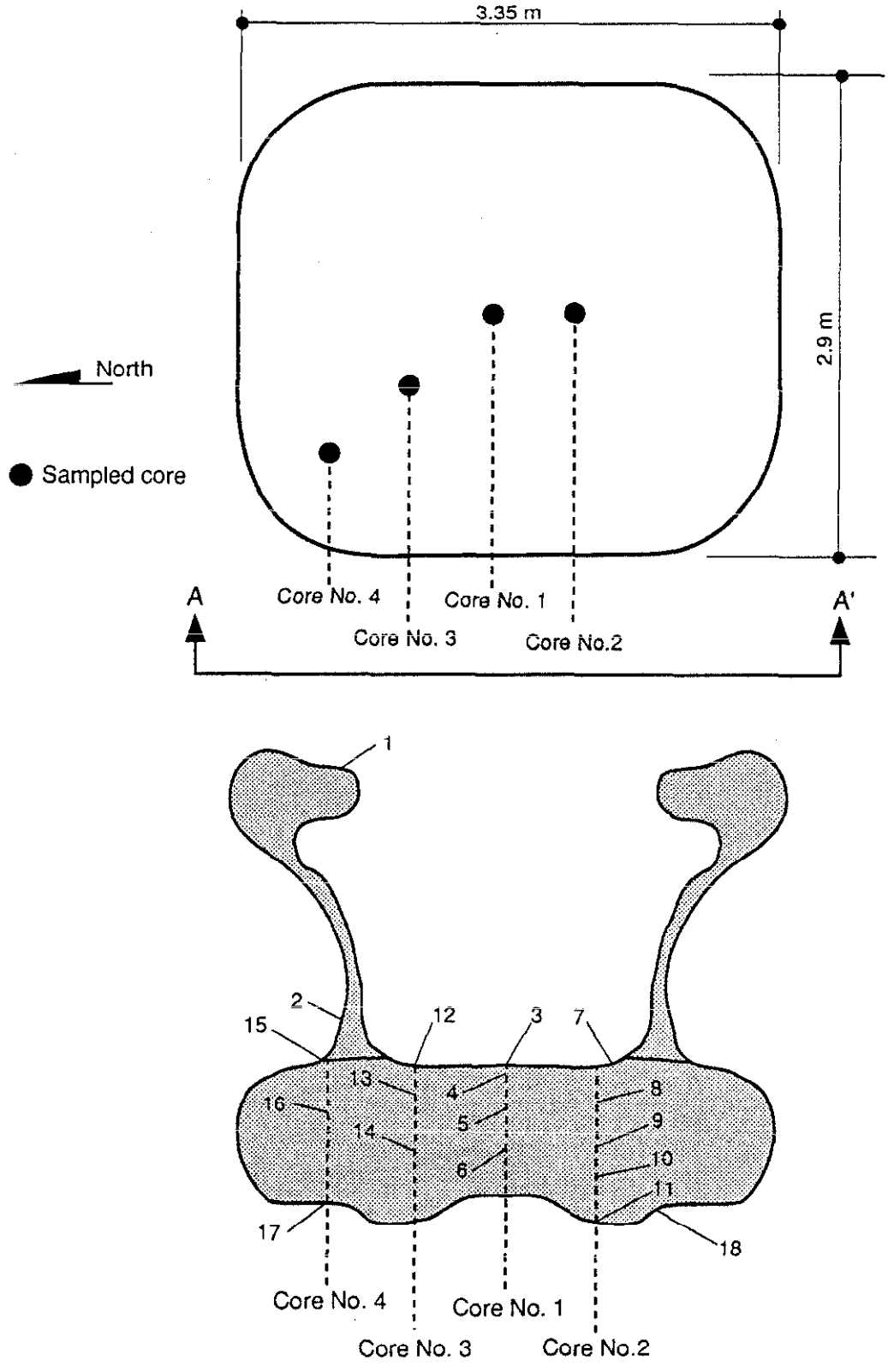

Figure 91. Product sample locations for Test Pit 2.

determinations was performed over a suitable concentration range. The quality control associated with the glass analysis included two internal standards, matrix blanks, duplicate samples, sample spikes and blank spikes. The quality control associated with the metal samples consisted of matrix blanks, sample spikes, and blank spikes. The quality control procedures and data were reviewed for compliance with acceptable limits. About one-third of the data were found to be suspect for many reasons. The suspect data are not included here. The reported mean percent spike recovery and the relative standard deviation of the duplicate samples are shown in Table 16. An additional test of the reliability of the data is that the sum of the major elements oxides of an acceptable analysis will be 100 ±5 weight percent. Many of the analyses do not meet this requirement.

Table 16. Reported QA/QC summary of ICP-AES analysis by the separations and analysis unit

	Si	Fe	Mg	Ca	Al	Na	K
Mean%Spike Recovery	74.6	101.6	96.1	N/A	91.2	N/A	103.3
Relative Standard Deviation on Duplicate Samples	3.3	0.4	1.2	0.9	2.2	3.8	6.3

Some of the major element bulk chemical data reported here, as well as all of the microchemical analysis, were carried out at the Idaho Geologic Survey/Comer Laboratories electron microprobe laboratory at the University of Idaho using an ARL-EMX electron microprobe operated at 15KV and 0.1 microamp beam current. Standard operating procedures and five well-characterized mineral standards were used. Polished thin-sections were used for both bulk analysis and also the microchemical observations and measurements. Each bulk analysis datum is the mean of about twenty individual measurements. The reported standard deviation of each oxide value ranges from a worst case 27% (Na_2O) to 1.5% (SiO_2) of the amount present. The reported sum of the major element oxides varies from 97.3 to 100.3 weight percent. In addition, a blind analysis of three National Institute of Standards and Technology (NIST) glass

standards was carried out. The agreement between the oxide values measured and the published values is excellent.

The Pacific Northwest Laboratory also carried out bulk chemical analysis of some of the samples described here as part of a study of the durability properties of the Intermediate Field test (IFT) waste form. Preparation of the samples was performed by $NaOH/Na_2O_2$ and KOH/KNO_3 fusions of samples ground to -200 mesh. The fusions were dissolved in deionized waster and analyzed by ICP-AES using standard procedures. The reported sum of the major element oxide data varied from 98 to 100.5 weight percent with the exception of sample IC048C90IW which had an 88 weight percent oxide sum.

Interlaboratory agreement of the data was checked by having duplicated samples analyzed by all of the laboratories. The agreement between the measurements made at the University of Idaho and PNL is excellent. Agreement between the data of the Separations and Analysis unit and both the other laboratories was not close in many cases. Since the PNL and University of Idaho data are in agreement, their oxide weight percent sums are close to 100%, and the University of Idaho methods were tested by blind analysis of three NIST glass standards, the data produced by these two laboratories are reported here except where noted.

X-ray powder diffraction analysis was carried out using an automated diffractometer equipped with a monochrometer and using Cu K_∂ radiation. The goniometer was used in step scan mode with 0.015 degree two theta per step and held one second per step. The goniometer scanned from 15 to 70 degrees two theta. CaF_2 was mixed with the powdered sample (< 100 mesh) and used as an internal standard. The data were automatically compared to the Powder Diffraction Files by computer match to obtain the identification of the crystalline compounds present in the sample. The compound identity selected by computer must be used with caution because compounds found in the ISV waste form are not necessarily those found in the computer file. The x-ray diffraction measurements were made by personnel in the Metals and Ceramic Unit, EG&G Idaho. Samples were also analyzed at the Idaho Geologic Survey/ Comer Laboratory and at PNL as part of the sample durability measurements.

Agreement among the three laboratories is excellent. Final interpretation of the data and compound identification was done by Jerry R. Weidner of the Waste Technology Development Department (WTDD) of EG&G Idaho using both the x-ray diffraction data and the microchemical data.

Apparent bulk density measurements of selected samples were performed by the Metals and Ceramics Unit, EG&G Idaho, using a standard procedure slightly modified from ASTM C-93-84 (the archimedean method). The procedure was tested using NBS 710 standard glass and achieved excellent agreement with the published values for this standard.

5.2.2 Results and Discussion

The products from Test Pits 1 and 2 are virtually identical and include several types of material. The outermost surface of the product was a grey-white, pebbly, and friable material, 1.27 to 1.91 cm (1/2 to 3/4 in.) thick, and was similar in both pits. This material is referred to as "rind," and is in direct contact with dark green-black glass on its inner surface (toward the test pit center) and loose soil on its outer surface. It is the calcined and sintered soil immediately adjacent to and in contact with the former melt. In general, the product from both pits consisted of a black (with green tints) glassy material containing variable amounts of bubbles and crystalline material. The amount of bubbles varied with position in the pits. Glass from the bottom of the pit generally contains less than 1 vol% bubbles, whereas glass from the upper regions of the pit near ground surface often contain greater than 90 vol% bubbles. Bubble diameter ranges from microscopic to several centimeters and the larger bubbles tend to occur within the glass areas having the largest portion of bubbles. Glass from the pit walls and top is generally dense and without voids adjacent to the rind, but becomes progressively more vesiculated toward the central cavity of the test pit. Some glass on the inner walls near the top of the pit are very vesicular (about 60 to 90 vol% vesicles as estimated by eye) and contain vesicles up to about 4 cm in diameter. The upper surface of the monolith, i.e., that surface in contact with gas in the bottom of the test pit central cavity, is similarly coarsely vesiculated (bubbly). In contrast, glass from the "glassy

boxes" (Test Pit 1) was generally without voids. Although the crystalline materials found in the products from the two test pits were very similar, the megascopic appearance of the materials was somewhat different. Glass was the principle phase found within the monolith. The outermost portion of the monolith, the most quickly cooled portion next to the "rind," was virtually pure glass (containing ≤2 vol% vesicles and opaque inclusions as estimated by eye). Grey spots, first appearing at about 10 cm from the monolith surface, increased in abundance (to about 60 vol% as estimated by eye) toward the interior of the monolith. The grey spots had a maximum diameter of about 3 mm. Examination of the spots using the scanning electron microscope, the petrographic microscope, and X-ray powder diffraction indicated that they were dendrites of crystalline material having a spherulitic structure and that small (<10μm) spherical metallic inclusions or bubbles often acted as nucleation sites.

Most of the material in the Test Pit 2 monolith was quite different in appearance from the black glass in the remainder of Test Pit 2 and all of the material in Test Pit 1. The Test Pit 2 monolith consisted of an outermost zone of black glass about 5.1 cm (2 in.) thick followed by an aphanitic white to beige zone and an aphanitic faint lavender porcelainous region 5.1 to 10.2 cm (2 to 4 in.) thick that graded into a phaneritic-appearing material. Examination using the transmitted light microscope and the scanning electron microscope indicated that the aphanitic materials were made of dendritic crystals (< 10μm) and glass. The phaneritic material constituted the bulk of the monolith. The phaneritic material had a green-black glassy matrix covered with up to 60% white spots that ranged in diameter from about 0.32 to 0.64 cm (1/8 to 1/4 in.). Figure 92 shows the texture of the Test Pit 2 monolith material. The spots are spherulites (i.e., 3-dimensional feather-like dendrites radiating from a common center) of dendritic crystals. A photomicrograph illustrating the typical dendritic microstructure is shown

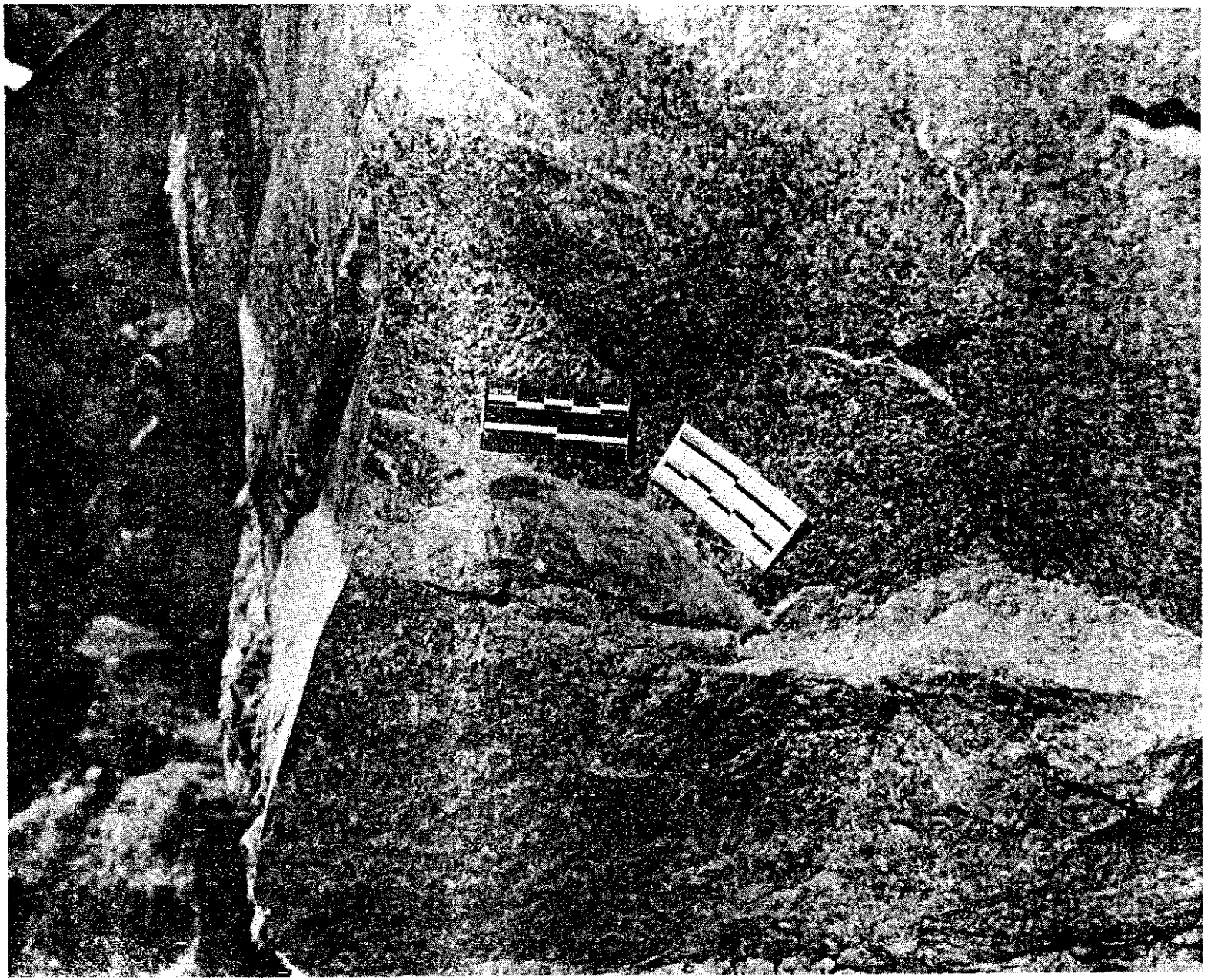

Figure 92. Test Pit 2 texture of vitrified monolith material.

in Figure 93. X-ray powder diffraction and microchemical analysis indicated that all of the dendritic materials found in both pits, indeed the only silicate mineral, was the mineral augite, a variety of clinopyroxene. Although quantitative analysis could not be made on individual crystals because the crystals were too small (<5μm) the data indicated that the crystals were chemically heterogeneous and zoned. Augite is a calcium-magnesium-iron rich silicate. The crystallization of this mineral caused the coexisting liquid to be enriched in sodium, potassium, aluminum, and silicon and depleted in calcium, iron, and magnesium. An example of magnesium depletion is illustrated by the x-ray photomicrograph Figure 94. Augite is a common, naturally occurring pyroxene found in volcanic rocks, such as the basaltic rocks found at the INEL, which have compositions and cooling histories similar to the vitrified material in the Intermediate Field tests reported here. The textural variations found between the test pits and within each pit are probably due to differences in cooling rate. Glass materials are the most quickly cooled and the phaneritic materials are the most slowly cooled. The heterogeneous nature of the crystals arises from the high rate of cooling of the test pit materials compared to the cooling rate required for equilibrium crystallization.

Twenty-three glassy samples were selected for bulk chemical analysis. Seven representative samples were selected from Test Pit 1; the remainder are from Test Pit 2. The data indicate that the bulk composition of all samples was virtually identical (within analytical uncertainty) and that the test materials were chemically homogeneous. The analyses are shown in Tables 17 and 18 with the analysis of a grab sample of INEL soil (<1 mm size fraction) from the Lost River Settling Area "A", which is just outside the boundary of the SDA, for comparison. Soil for the IFT test pits came from the Lost River Settling Area.

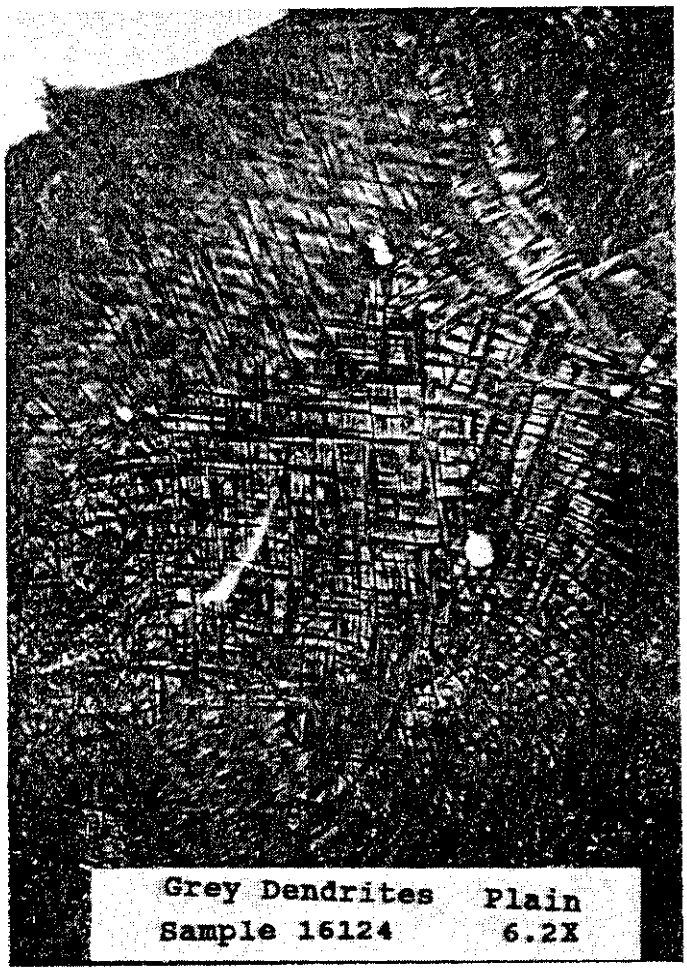

Figure 93. Typical dendritic microstructure showing glass (white) and needle-like augite crystals (photomicrograph white light, 6.2X), sample IC026I90I, Core #1 center of Pit 2 monolith, 28 cm below core top.

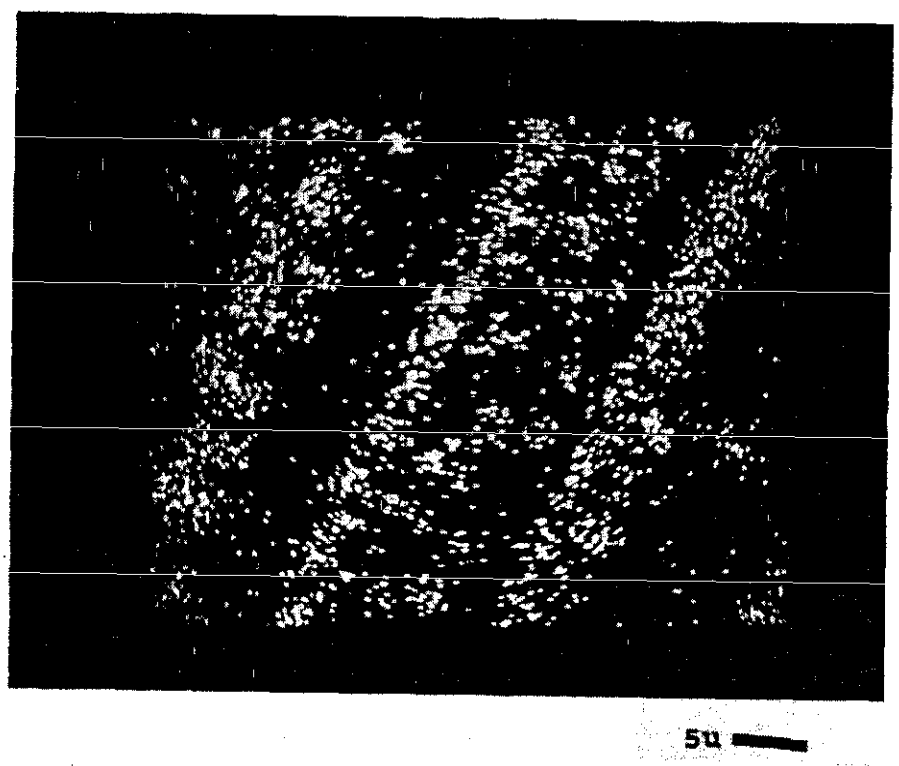

Figure 94. X-ray fluorescence photomicrograph (200X) showing magnesium concentration in dendrite crystals and depletion in glass matrix, sample IC026I90IE. Light areas show increased magnesium concentrations.

Table 17. Bulk composition of Intermediate Field Test Pit 1 Glass

Sample	Block Location	Oxide Weight Percent (SD) SiO_2	FeO	MgO	CaO	Al_2O_3	Na_2O	K_2O	Remarks
IC013C90IW	1	--	4.0	2.4	8.1	13.1	---	3.6	Glass, top of pit rim and edge
IC044B90IW[a]	2	63.6 (1.1)	4.7 (0.2)	2.8 (0.1)	8.6 (0.4)	13.4 (0.2)	1.2 (0.3)	2.8 (0.1)	Glass, top, central core (#5)
IC044D90IW[a]	3	66.6 (1.1)	4.8 (0.8)	2.7 (0.1)	9.0 (0.3)	12.9 (0.3)	1.2 (0.2)	2.8 (0.1)	Glass, dendrites core center
IC044H90IW	4	--	5.1	2.8	9.5	13.6	---	---	Glass, trace dendrite, core (#5) bottom
IC048B90IW[b]	5	65.6	4.4	2.6	8.8	12.5	2.0	3.1	Glass, top core #6
IC048C90IW[b]	6	65.3	4.2	2.7	8.5	12.5	2.7	3.2	Glass, dendrites, core #6, 30 cm below top
IC048H90IW	7	61.2	4.7	2.8	9.3	13.6	---	---	Glass,dendrites, core #6 bottom
Average		64.3	4.6	2.7	8.8	13.1	1.8	3.1	
INEL Soil[c]		71.0	4.3	2.3	7.5	12.2	0.3	2.5	

a. Electron-microprobe, University of Idaho, C. Knowles, analyst.

b. ICP-AES, Battelle North West, PNL.

c. Soil (<1 mm size fraction) from INEL Lost River Settling Area (EGG-WTD-9794) analysis.

analysis ---ICP-AES, Idaho Research Center, INEL, K. Messic, analyst.

Table 18. Chemical composition of Intermediate Field Test 2 Glass

Sample	Block Location	SiO_2	FeO	MgO	CaO	Al_2O_3	Na_2O	K_2O	Remarks
IC006C90IE	1	---	4.2	2.9	12.3	12.4	---	---	glass
IC007C90IE[a]	2	62.2	3.7	2.7	11.5	11.3	2.2	2.9	glass
IC026D90IE[b]	3	65.7 (0.5)	3.9 (0.1)	2.5 (0.3)	10.7 (0.4)	12.6 (0.5)	1.3 (0.3)	3.0 (0.05)	glass
IC026F90IE[b]	4	64.9 (1.8)	3.3 (0.9)	2.9 (0.9)	11.1 (0.8)	12.9 (0.1)	1.1 (0.1)	2.7 (0.2)	grey porcelain material
IC026I90IE[b]	5	64.6 (1.2)	3.9 (1.3)	2.0 (1.4)	11.1 (0.8)	12.8 (0.4)	1.2 (0.1)	2.8 (0.1)	aphanitic and spherulitic material
IC026M90IE65	6	7.7	4.1	2.6	10.7	11.8	1.5	2.5	glass and devitrifies material
IC027D90IE7	7	59.0	---	---	10.5	11.6	---	2.4	glass, top core #2
IC037B90IE[a]	8	64.3	3.9	2.6	10.7	12.2	2.3	3.2	asphanitic and devitrified material
IC037D90IE	9	56.5	---	---	11.4	13.3	---	2.5	devitrified glass
IC037F90IE	10	58.8	---	2.7	11.2	11.9	1.5	2.7	devitrified glass, core #2, 27 cm below IC037D90IE
IC038B90IE[a]	12	63.6	3.4	2.7	10.9	12.0	2.4	3.1	glass, top core #3, 46 cm NE core #1
IC038C90IE[a]	13	64.4	4.0	2.7	10.5	12.0	2.7	2.9	devitrified glass, ≈7 cm below IC038C90IE
IC038D90IE[a]	14	63.1	3.9	2.6	10.7	11.9	2.0	3.0	glass and spherulites, 46 cm below IC038B90IE

Table 18. (continued)

Sample	Block Location	SiO_2	FeO	MgO	CaO	Al_2O_3	Na_2O	K_2O	Remarks
IC043D90IE	15	60.3	---	2.7	11.2	12.1	1.5	2.7	glass, top core #4, 1.3 m NE core #1 inline with cores #1 & 2
IC043F90IE	16	---	4.2	2.6	10.7	11.7	2.6	2.6	glass dendrites core #4, 34 cm below IC043D90IE
IC043J90IE	17	58.2	---	2.8	---	14.4	---	2.6	grey, asphanitic material, bottom core #4, ≈63 cm below top
IC086C90IE[b]		62.9 (1.5)	3.8 (0.2)	2.6 (0.1)	1.3 (0.4)	12.6 (0.5)	1.1 (0.3)	2.6 (0.1)	melt sample
Average		62.0	3.9	2.6	11.0	12.2	1.8	2.8	
INEL Soil[c]		71.0	4.3	2.3	7.5	12.2	0.3	2.5	

a. ICP-AES, Battelle North West, PNL.

b. Electron-microprobe, University of Idaho, C.Knowles, analyst.

c. Soil (<1 mm size fraction) INEL Lost River Settling Area (EGG-WTD-9794); normalized volatile-free analysis-ICP-AES, Idaho Research Center, INEL, K. Messic analyst.

The data indicate that the ISV test product is identical to the INEL soil except for the greater quantity of silica and lesser amount of sodium in the soil grab sample, presumably indicating that the grab sample contains slightly more quartz and less feldspar. Note also that the composition of the "melt sample," IC086C90IE, is virtually identical to the average value. The "melt sample" was collected by pushing a 2.4 cm (1 in.) steel rod directly into and then withdrawing it from the still molten silicate material immediately following the termination of Pit 2 processing. The sample was taken from the material adhering to the rod. The close agreement between the average values and the "melt sample "values indicates that such melt sampling and subsequent rapid chemical analysis provides an excellent first-look data set for predicting the composition and, therefore, the properties of the monolith before it has cooled. This suggests that the composition analysis of a full-scale melt could be taken, analyzed, and modifications could be made to the melt by additives during processing.

The bulk density values of seven glassy samples from both pits (see Table 19) are also nearly identical and also show that the test pit materials are homogeneous. The minor density variations are probably due to the variation in the number of bubbles and metallic inclusions in the samples.

Three distinguishable classes of metallic materials are found in both pits. One category is the metal found with the shape of the original scrap, i.e., cans, bars, plates, sheets, turnings, and various artifacts of mild steel, carbon steel, and stainless steel. This class of metals was not melted during ISV processing, otherwise the original morphology would have been destroyed. In general, cans, turnings, and sheet stock (thinner than about 1 mm) were not observed within the monolith and probably were dissolved/melted when incorporated into the melt. The unmelted metal within the lithified (previously melted) regions appeared to be only the massive pieces of scrap metal such as machine parts or thick plates. The massive metal scrap is concentrated into the lower one-quarter of the monoliths, suggesting that some of the metal settled toward the bottom of the silicate melt pool. The second class of metal occurs as megascopically observable spherical particles to nodular lumps. This morphology indicates that these materials have undergone some transformation, most likely melting, during the ISV processing. Because

Table 19. Intermediate Field Test glass density

Sample	Block Location	MEAN DENSITY (sd) gr/cm^3	Remarks
IC026M90IE (Pit 2)	6	2.619 (±0.002)	glass and dendritic material, core #1, Pit 2, ≈54 cm below top
IC027D90IE	7 (Pit 2)	2.550 (±0.001)	glass, top of monolith core #2, 43 cm south of core #1, Pit 2
IC037D90IE	9 (Pit 2)	2.624 (±0.003)	devitrified glass, core #2, ≈38 cm below top
IC044F90IW	3 (Pit 1)	2.538 (±0.001)	glass and dendritic material core #5 center of Pit 1 monolith, 28 cm below top
IC044H90IW	4 (Pit 1)	2.526 (±0.001)	glass and dendritic material core #5, Pit 1,≈56 cm below top
IC048D90IW	5 (Pit 1)	2.520 (±0.002)	glass, top of core #6, 76 cm NNW of Pit 1 central core
IC087A90IE	--	2.539 (±0.004)	glass, melt sample, Pit 2

the megascopically observable metal was found associated with unmelted and partially melted scrap metal, for example in the glassy boxes, some of it was apparently produced by melting the scrap metal. This interpretation is also indicated by the chemical analysis (see Table 20) which shows that some of the metal contains chrome and nickel, an indication of melted stainless steel scrap. Nodular lumps of metal are concentrated at the base of the monolith below the electrodes. The nodular lumps are aggregates of spheres and are predominantly iron with minor amounts of chromium, nickel, and non-metallic inclusions. Chemical analysis of this material is included in Table 20. The spacial association of the metal lumps with the electrodes suggests that the high temperature and reducing nature of the graphite electrodes reduced ferrous iron dissolved in the silicate melt to the metallic state in a manner analogous to the industrial production of steel using the electric furnace. The density contrast between iron and silicate probably caused the molten metallic iron to settle to the bottom of the silicate melt pool. Figure 95 shows an example of the metallic balls formed below electrodes. The third class of metallic materials includes the microscopic (<10 μm) spheres of opaque metallic material, mostly metals, found in all samples that were examined in detail. Usually the amount of opaque material is one volume percent or less (as observed in thin-section using the petrographic microscope and estimated by eye). Microchemical analysis indicates that the composition of the opaque particles is often complex (see Table 20). The most common opaque particles include (a) virtually pure metallic iron, (b) iron phosphide, probably Fe_3P, (c) complex spheres having an iron core and an iron phosphide rim, and (d) iron alloys containing small amounts of chromium and nickel, probably derived from stainless steel in the scrap metal.

5.3 Product Durability

There are currently no specific durability specifications established for ISV waste forms. The minimum expected testing requirements will be those currently established for RCRA hazardous materials landfill disposal, the Toxicity Characterization Leach Procedure (TCLP). Passing the appropriate

Table 20. Composition of Intermediate Field Test metals

Sample	Block Location	Weight Percent Fe	Al	Cr	P	Ni	Remarks
IH037J90IE	11 (Pit 2)	80.3	7.21	3.8	0.5	6.3	massive metal and traces of glass, bottom of core #2, Pit 2 monolith
IH061D90IW	8 (Pit 1)	96.9	3.5	1.5	0.2	0.9	nodular metal from the bottom center of Pit 1 monolith
IH074D90IE	18 (Pit 2)	96.1	6.1	0.4	0.2	0.8	nodular metal from the bottom of Pit 2 monolith, 1m. toward monolith center from the NE corner
IC007D90IE[a]	2 (Pit 2)	100	ND	ND	1.2	ND	opaque inclusion in glass, lower "funnel"≈1.5m. below ground surface Pit 2
IC026D90IE[a]	3 (Pit 2)	94.1 77.0	ND ND	ND ND	1.3 25.2	ND ND	opaque inclusions in glass, top of center monolith core #1 Pit 2 monolith
IC086C90IE[a]	--	90.5	ND	ND	21.3	ND	opaque inclusion in glass, melt sample, Pit 2

a. Electron-microprobe, University of Idaho, C. Knowles, analyst

ND not detected
analysis---ICP-AES, Idaho Research Center, INEL, K.Messic, analyst

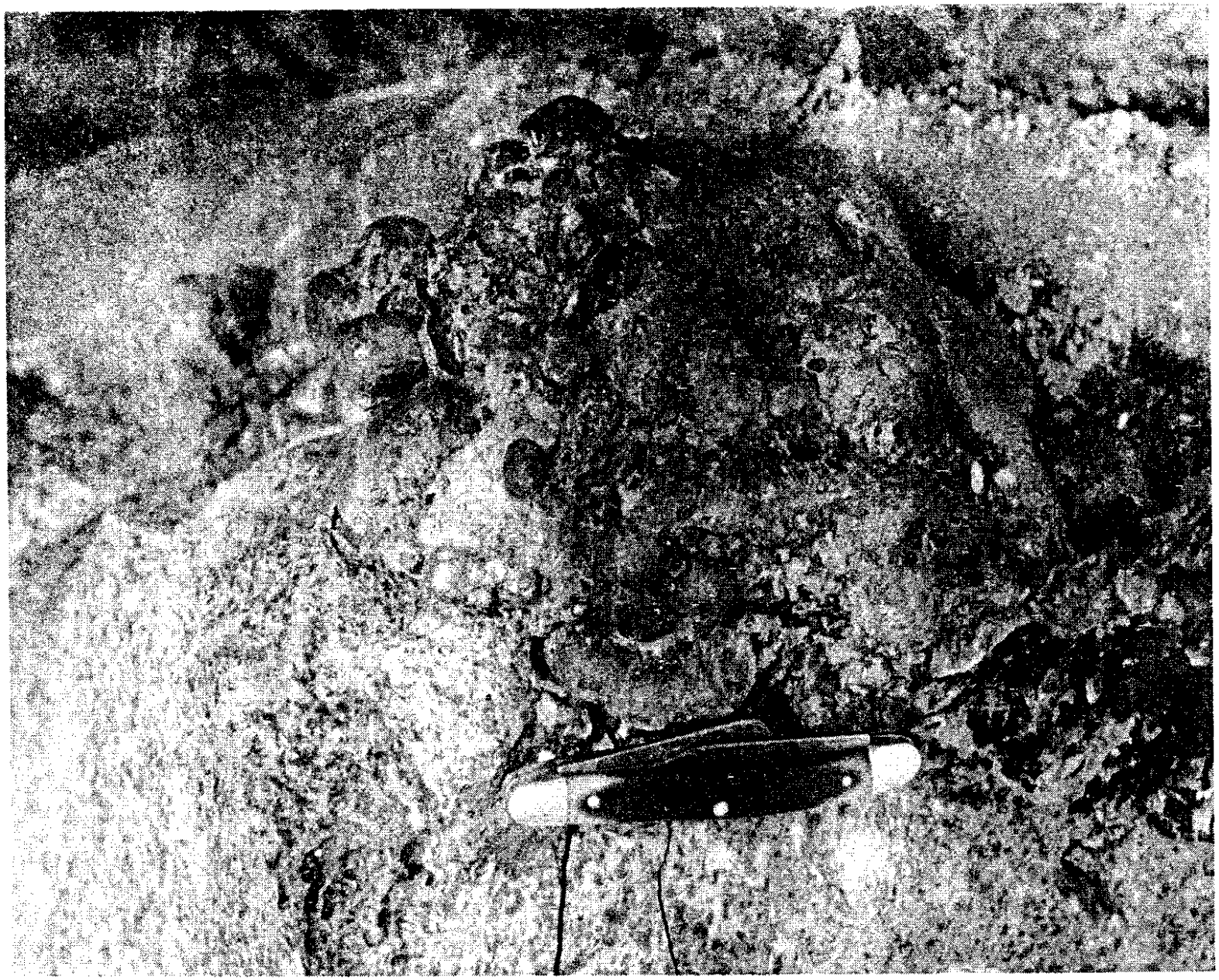

Figure 95. Metallic balls in Test Pit 2.

test only classifies the waste form as RCRA-regulated for TCLP characteristics. However, the TCLP does not: (a) address radioactive waste components, (b) provide a technical basis for assessing long-term durability, (c) provide a basis for a comparison to highly durable waste forms or natural analogs, or (d) provide an assessment of the source term release rate of the waste component for risk assessment models. To provide this information, additional durability tests must be conducted. These additional tests fall into two categories: comparative testing (comparing ISV waste forms to similar waste forms and natural analogs) and testing to determine the forward rate of waste form dissolution (k_+). Each category of durability testing is discussed in detail in the following subsections. A detailed account of the method development, procedures, results, and calculations is presented else where.[12]

For each type of durability testing, all major phases within the ISV monolith were tested, if possible. Where multiple phases could not be separated, such as when devitrification produces an intimate mixture of different small grain crystalline phases, these phase mixtures were tested as a single phase.

5.3.1 Toxicity Characteristic Leach Procedure (TCLP)

The required regulatory testing for retention of waste components is the TCLP test. Waste is hazardous by definition if it displays the characteristics of ignitability, reactivity, corrosiveness, and/or TCLP toxicity. After being formed at temperatures greater than 1300°C, the ISV waste forms are neither ignitable, reactive, nor corrosive. The TCLP test is designed to simulate the rainwater leaching process a waste would undergo if disposed of in a sanitary landfill.

The TCLP is designed to simulate rainwater leaching of certain metals from landfill wastes. The testing consists of extracting 100 g of crushed waste form with 1600 g of deionized water (DIW). One of two acetic acid

Table 21. Maximum concentrations allowed for TCLP and testing results.

	SAMPLE IDENTIFICATION NUMBER						
Element	IH064B90IE	IC066B90IE	IC068B90IE	IC069B90IE	IC052B90IW	IH053A90IW	Max. Conc. (µg/L)
Arsenic	<250	<250	<250	<250	<250	<250	5000
Barium	44.0	64.7	77.8	57.0	50.7	76.8	100000
Cadmium	26.0	<5.0	<5.0	5.9	7.3	34.1	1000
Chromium	1960	8.4	<5.0	8.2	11.1	532	5000
Lead	<150	<150	<150	<150	<150	<150	5000
Mercury	0.08	0.31	0.56	0.32	0.21	0.15	200
Selenium	<300	<300	<300	<300	<300	<300	1000
Silver	<10.0	<10.0	<10.0	<10.0	<10.0	<10.0	5000

extraction fluids (pH 2.88 ± 0.05 or pH 4.93 ± 0.05) are used and the temperature is maintained between 20 and 40°C. The duration of the TCLP is 24 hours. The extract is then analyzed by ICP or Atomic Absorption Spectrometry (AA) (Hg and Cs). The maximum concentrations allowed for inorganic elements are listed in Table 21 with the results from the samples from the two pits. No organic will be present in the glass due to the high ISV processing temperatures; therefore, the organic analysis portion of TCLP is not required.

Samples of both glass/crystalline and metal phases were taken from various parts of the waste forms. A description of these samples is presented in Table 22. There was no hazardous materials placed in the pits. However, some of the materials placed in the pits and the soil have small amounts of TCLP metals in them (i.e., barium in the soil and chromium in the stainless steels). TCLP testing was conducted to document that the ISV waste form could be disposed of in a landfill. The data summarized in Table 21 demonstrate that the samples do not exhibit hazardous characteristics of TCLP toxicity. In most cases, the TCLP results are below detection limits or 10 to 100 times lower than the maximum acceptable concentrations. The two metal samples, IH064B90IE and IH053B90IW, have concentrations 10 to 40% of the maximum acceptable concentration for chromium. This is thought to be due to the stainless steel in the samples.

5.3.2 MCC-1 and MCC-3 Testing

To provide a scientific basis for evaluating the short- and long-term durability of ISV waste forms, additional testing will be required. While the TCLP test satisfies compliance with EPA requirements for hazardous waste disposal, this test has little value in quantifying the release characteristics of the ISV waste form. The waste form produced from the ISV process is similar to a number of natural analogs, and also the waste forms evaluated for high-level nuclear waste. By comparing test results for ISV waste forms to other well documented waste forms and to natural analogs, a baseline can be established for assessing the durability of the ISV waste forms.

Table 22. Description of samples used in TCLP testing

Sample Number	Description
IH064B90IE	Metal sample taken from Pit 2 from approximately 3 feet into monolith on north side and bottom. Large magnetic metal chuck of molten metal with glass adhered to the metal in crevasses glass covers 20% of the surface.
IC066B90IE	Crystalline, aphanitic, very pale purple, porcelain-like material from Pit 2, bottom level, east side.
IC068B90IE	Bottom of Pit 2, east side of melt, darker green glass (with less than 1% of the total sample consisting of small white phase). Small gas bubbles the glass, grayish glass interfacing with green glass, also glass looks like it was next to some metal and has very small amount of rust-colored flecks.
IC069B90IE	Course texture of approximately 1/8 in. crystals that are green, gray and greenish gray in color, with irregular grain pattern. Taken from Pit 2 east side of pit at bottom of melt.
IC052B90IW	Random glass sample taken from storage boxes from Pit 1.
IH053A90IW	Random metal sample from Pit 1 pulled from storage box. Metal was molten at one time during the test. Sample was magnetic and has some glass fixed to them. They are dull, metallic-gray in color.

To allow for direct comparison of waste forms, the test method, leachate, temperature, and surface area/volume (S/V) used in testing the ISV waste form should be the same as those used in testing glass waste forms chosen for high-level nuclear waste. The differences in application (repository conditions such as groundwater saturation and temperature) and the nature of the waste form (multiphase ceramic-glass versus single-phase glass) make such comparisons difficult. Most high-level nuclear waste glasses have been tested at 90°C. The MCC-1 and MCC-3 test methods were originally developed, and the current procedures written, for application to high-level waste repositories in deep geological environments. The primary applications of the MCC tests will be to compare ISV waste forms and will have limited utility for mass transport analysis. By conducting the MCC-1 and MCC-3 leach testing at 90°C, the results can be compared to the existing large data base of leaching data on the high-level glasses. The MCC tests will be used because of the large data base of data glassy materials.

To allow comparison of leach tests results from waste forms with different compositions, results are given in terms of normalized elemental mass release for the MCC-1 and MCC-3 tests and normalized concentration for the modified MCC-3 test.

The MCC-1 static leach test[13] measures the elemental mass loss of a glass sample as a function of time. For this test, a glass monolith is suspended within a sealed Teflon™ container. The surface-area-to-volume ratio (surface area of sample/volume of leachant, S/V) of 10 m^{-1} was used. The leachant was deionized water (DIW). The sealed containers were maintained at 90°C for 7, 14, 28, and/or 90 days. The test results are based on leachate elemental analysis from which the total concentrations of materials leached from the sample are determined. The most commonly used test parameters are an S/V of 10 m^{-1} in DIW at 90°C for 28 days. These were used for ISV testing to allow for comparison with the largest amount of data. One drawback to this type of test is that the MCC-1 procedure requires a small monolith of sample. Inhomogeneities in the test samples, such as varying amounts of exposed crystalline phases or metals, may result in inconsistent results.

5.3.3 MCC-3

The MCC-3 agitated powder leach test[14] is similar to the MCC-1 test procedure, with two exceptions: the glass is in a powdered form, and glass powder and leachant are agitated by rotating the Teflon container in which the sample is placed. The elemental leachate concentrations from MCC-3 tests are estimated to be representative of longer-term (more saturated leachates) extrapolation of MCC-1 test results. This objective is achieved more rapidly in the MCC-3 test because higher S/V ratios are used than those used for the MCC-1 tests. For evaluation of ISV waste forms, tests were conducted with an S/V of 1000 m^{-1} in DIW at 90°C for 28 days (a large amount of 7 to 90 day data also exist). Because of the higher S/V used in the MCC-3 testing compared to that used for MCC-1 testing (2000 m^{-1} and 10 m^{-1}, respectively), the leachants in the MCC-3 tests became saturated much sooner than the leachants in the MCC-1 tests. This saturation slows the dissolution process. Therefore, direct comparison of normalized release values from the MCC-1 and MCC-3 tests is not appropriate. Because a powdered sample is used for the MCC-3 tests, combinations of glass and devitrified phases may be tested together. At this time, a modified MCC-3 test called the Product Consistency test (PCT)[15] is now the standard test MCC-3 method being used.

Previous testing of samples from the ISV laboratory scale test ES-4 had shown that allowing leachates to cool to room temperature prior to filtering and acidification may result in the precipitation of secondary phases in the leachates. To prevent this, the IFT samples were treated in a different manner as follows: the container was removed from the leaching oven and weighed, then placed in a pre-heated metal block machined to fit the knurled leach containers. Immediately, 10 mL of leachate (each) was filtered, using a 0.45 μm filter, and placed in three polyethylene vials. The pH was then measured of the remaining leachate in the container. The temperature was measured immediately after pH measurement and the temperature was found to be 75 ±5°C. The pH was also remeasured at room temperature. As before, two of the leachates were acidified, one for inductively coupled plasma atomic emission spectroscopy (ICP-AES) analysis and another for storage. The unacidified sample was analyzed by ion chromatography (IC).

5.3.4 MCC-1 and MCC-3 test Matrix

A series of closed-system, isothermal experiments were designed to elucidate the dissolution behavior, alteration phase formation, and elemental solubilities for the INEL ISV glasses. The test matrix is given in Table 23. Three different surface area-to-volume (S/V) ratios were investigated with overlapping (S/V)·time as illustrated in Figure 96. This range was selected so that sufficient glass reaction occurs to saturate the leachate with respect to the major elements of concern. The 10 m^{-1} experiments were performed with the MCC-1 method and the higher S/V tests used the modified MCC-3 test, PCT. The test matrix shown in Table 23 was performed in its entirety for samples IC007C90IE, IC027B90IE, IC038C90IE, and IC048B90IW. Samples IC038B90IE, IC038D90IE, and IC048C90IW were tested in triplicate for 28-day duration using both MCC-1 and PCT test methods. A short description of each of these samples is found in Table 24. The elemental and $Fe^{+2}/\Sigma Fe$ for these samples (as analyzed at PNL) are reported in Table 25.

At the present time, only experiments at 90°C in deionized water have been conducted. Although 90°C is far above the expected temperature range where the ISV waste form may be contacted by water, the elevated temperature permits the more rapid formation of crystalline alteration products that may be identified by surface analysis techniques and gives a greater extent of alteration in a short period of time. Both of these factors simplify comparison of the experimental results and model with model predictions. It has also been recently demonstrated that the basic mechanism of the reaction of a complex waste glass with water does not change up to 200°C.[16] Also, 90°C has been a *de facto* standard for the majority of dissolution experiments that have been conducted with nuclear waste glasses. Comparisons of the performance of INEL ISV glasses with this extensive database are facilitated by using the same conditions. However, low temperature experiments should be planned in future work to validate the model at lower temperatures.

The results from both MCC-1 and PCT tests with the IFT samples are shown in Figures 97 and 98. Only results from 7 & 28 day duration experiments are available at this time. However, the data do show differences

Table 23. Static testing for ISV product evaluation

				No. tests				
Material	test	S/V, m^{-1}	Temperature	7d	14d	28d	56d	91d
ISV Glass	MCC-1	10	90°C	1	3	1	1	3
Blank				1	1	1	1	1
ISV Glass	PCT	100	90°C	3	1	3	1	3
	PCT	1000	90°C	3	1	3	1	3
Blank				1	1	1	1	1

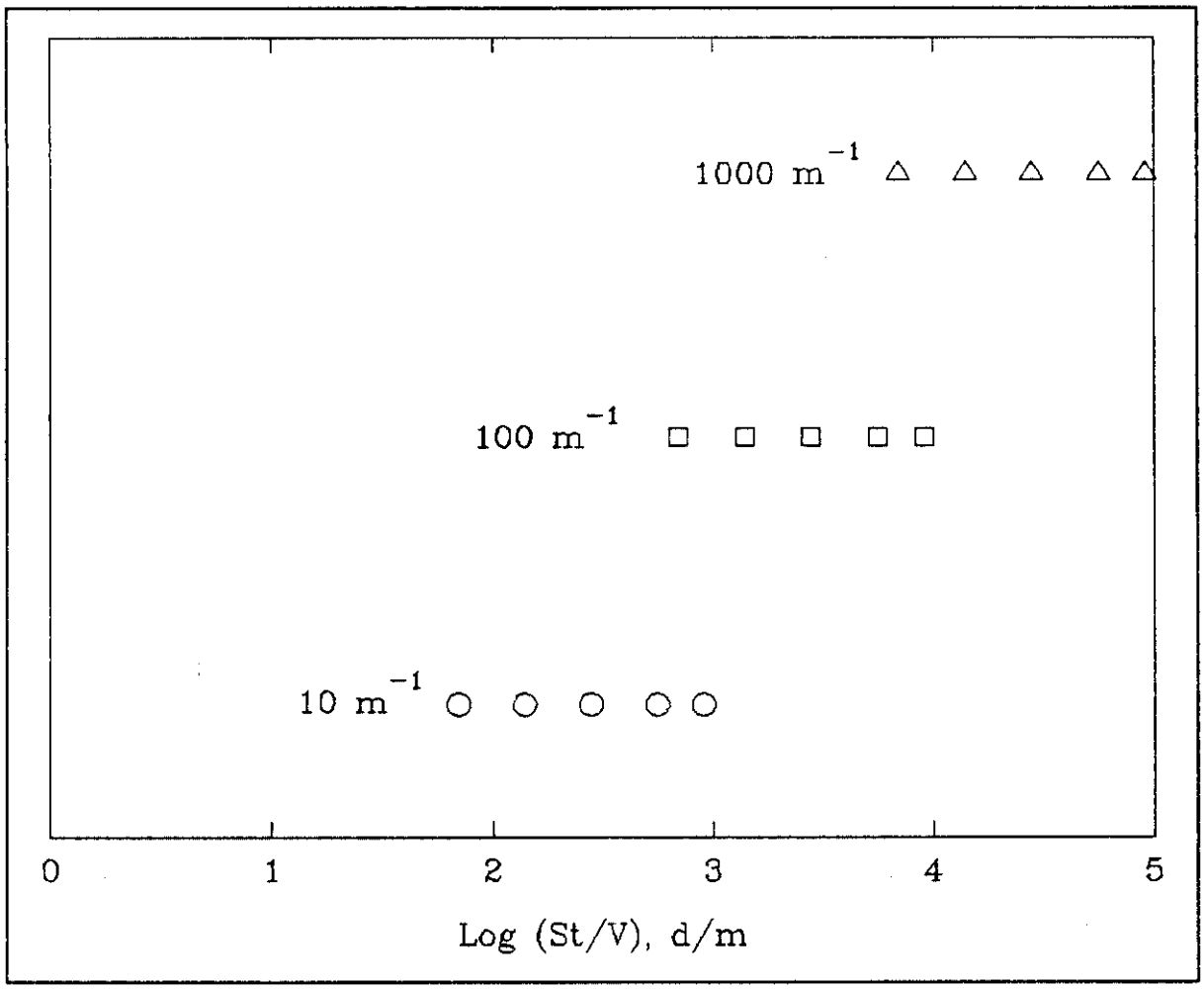

Figure 96. Range of glass surface area/leachate volume times time (ST/V) values used to investigate the static dissolution behavior of INEL ISV glasses.

Table 24. Description of samples used in durability testing

Sample Number	Description
IC007C90IE	ISV Pit 2 Glass sample from lower "funnel" taken from east side. Very dark green glass with 3% of volume being gas bubbles <2 mm. The glass interfaces with two different substances (a) a light gray hard substance resembling dirt and (b) small undissolved pieces of rocks.
IC027B90IE	Core Pit 2, hole two taken from a larger piece of core material located at bottom of core. Neutral gray glass that is not see-through, makes up 50% of the composition. Large crystals are mixed in with the neutral gray glass. Crystals are 3 mm to 5 mm in width; they are slightly darker gray/green glass covering 50% of the surface area.
IC038B90IE	Pit 2, third hole, 18" NE of hole 1, drilled to 2'-3 1/4", 5 cm to 13.5 cm down from top of core. The top is dark-green shinny glass with gas bubbles of different sizes and shapes. Top of green glass is where gas bubbles have come to the surface. A 90% gas interface with bubbles. Bottom of sample has gas bubbles 1 cm x 1.5 cm and smaller covering 5% of the surface area. Medium gray crystals mixed in with the green glass, covers approximately 2% of the surface, ranges in size from 1 cm to 1.5 cm. The bottom of the sample is optic & medium-grayish green.
IC038C90IE	Pit 2, third hole, 18" NE of hole one; top of sample is optic grayish-green glass. Medium gray crystals are mixed with the green glass (approx 2% of the surface, ranging in size from 1 cm to 1.5 cm). Gas bubbles are 1.3 cm x 2 cm in diameter and make up 25% of surface. Three metal beads are located near the center; they are magnetic and are <1 mm in diameter.
IC038D90IE	Pit 2, third hole, 18" NE of hole one, 1'-6" from top of core. Neutral gray, medium gray, and green crystals, 5 mm to 1 cm in size. Gas bubbles make up <1% of surface, size <1 mm.
IC048B90IW	Pit 1 core 6, depth 1'-10" (core depth), 1'- 4" recovered. North-northwest of center core #5. Glassy phase, gas bubbles cover 30% with size of 1 cm x 2 cm to 1 mm. Medium gray crystals mixed in with the glass (approximately 25% of the surface, <1 mm in diameter).
IC048C90IW	Pit 1 core 6, 12" from top of core. Glassy phase with gray crystals 1 mm in diameter cover 50% of the surface area. Gas bubbles are <1 mm in diameter and make up <1% of the surface mass.

Table 25. Bulk chemical analysis of IFT samples

Oxide	IC007C90IE	IC027B90IE	IC038B90IE	IC038C90IE	IC038D90IE	IC048B90IW	IC048C90IW
Ag_2O	0.00	0.00	0.00	0.00	0.00	0.00	0.00
Al_2O_3	11.30	12.20	12.00	12.00	11.90	12.50	12.50
BaO	0.40	0.09	0.09	0.09	0.09	0.09	0.09
CaO	11.50	10.70	10.90	10.50	10.70	8.77	8.48
Cr_2O_3	0.00	0.26	0.27	0.26	0.26	0.13	0.14
FeO	3.68	3.94	3.36	3.96	3.90	4.42	4.21
Fe_2O_3	0.47	0.17	0.79	0.22	0.24	0.19	0.39
K_2O	2.90	3.20	3.10	2.90	3.00	3.10	3.20
MgO	2.70	2.60	2.70	2.70	2.60	2.60	2.70
MnO	0.08	0.19	0.19	0.19	0.19	0.13	0.13
Na_2O	2.15	2.30	2.40	2.70	3.18	2.00	2.70
SeO_2	0.00	0.00	0.00	0.00	0.00	0.00	0.00
SiO_2	62.20	64.30	63.60	64.40	63.10	65.60	65.30
SrO	0.03	0.03	0.03	0.03	0.03	0.03	0.03
TiO_2	0.54	0.58	0.58	0.57	0.58	0.61	0.62
TOTAL	97.95	100.56	100.01	100.52	99.77	100.17	87.99
Fe^{2+}/Fe	0.897	0.963	0.827	0.952	0.947	0.963	0.924

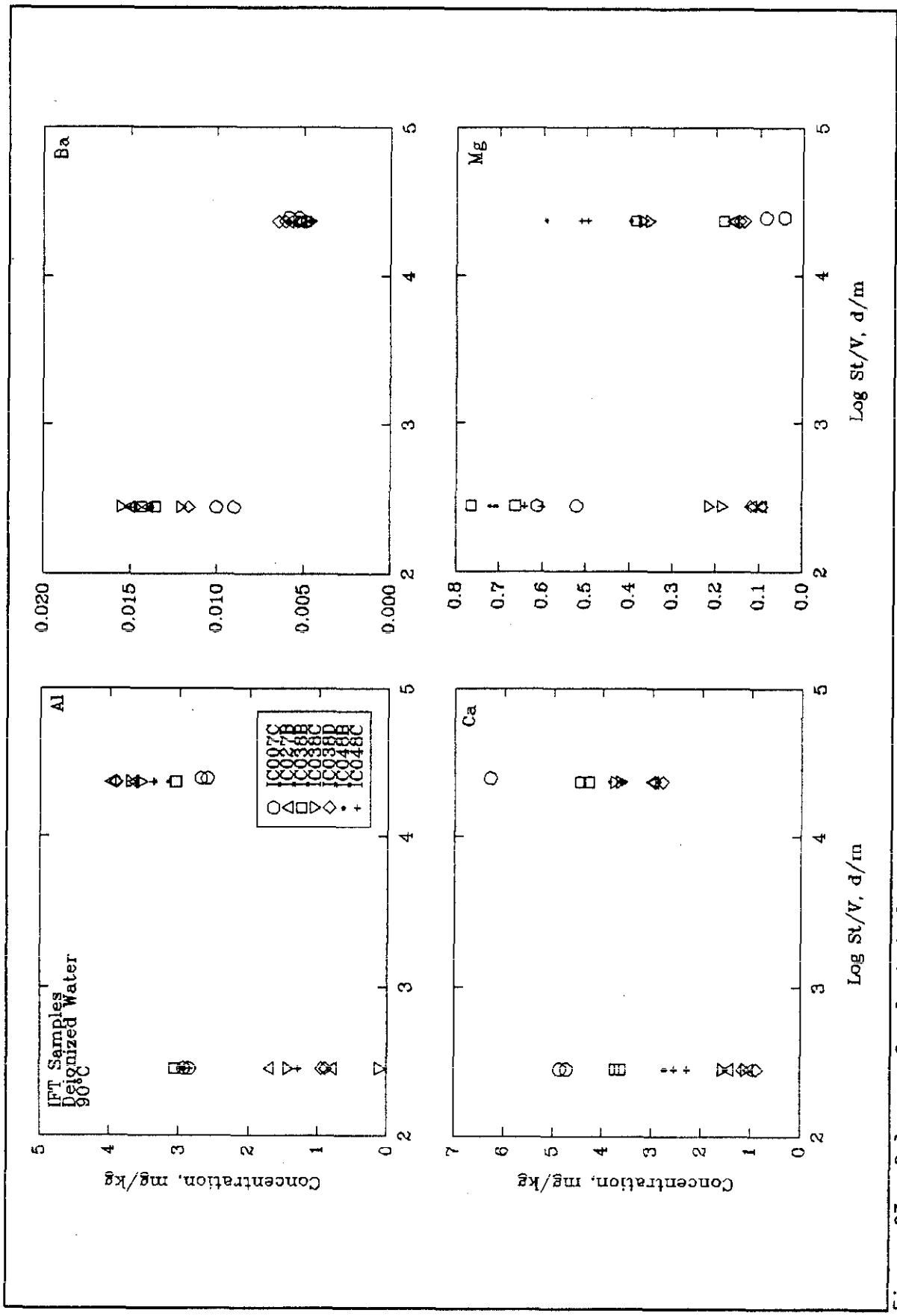

Figure 97. Release of selected elements from IFT samples in MCC-1 and modified PCT tests.

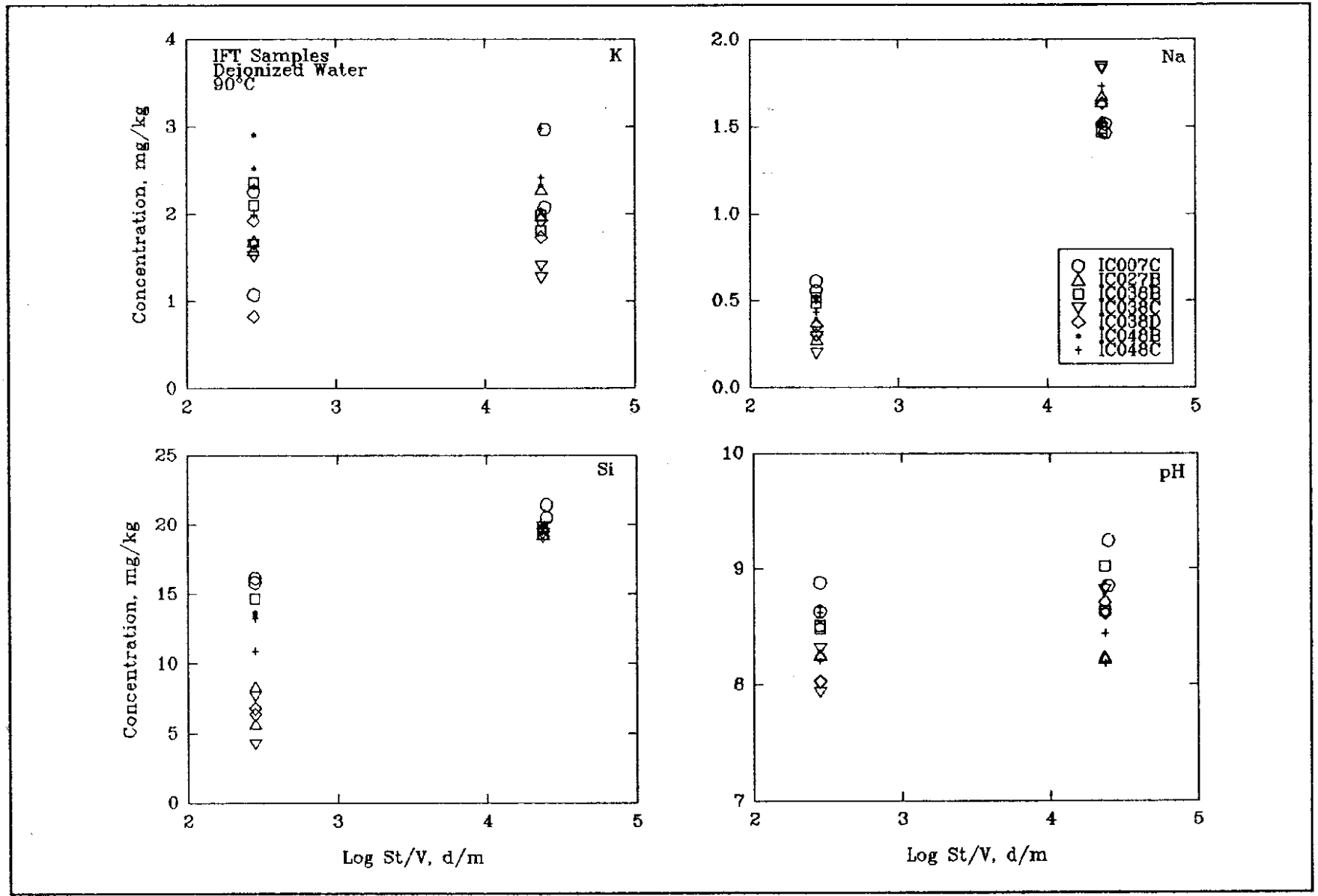

Figure 98. Release of selected elements and pH of IFT samples in MCC-1 and modified PCT tests.

among the field samples that appear to correspond to the degree of crystallinity in the samples. While not statistically differential, the trend appears to be consistent. Sample IC038C90IE appeared to the eye to be completely devitrified and this sample shows consistently lower releases for Ca, Mg, Al, and Si compared with sample IC007C90IE that analyzed X-ray amorphous. The releases of Ca and Mg are as much as 2 to 3 times smaller for the other devitrified samples. Because most of the ISV monolith is devitrified, these lower release rates for the devitrified phase of the ISV waste form may result in a lower source term for heath-based risk assessments.

Table 26 and Figure 99 compare MCC-1 and MCC-3 results for the IFT ISV waste form with typical high-level nuclear waste glasses and natural analogs. The IFT waste form is comparable to obsidian and granite, and 4 to 10 times more durable (based on MCC-1 testing) than typical high-level nuclear waste glasses.

Table 26. Comparison of MCC-1 data for IFT, other waste forms and Natural Analogs

SAMPLE	Normalized Concentration g/m^2
IC07C90IE	5.50
IC027B90IE	2.33
IC038B90IE	4.93
IC038C90IE	1.97
IC038D90IE	2.22
IC048B90IW	4.43
IC048C90IW	3.95
IFT AVERAGE	3.62
High Level Waste Class	16
ISV Hanford Soil	4
Pyrex	1.3
Obsidian	1.2
Granite	0.98

5.3.5 Intrinsic Rates of Dissolution

The fastest rate at which a glass/ceramic will dissolve is the forward rate of dissolution (k_+). This glass parameter has the most technical

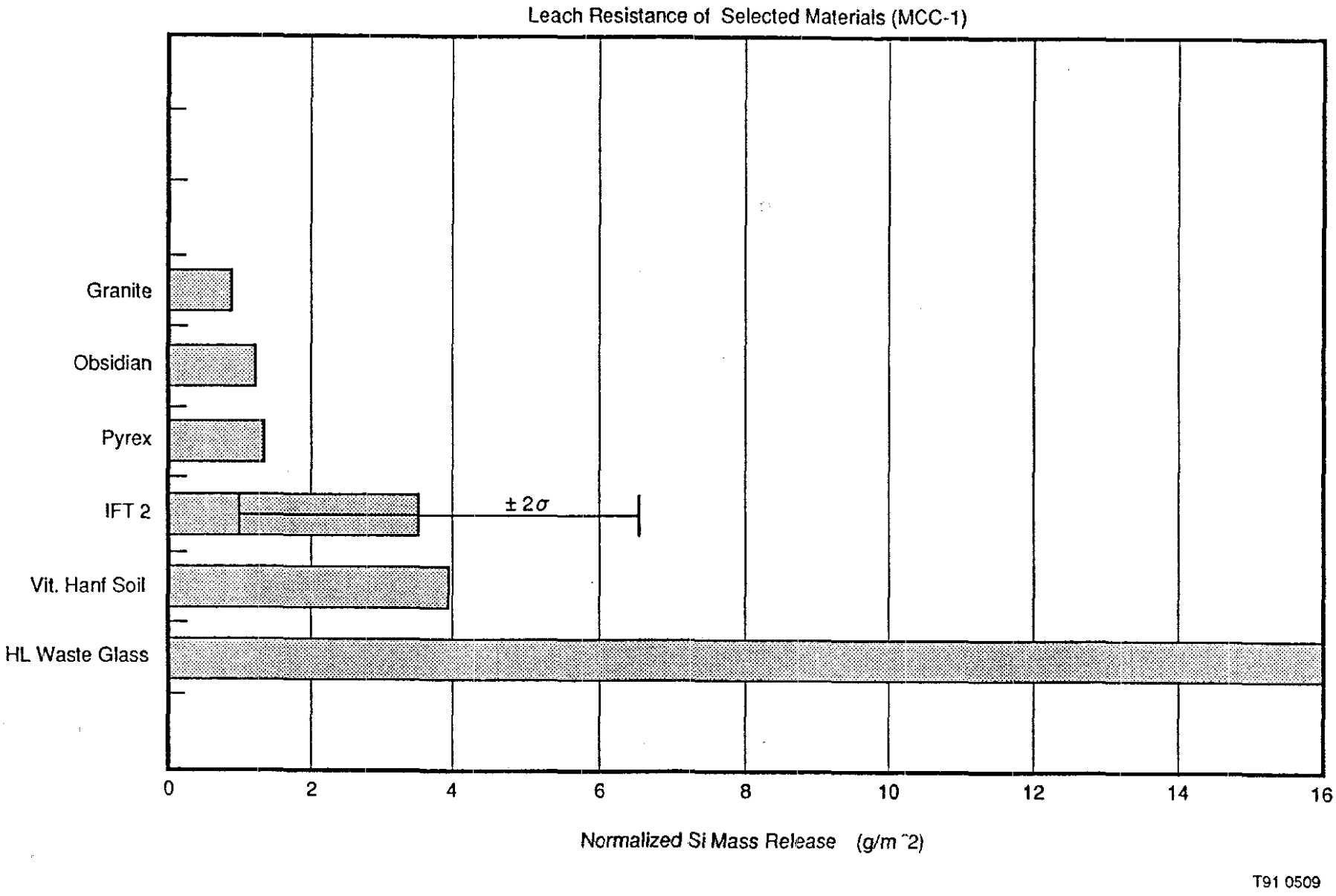

Figure 99. Comparison of durability of ISV samples based on MCC-1.[17]

relevance when evaluating and predicting the dissolution (durability) behavior of the glass (see Reference 9).

To understand the forward rate, it is beneficial to discuss the three different regimes typically observed in glass dissolution: (a) the period in which the glass first contacts a leachate and the glass dissolution rate is uninhibited by any solubility effects, (b) a transient regime where the increasing concentrations of dissolved glass components in the leachate slows the dissolution rate through solubility effects, and (c) a steady-state regime in which the dissolution rate is constant because alteration processes (saturation) have reached a steady-state. Typical release data can be plotted as the elemental concentration in the leachate versus (S/V) · time, which shows these different regimes. This behavior can be understood by considering what happens at the beginning of glass dissolution (no saturation effects) and under conditions where the leachate has high concentrations (near saturation) of dissolved glass or groundwater components.

At both ends of the dissolution curve, there are linear portions at which the dissolution rate is linear. At early times, the glass matrix dissolves with the forward dissolution rate (k_+) because there is nothing in solution or on the surface of the glass to impede the dissolution process. The forward dissolution rate is the slope of the linear portion of the curve at low saturation smaller values of (S/V) · t. As the leachate becomes saturated, the dissolution rate of the glass decreases. These are the slower rates observed in a static test, such as MCC-1 and MCC-3.

Low values of (S/V) · t (and the resulting solution concentrations) are analogous to the ambient (low solution saturation) conditions expected for the ISV waste form as unsaturated surface water percolates past the waste form. Data obtained over this range of (S/V) · t products can be used to compare the relative chemical durability behavior of glasses in a way that is more relevant than a single static test condition which may be in the transient regime. Because the ISV waste form will be in a near-surface environment where water flow rates could be postulated to a relatively high, saturation of the water may not occur and the forward rate of dissolution will limit the

release rate. In addition, because k_+ represents the absolute maximum dissolution rate, a conservative source term can be derived from an accurate determination of this parameter of the ISV products. This source term can be used in health-based risk assessment modeling. The k_+ is also required for predictive modeling of waste form dissolution as a function of waste form composition and solution chemistry.[18,19]

Reaction rates, such as the forward rate, are known to have strong temperature dependence. Because of the high durability of waste forms, such as those produced from ISV, it may not be possible to conduct leach testing at ambient ground temperatures ($\leq$ 20°C) and have concentrations in the leachate above analytical detection limits. Conducting leach testing at higher temperatures ($\approx$40 to 90°C) will provide adequate leachate concentrations. If conducted at three or more temperatures, the forward rate's Arrhenius activation energy can be determined, which will allow the temperature dependence to be established. Using this temperature dependence, the forward rate at ambient storage conditions can be calculated.

The forward rate of dissolution has been measured using a number of techniques.[20,21,22] One technique that is promising for k_+ measurements is the pH stat method. This method has significant advantages over other techniques such as Soxhlet extraction, MCC-1 tests, or MCC-3 tests because the solution pH is held constant over the course of the test and a large quantity of data is generated in a short time.

Extensive Soxhlet extraction data have been obtained on nuclear waste glasses at temperatures ranging from 50 to 200°C.[23,24] Because the Soxhlet extractor provides a continuous flux of distilled water over the sample, dilute conditions are maintained throughout the duration of the test as required to accurately measure k_+. The primary disadvantage of the Soxhlet device is the difficulty in applying reduced pressures to run at temperatures lower than 100°C and the difficulty in measuring and controlling the pH of the distillate.

A modified Soxhlet extraction apparatus was developed for these measurements. All wetted parts of the reactor were made from Teflon® PTFE to minimize Si or Na contamination of the extract. Approximately 1 g of -100 +200 mesh glass was placed in the overflow cell and the Soxhlet extractor assembled. A 5 mL sample of the extract was obtained approximately every 24 hours using a syringe. The sample was immediately acidified to 1% HNO_3. The 5 mL sample was replaced with 5 mL deionized water to maintain a constant volume of water. For the current series of tests, run durations were limited to 7 days.

The pH stat method[25] has significant advantages over other dissolution rate measurement methods because the solution pH is held constant over the course of the test automatically by adding small quantities of a strong acid or base to the solution. A high density of data is thereby generated in a short time. For simple alkali silicate glasses, the rate of glass reaction can be precisely determined from pH stat alone by relating the one-to-one correspondence between alkali and hydronium ion exchange to the reaction rate. Unfortunately, the utility of pH stat is limited with more complex glasses because precipitation of highly insoluble secondary phases (such as gibbsite and ferrihydrite) may consume or release OH, making interpretation of the pH stat data extremely difficult, if not impossible. In addition, the measurements are restricted to near-neutral pH where the sensitivity to changes in solution pH from glass dissolution are maximized.

To overcome these limitations with the pH stat technique, the method was modified. The time rate-of-change in the concentration of a soluble glass component, such as Na, was monitored along with the H_3O^+ consumption, and an ion-selective electrode was used to monitor the selected cation concentration. Commercially available electrodes are capable of measuring M^+ concentrations as low as 10^{-6} M and will tolerate prolonged exposure to temperatures between 70 and 80°C.

Figure 100 shows typical results from the Soxhlet tests for IC007C90IE IFT glasses. Because of the scatter in the results for several elements and the lack of clear trends for other elements (such as K), dissolution rates for the samples were calculated from least squares fits to Na and Si only. The results from these fits for all of the INEL ISV glasses tested to date are given in Table 27. Note that these are the dissolution rates at 100°C.

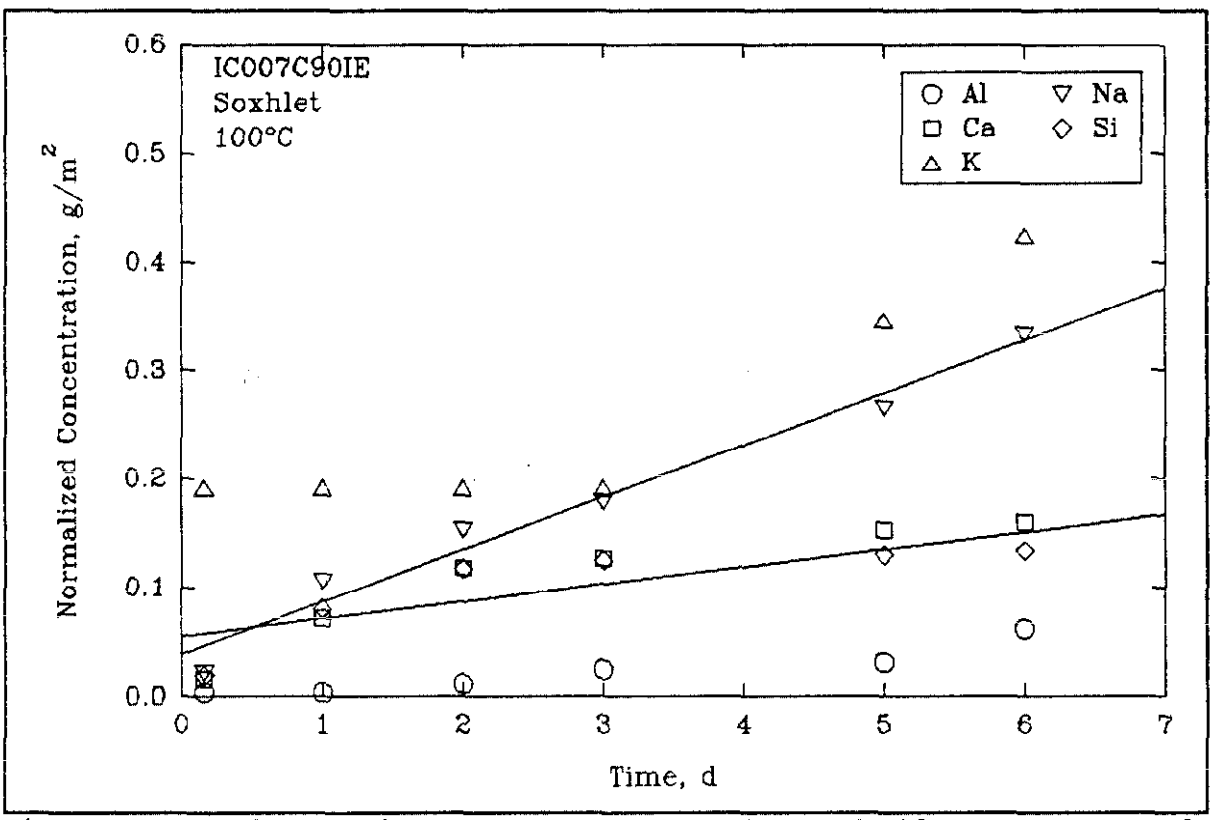

Figure 100. Selected element concentrations during Soxhlet extraction of IFT sample IC007C90IE at 100°C.

Figure 101 summarizes the results from pH stat/ISE experiments conducted with IFT sample IC007C90IE. The dissolution rates are for the ISV glasses are approximately one tenth compared to the reference waste glass at 80°C. Because of the small dissolution rate and low Na content of the ISV glasses, absolute concentrations of Na were nearly two orders of magnitude smaller than for the waste glass and near the detection limit for the ISE. This results in a small signal to noise ratio as is evident in the data in Figure 101. Accuracy and reproducibility are also poor because at Na^+ concentrations near 10^{-3} M, the response of the ISE is poor and non-linear with respect to Na^+

Table 27. Dissolution rates measured for INEL ISV glass samples by Soxhlet extraction at 100°C

Sample ID	Dissolution rate [g/(m^2·d)]	
	Na	Si
IC007C90IE	0.048 ± 0.004	0.016 ± 0.006
IC038B90IE	0.024 ± 0.002	0.004 ± 0.003
IC038C90IE	0.027 ± 0.001	0.014 ± 0.004
IC048B90IW	0.035 ± 0.002	0.002 ± 0.001

concentration. Although several attempts were made to adjust S/V ratios and reduce interferences from competing cations (such as NH_4^+ leakage from the pH and ion-selective electrodes), consistently satisfactory results could not be obtained with the technique. Consequently, we conclude that an alternate experimental method, such as a single-pass flow-through cell is needed to accurately measure k_+ for the INEL ISV glasses. Design and construction of such an apparatus is in progress. Because the release at 80°C was near the detection limit, testing at lower temperatures was not possible and the activation energy could not be determined. Determination of k_+ down to the ambient temperature is expected for final disposal of the ISV waste form

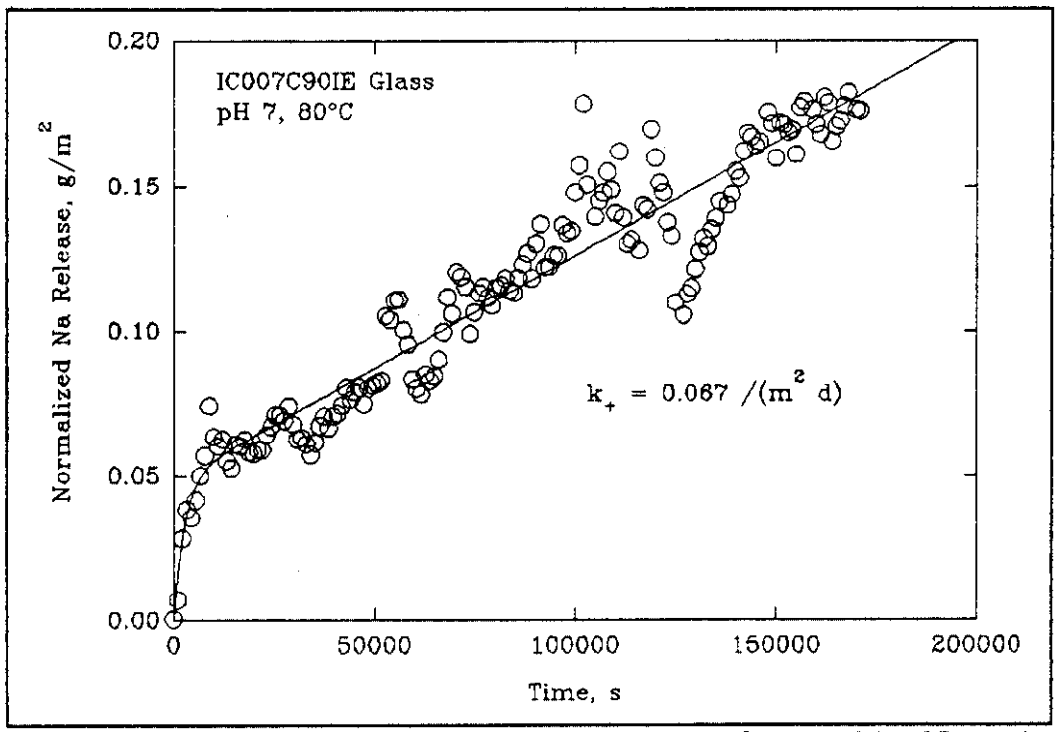

Figure 101. Dissolution behavior of IFT sample IC007C90IE at in situ pH 7 and 80°C.

(approximately 20°C). Because k_+ will decrease as the temperature decreases, the k_+ at 80°C can be used as a conservative value until the activation energy can be determined. Based on these results, a preliminary evaluation was also performed to evaluate the effects (if any) that devitrification of the IFT samples may have on the solution chemistry. Although the results are still preliminary, the static tests indicate that the devitrified samples have lower releases of several key elements including Ca, Mg, Al, and Si. This difference may be due to smaller dissolution rates for the glass matrix, the crystalline phase(s), or both. The smaller release could also be due to a smaller thermodynamic driving force for the irreversible dissolution of the crystalline phase(s) in the devitrified samples. Although dissolution rates of diopside (Ca, Mg, SiO_2) have been reported,[26,27] reliable kinetic data are not available for the pyroxene solid solution identified in the IFT samples. However, we have used the EQ3/6 code[28] to analyze the thermodynamics for the irreversible dissolution of the pure end member phases, diopside and hedenbergite. Diopside and hedenbergeite are very similar in composition, structure, and behavior to the augite found in the IFT waste forms and are suitable models. In performing this calculation, the analyzed bulk composition for sample *IC038D90IE* was used, assuming that the entire Mg inventory is partitioned to the end member diopside and the remaining elements (Ca, Fe, Si, and O) partition according to their stoichiometric amounts in both the diopside and hedenbergite phases. This procedure left a residual glass completely depleted in Mg and partially depleted in Ca and Fe. The data show a large driving force for the dissolution of both end-member phases at reaction progress values less than 10^{-3} mol/kg. Consequently, the smaller release rates observed in the static tests with the IFT samples cannot be attributed to smaller chemical affinities associated with the dissolution of the crystalline phases. Smaller dissolution rate constants appear to be the most likely cause for the smaller releases observed with the devitrified IFT samples.

In all of the above calculations, we have fixed the O_2 and CO_2 gas fugacities to correspond with the conditions of the dissolution experiments, i.e., essentially open to the atmosphere. Because of the oxidizing conditions and unlimited availability of carbonate, the release of many of the hazardous elements are predicted to be congruent with the dissolution rate of the glass (i.e., Se, As, Pu). However, water contacting the interior of ISV product,

where the hazardous elements are immobilized, must migrate through a series of cracks or channels that may not be open to direct contact with the atmosphere. We have used the EQ3/6 code to simulate this effect by allowing air-equilibrated deionized water to react with IFT sample IC007C90IE under closed-system conditions, i.e., mass balance constraints are allowed to determine the fO_2 and fCO_2. Under these conditions, those elements with multiple oxidation states will be reduced and, for several key elements such as Se and Pu, the calculated solubilities will be several orders of magnitude smaller. These elements would be sequestered in the alteration layers on the glass surface and, therefore, released at a rate less than the matrix dissolution rate. Accounting for the chemical interaction of the ISV product with water under closed-system conditions could provide smaller predicted release rates than by matrix dissolution alone.

In summary, a series of experiments was performed to determine the dissolution behavior of samples produced from the ISV processing of typical soils from the INEL Subsurface Disposal Area. Preliminary results from intrinsic rate constant measurements using pH stat/ISE and Soxhlet extraction methods showed that the dissolution rates of the ISV samples range from 0.01 to 0.06 $g/(m^2 \cdot d)$ at 90°C and pH 7. These values are 10 to 100 times smaller than measured for a typical borosilicate nuclear waste glass (see Reference 24). Devitrified samples from an intermediate-scale field test showed a possible trend to have slower dissolution behavior then amorphous samples of equivalent bulk composition. Additional thermodynamic and kinetic data on the clino-pyroxene minerals will be required to adequately explain the differences in the dissolution behavior of the partially-devitrified ISV products. Solids characterization of the ISV products showed that the ISV melts are reducing, resulting in Fe^{2+}/Fe ratios > 90%. Under equivalent closed-system conditions, as might occur during the slow migration of water through cracks in the solid mass, the reaction of the ISV glass with water reduces the redox potential to the lower stability limit of water. Under these conditions, several redox sensitive elements such as Se and Pu are expected to be sequestered in an alteration layer on the glass surface resulting in a smaller predicted release rate than calculated from the matrix dissolution rate alone.

5.4 Other Issues and Observations

Several observations that provide the basis for qualitative estimates of thermal gradients (edge effects) and of the probability of underground fires in the simulated waste materials in contact with the ISV melts are described below.

5.4.1 Alteration of Materials and Thermal Gradients

The simulated waste materials included wood, paper, cloth, sludge, scrap metal, and concrete/scrap glass contained within covered but unsealed steel cans. Cardboard boxes contained scrap metal or concrete/scrap glass. In general, cans containing concrete/scrap glass, simulated sludge (i.e., calcium silicate), and scrap metal showed no visible effects that could be attributed to the thermal effects of the melt. All of these materials appeared to be unaffected even when in physical contact with the melt. The cans of sludge were dry when within about 25 cm (10 in.) of glass, otherwise, the cans of sludge had minor (<25% interior area) surface rust on can interiors, presumably corrosion generated by the very basic solutions produced by wet sludge and not by thermal effects from the melt. Combustible materials included paper, cloth, cardboard, and wood.

In general, these combustible materials showed significant effects of thermal alteration. The alteration ranged from no effect to complete carbonization. Grey-white ash, indicating oxygen-rich combustion, was observed in only two cans, both within 0.76 to 0.91 m (≈2.5 to 3 ft) of a surface in contact with air. These cans also contained carbonized material, which indicates the environment became oxygen deficient before combustion was complete. The degree of alteration is directly related to distance from the melt and, thus, temperature. In general, in both pits visible alteration effects were observable up to about 46 cm (18 in.) maximum from the melt, at which distance only a very slight darkening of the combustible materials was evident. At distances progressively closer to the melt, the combustible wastes were increasingly carbonized. Black materials coated the insides and lids of the cans and the adjacent soil. The black coating on the cans and soil is presumably the carbonized remains of organic tars or similar substances driven from the combustible waste during the heating process.

Figure 102 shows typical carbonization of a paper-filled can when located within about 30 cm (12 in.) of the melt. Note the black deposits on the can lid in the figure. Often, carbonized paper and cloth are in direct contact with the glass which is indicative of an oxygen deficient environment. The effects in Test Pit 1 are similar to Test Pit 2. Alteration effects are often restricted to distances much less than the 46 cm (18 in.) noted above. For example, molten steel sheet metal was observed within about 5 cm (2 in.) of unaltered cardboard (see Figure 103). Many other examples were also observed. The extent of alteration, and therefore the thermal gradient, is probably a function of both the temperature and mass of nearby melt and is highly variable from point to point around the pits. The above observations indicate the probability of underground fires is very low provided that there are no oxygen sources.

The soil adjacent (less than approximately 10 cm [4 in.]) to glass usually shows thermal alteration effects as well. Such soil within about 10 cm (4 in.) of the ground surface is salmon colored, but becomes bleached grey-hite at greater distances from ground surface. A very dark brown soil zone is found directly outside the grey-white region. Soils outside the dark brown zone appeared to be unchanged.

Figure 102. Carbonization of paper outside of vitrification zone for Test Pit 2.

Figure 103. Edge effect showing molten steel near cardboard in Test Pit 2.

6. TRACER STUDY

6.1 TRACER BACKGROUND

During preparation of the test pits, rare-earth tracer elements were added to selected waste containers. The added tracers were oxides of dysprosium, terbium, and ytterbium (Dy_2O_3, Tb_4O_7, Yb_2O_3). These tracers were added with the intent to use them as simulants of PuO_2 (see Reference 29). Rare-earth tracers (i.e., lanthanide series elements) have been previously used as simulants for Pu (an actinide).[30, 31]

The retention of elements or compounds in the glass, or alternatively the transport of materials to and within the off-gas system, is governed by a number of thermodynamic and/or transport properties. Thermodynamic properties such as boiling points, equilibrium solubilities in the various phases, and redox potentials are significant parameters which affect the retention of actinide components. Additionally there are transport mechanisms which can result in material transport from the melt and into the off-gas system; these include direct entrainment in gases released from the melt and steam transport, as well as ejection of material from the surface of the melt from collapsing bubbles.

The relative amount of retention of elements within the ISV melt is generally defined by the decontamination factor (DF). The DF of an element or compound is defined as m_i/m_e, where m_i is the initial input mass of contaminant in the control volume (soil) per unit time and m_e is the exit mass from the control volume per unit time. DFs can be presented to show what the relative retention of an element is in the melt relative to escape to the off-gas (i.e., soil-to-off-gas DF). A total DF for the ISV processing can be calculated which takes into account the additional retention of elements within the off-gas processing system.

Data from previous ISV testing have been published (see Reference 2) which indicate that Pu is primarily retained within the melt during ISV

processing. This is consistent with thermodynamic considerations, as well as previous data for Pu solubility in basaltic rock.[32] Data from a PNL pilot-scale radioactive test indicate a decontamination factor from the soil to off-gas of 4.5×10^3 (see Reference 2). An additional observation made during previous testing is the apparent greater retention of elements within the melt if they are initially buried at greater depth.

As indicated above, the retention of an element within the ISV melt is dependent on multiple factors. Transport factors such as direct entrainment of elements into melt gases, are of particular concern for ISV processing of buried waste, since these mechanisms offer the potential to increase the amount of released material in spite of equilibrium thermodynamic properties which may favor retention in the melt. The effect, if any, of these additional factors must be determined for the case of ISV buried waste processing.

The use of tracers in these Intermediate Field Tests provides some qualitative indication of potential for element release from the melt. The tracers were added to the pretest waste to simulate Pu behavior; however, a direct correlation between tracer behavior and Pu behavior remains uncertain. In addition, as discussed below, the uncertainties introduced during the sampling and analyses also act to prevent a rigorous quantification of the amounts of tracer released.

6.2 Tracer Study Objectives

The above considerations have resulted in modifications of the objectives of the tracer study as originally proposed. Despite the chemical similarities between the tracer materials and Pu, there remains no way to infer quantitative amounts of Pu retention/transport from tracer data. Despite uncertainty in the quantitative correlation between tracer behavior and Pu behavior, and the uncertainties introduced during the sampling and analyses,

essential information can be derived from the study. The modified objectives of the tracer study are as follows:

- Assess presence or absence in off-gas treatment system. Provide order of magnitude estimates of amounts.

- Determine relative amounts of tracer materials found retained within block, on hood and off-gas line surfaces, within the scrub system, and on the exit HEPA filter.

- Determine tracer release patterns over time.

- For Test 1, assess the amounts of tracer on the air inlet filter. This tracer could only be deposited as a result of positive pressure transients. The amount, if any, of tracer captured on the air inlet filter may allow evaluation of significance of direct air entrainment as an element release mechanism.

- Evaluate whether the tracers are found homogeneously within the block. This provides a measure of the amount of mixing of the block.

- Determine the partitioning of tracer material between solid phases in the final waste form.

6.3 Tracer Placement in Pit 1

Three tracers were placed in Pit 1 as shown schematically in Figure 104. The amounts of added tracer were as follows: Dy_2O_3 - 1.336 kg; Tb_4O_7 - 1.337 kg; and Yb_2O_3 - 1.331 kg. Each tracer was equally divided and placed into six paper bags. Each bag was placed into an individual can of waste materials. During placement, the contents of the bag were dumped into the can and a

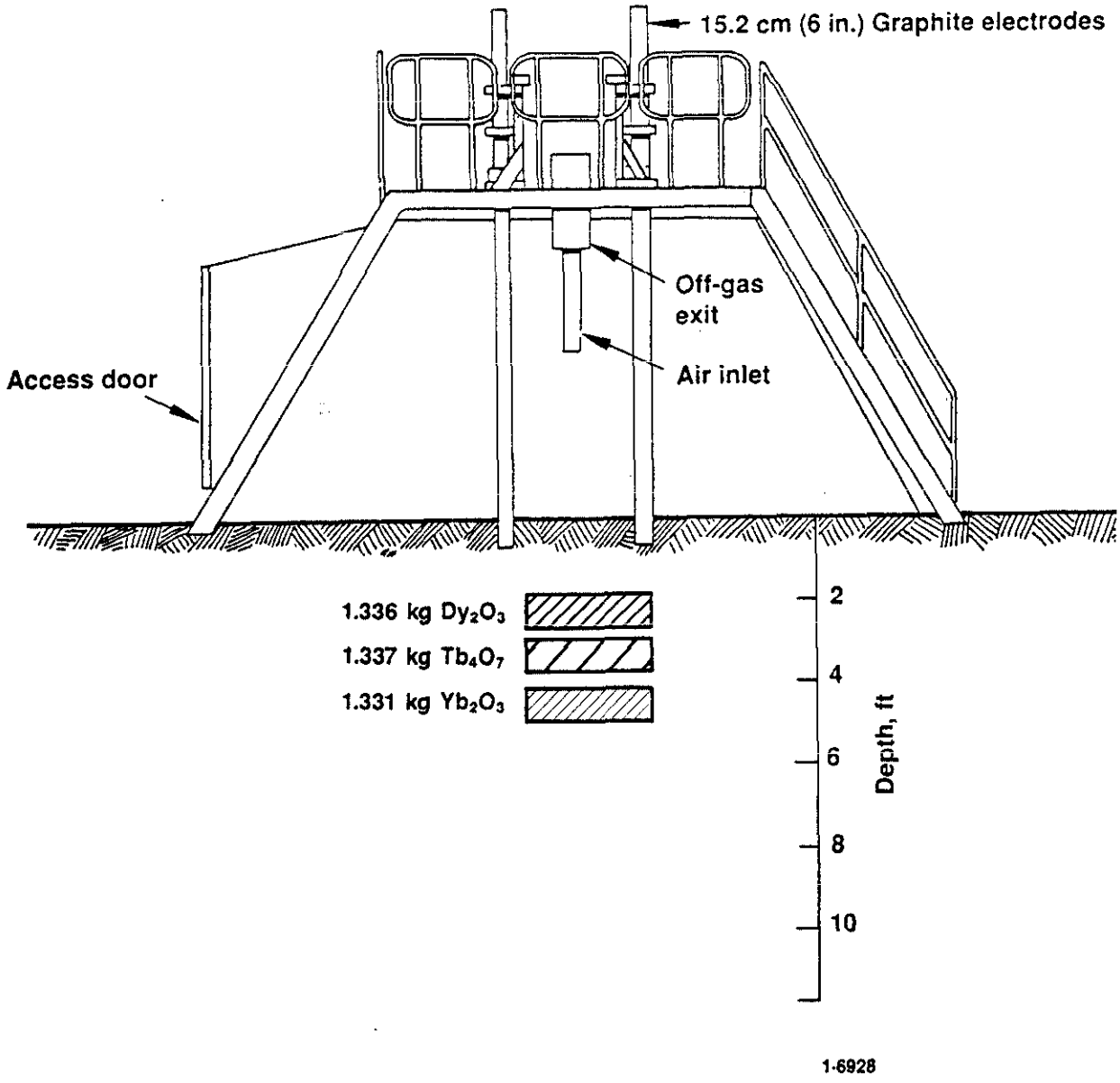

Figure 104. Tracer placement location for Test Pit 1.

limited attempt made to disperse the tracer material. The six cans containing each tracer represented the diversity of can waste materials: 1 can containing sludge, 2 cans containing cloth and/or paper, 1 can containing metal, 1 can containing concrete/glass, and 1 can containing wood. Placement of tracers in the pit during construction is shown in Figures 13 and 14; the cans containing tracer materials were placed near the center of the pit to ensure that they would be processed by the melt.

6.4 Tracer Placement in Pit 2

Only one tracer material was placed in Pit 2 as shown schematically in Figure 105. The amount of added tracer was Dy_2O_3 - 2.282 kg. The tracer was equally divided and placed into ten paper bags. Each bag was placed into an individual can of waste materials. During placement, the contents of the bag were dumped into the can and a limited attempt made to disperse the tracer material. The ten cans containing each tracer represented the diversity of can waste materials: 3 cans containing sludge, 5 cans containing cloth and/or paper, 1 can containing metal, and 1 can containing concrete/glass. Placement of the tracer cans in the pit during construction is shown in Figure 52; the cans containing tracer materials were placed near the center of the pit to ensure that they would be processed by the melt.

6.5 Tracer Sampling Strategy

Sampling of the following major areas was performed for each test: (a) glass product, (b) confinement hood, (c) off-gas ducting, (d) off-gas scrub solutions, (e) off-gas HEPA and inlet filters, (f) soil and sand used in pit preparations, and (g) soil adjacent to the glass product. Sampling strategies of these areas are described below. Sampling procedures are described in the sampling and analysis plan[29] for the field tests.[a]

---

a. Smears were collected from 100 cm^2 area, a deviation from the sampling and analysis plan.

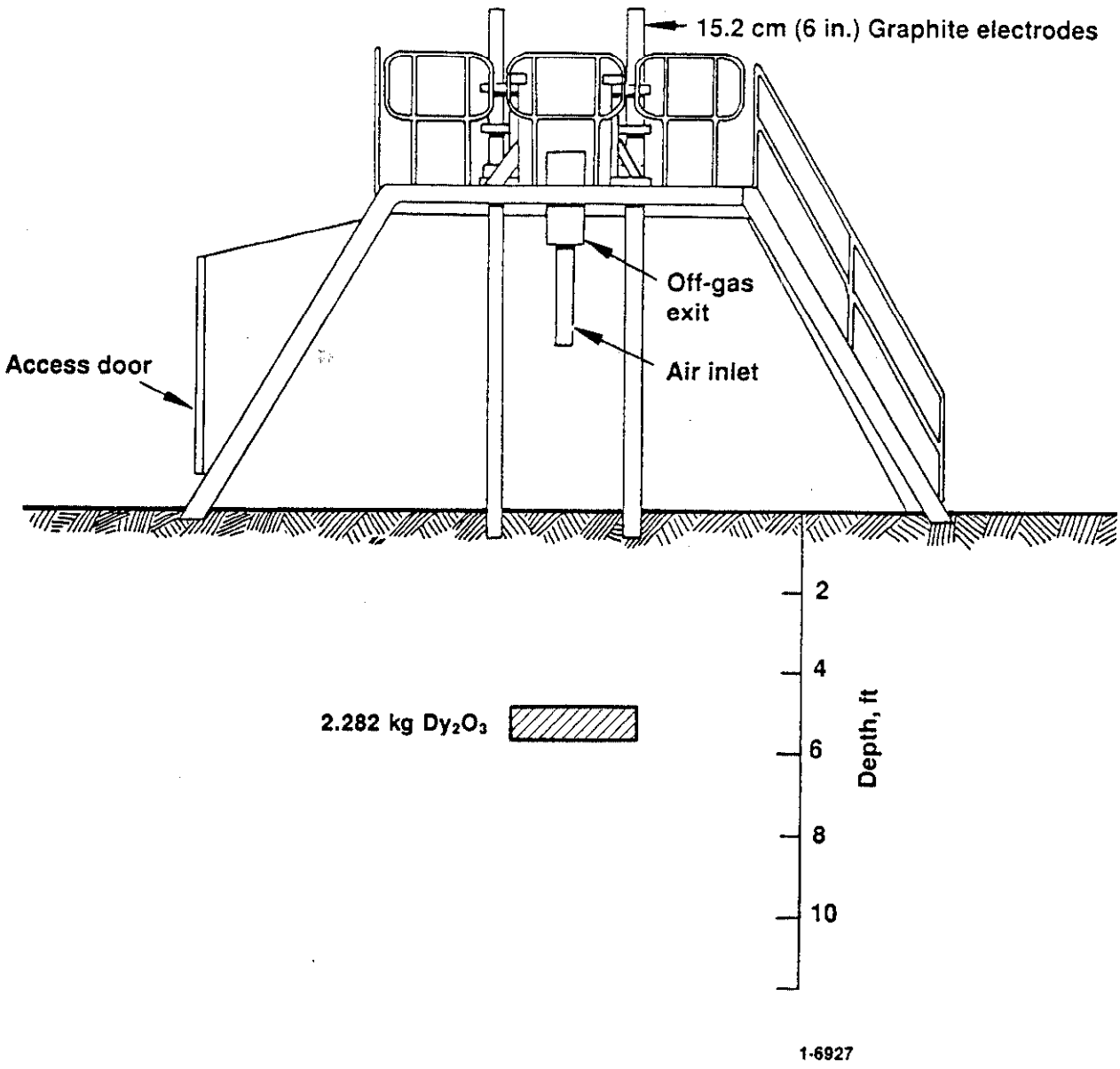

Figure 105. Tracer placement location for Test Pit 2.

Product

Grab and core samples were collected from the product block of each test. The sampling strategy focused on selection of material from different phases observed, and from various spatial locations within the product. See Figures 90 and 91 for the core and sample locations in plan and cross-sectional view for Tests 1 and 2, respectively. No field quality control samples were collected.

Hood

Smears were collected from top and side panels of the inside of the hood before and after each test.[a] Three top smears were collected 0.3 m (1 ft) from the edge of the hood and three[b] side smears were collected 0.6 m (2 ft) from the floor. Blank smears were prepared in each sampling episode.

Off-gas Duct

Smears of the off-gas ducting were collected at five locations before and after each test. The approximate locations (1-5) are shown in Figure 106. The samples were collected from the inside 2.5 cm (1 in.) of the entire circumference at each location. Smears were collected in the same sampling episode as hood smears, which included field smear blank preparation.

Off-gas Scrub Solution

Samples of the off-gas scrub solutions were collected at approximately two hour intervals during each test. The samples were collected from both scrub tanks at each sampling time.[c] Eight duplicate samples were collected.

---

a. Sample identification was inferred from sample logbook and chain-of-custody information.

b. In pretest sample for Test 1, two smears and one blank were collected.

c. Sample identification was inferred from the sample logbook, operations log, and chain-of-custody records in cases of discrepancies. Discrepancies that could not be satisfactorily resolved resulted in omission of data points. Some missing data result from no record of tank volumes and sampling times.

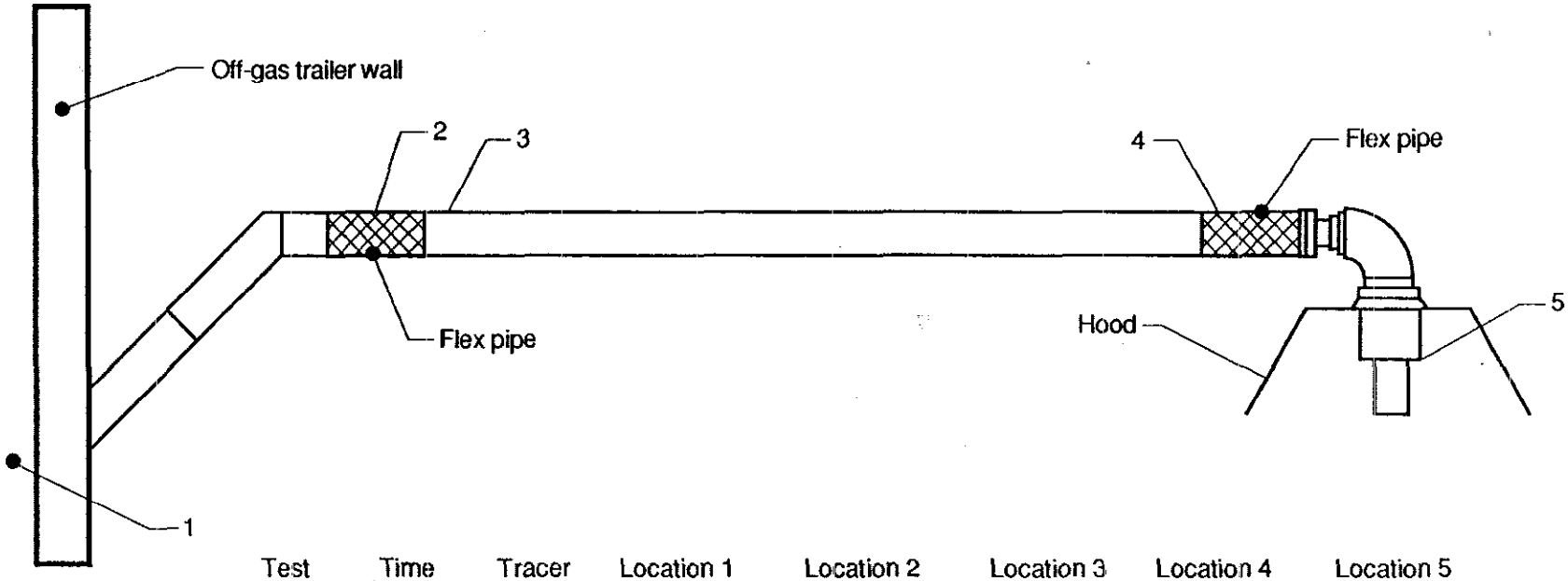

Test	Time	Tracer	Location 1		Location 2		Location 3		Location 4		Location 5	
			Amount (µg)	Flag	Amount (µg)	Flag	Amount (µg)	Flag	Amount (µg)	Flag	Amount (µg)	Flag
Test 1	Pretest	DY	2.2	B	1.0	U	1.0	U	1.0	U	1.0	U
Test 1	Pretest	TB	1.0	U	1.0	U	1.0	U	1.0	U	1.0	U
Test 1	Pretest	YB	1.0	U	1.0	U	1.0	U	1.0	U	1.0	U
Test 1	Post test	DY	5860.0		2370.0		6930.0		3140.0		944.0	
Test 1	Post test	TB	79400.0		35900.0		23200.0		40700.0		5180.0	
Test 1	Post test	YB	24500.0		11300.0		7380		16400.0		1940.0	
Test 2	Post test	DY	2260.0		1650.0		394.0		658.0		343.0	
Test 2	Post test	TB	7450.0		5340.0		438.0		1250.0		921.0	
Test 2	Post test	YB	2090.0		2030.0		274.0		1460.0		418.0	

T91 0479

Figure 106. Schematic showing off-gas duct smear locations and tracer analysis results. (Flag values are defined in Table 28.)

Filters

Eight samples were collected from the primary HEPA filters in the off-gas system and the air inlet filter in the hood.[a] Three samples were collected from the Test 1 air inlet filter, three samples were collected from the Test 2 primary HEPA filter, and two samples were collected from the Test 1 primary HEPA filter. One of each of the sets of three was sampled first and analyzed separately from the remaining samples. A blank of the HEPA filter material from the manufacturer was also submitted for analysis in the second submittal.

Soil

Pretest soil samples were collected from the pile of soil that was used in preparing the test pits. Samples were collected at different locations along the long axis of the pile at different depths; one duplicate sample was collected. In addition, sand used in preparation of the starter path (see Section 1.3.3) for the test pits was sampled in two locations from a pile.

A composite sampling scheme was used in posttest sampling of the soil adjacent to the products from Tests 1 and 2. Composite samples for the sides and bottom of the product blocks at two distances [15.2-20.3 cm (6-8 in.) and 25.4-30.5 cm (10-12 in.)] from the block-soil contact were collected. The number and locations of individual samples that composed each composite varied; the number of individual samples is shown below with the number of splits prepared for each composite. Volumes of individual samples contributing to the composites were not measured.

---

a. The sampling was performed after filters had been removed from the frames and sampled for other analyses. Filter identification was inferred from sampling notes.

	TEST 1 side 15.2-20.3 cm	TEST 1 side 25.4-30.5 cm	TEST 1 bottom 15.2-20.3 cm	TEST 1 bottom 25.4-30.5 cm
Samples:	9	9	3	3
Splits:	2	3	2	2

	Test 2 side 15.2-30.5 cm	Test 2 side 25.4-30.5 cm	Test 2 bottom 15.2-20.3 cm	Test 2 bottom 25.4-30.5 cm
Samples:	4	4	6	6
Splits:	2	2	2	3

6.6 Tracer Analysis

All samples were analyzed for Dy, Tb, and Yb, with the exception of Posttest 2 composite soil samples, which were analyzed for Dy only. The EG&G Idaho Environmental Chemistry Unit analyzed all samples, except product samples. Product samples were analyzed by the EG&G Idaho Separations and Chemical Analysis Unit.

Product Analyses

The product tracer analyses were performed by ICP-AES using an ARL 3410 instrument. The preparation of glass samples involved first crushing, then dissolution using HF and nanopure water, followed by two additions of HNO_3 and nanopure water. The metal samples were prepared using the described HF dissolution on metal shavings. The ICP analyses were performed using standard techniques. A multipoint calibration with replicate standard determinations was performed over a suitable concentration range.

The samples were submitted for analysis under chain of custody.[a] No special preservation or storage of the samples was required. The quality control associated with the glass analyses included two internal standards, matrix blanks, duplicate samples, sample spikes, and blank spikes. The

a. Chain of custody was adequate, with the exception that one sample label was misprinted.

quality control associated with the metal analyses consisted of matrix blanks, sample spikes, and blank spikes. The spikes were of analytes other than the tracers.

The quality control procedures and data[a] were reviewed for compliance with acceptable limits. Over one-third of the analyses were found to be suspect for several reasons. No analytical or matrix spikes were performed on any samples submitted for Dy, Tb, or Yb analysis. For all three tracers, selected sample analytical results are suspect because recoveries on associated standards exceeded procedure limits but were not reanalyzed. The reported mean percent error of standards (bias) is 7.4, 0.6, and -0.1 for Yb, Dy, and Tb analysis of glass samples, respectively. The relative standard deviation of the duplicate sample for Dy analysis of glass samples is 7.8%.

Hood, Off-Gas Duct, Scrub Solution, Filter, and Soil Analyses

EPA SW-846 Method 3020 was used for sample preparation of scrub solution and soil samples. A modified method was used for preparation of smear and filter samples. Method 6020-M Rev. 1 was used for analysis with Cesium-133 as the internal standard.[b] The instrumentation used was a VG Elemental PlasmaQuad II+ ICP-MS, equipped with an autosampler. Sample analyses were performed using peak-jumping mode in the pulse-counting detector. Some samples were analyzed in Extended Dynamic Range due to high analyte concentrations in the samples. All reported sample and quality control (QC) results were quantitated using blank subtraction. No isobaric elemental or molecular-ion interferences occurred at the masses of interest for the three rare-earth analytes, so isobaric interference correction factors, though applied, did not affect reported data. Matrix spikes and matrix spike duplicates were not performed on smear samples because of the impossibility of evenly splitting the samples. To obtain indicators of precision and accuracy for smear analyses, two laboratory control samples (spiked clean paper towels of identical brand as the analysis batch) were processed with the samples.

---

a. Only summarized, no raw data was available for review; therefore, initial and continuing calibration of the instrument was not verified.

b. In one instance, rhodium was used as an internal standard because cesium was detected in the sample.

The samples were submitted for analysis under chain of custody. Sample integrity was found to be adequate except in cases where the pH of the scrub samples was greater than two, which could lead to a low bias in the results. Required refrigeration was maintained and holding times were met. Quality control was measured with initial and continuing calibration verification standards, low-level standards, method and calibration blanks, matrix spikes, matrix spike duplicates, and laboratory control samples.

Because of the scoping nature of the IFT as the first testing of ISV processing of buried waste and the intended use of the tracer data as indicators rather than quantification of element retention, a detailed quality control review inclusive of raw data was not performed. However, the quality control procedures and summary statistics were reviewed for compliance with acceptable limits.

All pretest soil samples are associated with out-of-limit spike recoveries for Dy, indicating that the sample bias could be as high as 43%. QC associated with Posttest 2 smear samples showed a small bias in the blanks (on the order of 0.01 ug or less) for Dy, Tb, and Yb. One smear analysis batch had poor matrix spike recoveries; one of the post-digestion matrix spike recoveries was below the lower control limit.

Virtually all scrub solutions had poor matrix spike recoveries because the amounts added to the samples were much less than sample amounts.[a] However, out-of-limit low post digestion matrix spike recoveries occurred in one Test 1 scrub solution batch for Dy, Tb, and Yb and in two Test 2 scrub solution batches for Yb. Samples with high pH occurred in five of eight scrub solution analysis batches; this could result in a low, but unquantifiable, bias in results. One Test 2 scrub solution batch had a contaminated preparation blank (on the order of 0.1 ug/l) for Dy, Tb, and Yb and another had an initial calibration recovery for Tb slightly less than acceptable. Some laboratory control sample recoveries less than 75% were reported for both Test 1 and Test 2 scrub solutions. The poor matrix spike, initial

---

a. In some cases, the matrix spikes are virtual duplicates of the original sample; however, the analysis results show poor precision. Analysts believe this could be due to the presence of solids in the solutions, which affect the representativeness of the splits.

calibration, and laboratory control sample recoveries and contaminated blanks indicate that scrub solution sample results are biased low, in varying amounts. The bias is not estimated here because of the ubiquitous nature of the problems and the scoping nature of the data analysis.

For tracer analysis of the filters, all calibration verification QC, laboratory control sample, and preparation blank results were in control.[a] Matrix spike recovery problems similar to those in scrub solution analyses were experienced for two of the filters, possibly because of inhomogeneous distribution of analytes on filter surfaces and the high absorbency that is characteristic of HEPA filter media.

The analytical results are discussed below by media and ISV system component. Complete listings of data discussed are presented in Appendix A. In the Appendix and following sections, qualifiers to the data may be shown.[b] The qualifiers and their respective definitions are in Table 28.

In analysis of the results, values flagged with a B are used as actual measurements unless otherwise noted and values flagged with a U are treated as less-than-detectable (LTD) measurements.

Table 28. Data qualifiers and definitions

Qualifier	Qualifier Definition
U	Analyte was analyzed for but not detected (value reported as the IDL followed by a U flag)
B	Value is less than the minimum reporting level (MRL) but greater than the IDL (potential for false positives and or low/high bias exists)
N	Matrix spike or duplicate matrix spike recovery not within control limits
*	Duplicate analysis not within control limits

a. Relative percent difference between duplicates for Tb, 38%, is the exception.

b. If the matrix spike amount was much less than the sample amount and the recovery was not within control limits, the flag 'N' was not reported by the laboratory. ISV product analyses were flagged only as less-than-detection where appropriate; an overall quality flag is reported here with the data.

6.7 Test 1 Tracer Results

Product

Glass, crystalline, and metal phases of each test product were analyzed for Dy, Tb, and Yb. Analysis results are given in Table 29. The table also identifies the analysis results that have questionable quality, as discussed above. With one exception, the tracers were detected in every sample; the exception has questionable analytical quality.

Table 30 gives estimates of the mean (or average) and 90% confidence limits for the mean for glass and crystalline product samples. To compute the statistics, questionable data were removed from the data set. The results imply the following:

- there is a 90% chance that the true mean concentration of Dy in the nonmetal phases of the product is between 172 and 201 ug/g
- there is a 90% chance that the true mean concentration of Tb in the nonmetal phases of the product is between 209 and 267 ug/g
- there is a 90% chance that the true mean concentration of Yb in the nonmetal phases of the product is between 325 and 396 ug/g.

The confidence interval width is influenced by the number and variability of samples; the interval widths and the data themselves indicate that nonmetal product materials from different block locations have relatively similar tracer amounts.

The mass of the Test 1 product has been estimated at 8267 kg. Using the means from Table 30, the estimated tracer amounts in the product are 1538, 1968, and 3009 g Dy, Tb, and Yb, respectively, or 1765, 2314, and 3398 g Dy_2O_3, Tb_4O_7, and Yb_2O_3, respectively. The respective confidence intervals for the tracer oxide amounts, using the limits in Table 30 and ignoring any

Table 29. Product tracer analyses[a]

Location	Block Location	Phase	DY	DY Flag	TB	TB Flag	YB	YB Flag	DY Quality	TB Quality	YB Quality	Units
TEST 1	1	GLASS	58		42	U	5	U	Q	Q	Q	ug/g
TEST 1	2	GLASS	169		199		320					ug/g
TEST 1	3	GLASS AND DENDRITES	187		227		359					ug/g
TEST 1	4	GLASS, TRACE DENDRITES	224		284		362		Q		Q	ug/g
TEST 1	5	GLASS	192		240		390					ug/g
TEST 1	6	GLASS AND DENDRITES	197		241		374					ug/g
TEST 1	7	GLASS AND DENDRITES	188		233		378		Q	Q	Q	ug/g
TEST 1	8	METAL	6	U	42	U	5	U	Q	Q		ug/g
TEST 2	.	GLASS	195		42	U	6		Q	Q		ug/g
TEST 2	1	VESICULATED GLASS	6	U	42	U	6		Q	Q	Q	ug/g
TEST 2	2	GLASS	84		42	U	5	U	Q	Q		ug/g
TEST 2	3	GLASS	186		42	U	5	U				ug/g
TEST 2	4	GREY PORCELINOUS MATERIAL	183		42	U	5	U		Q		ug/g
TEST 2	5	GLASS AND APHANITIC MATERIAL	182		42	U	5	U		Q		ug/g
TEST 2	6	GLASS AND DEVITRIFIED MATERIAL	177		42	U	5	U		Q		ug/g
TEST 2	7	GLASS	172		42	U	5	U				ug/g
TEST 2	9	DEVITRIFIED GLASS	181		42	U	5	U				ug/g
TEST 2	10	DEVITRIFIED MATERIAL	171		42	U	5	U				ug/g
TEST 2	11	METAL	6	U	42	U	5	U	Q	Q		ug/g
TEST 2	15	GLASS	173		42	U	5	U				ug/g
TEST 2	16	GLASS AND CRYSTALLINE	155		42	U	5	U				ug/g
TEST 2	17	GREY APHANITIC MATERIAL	6	U	42	U	8					ug/g
TEST 2	18	METAL	6	U	42	U	5	U	Q	Q		ug/g

a. Questionable data identified with Q.

Table 30. Nonmetal product tracer analyses means and 90% confidence limits (ug/g). Questionable and less-than-detection data removed.

Location	Tracer	Mean	Lower Limit	Upper Limit
Test 1	DY	186.250	171.891	200.609
Test 1	TB	238.200	208.928	267.472
Test 1	YB	360.750	325.484	396.016
Test 2	DY	175.556	169.756	181.355
Test 2	YB	7.000	0.686	13.314

uncertainty (possibly substantial) in the product mass value, are (1632, 1907), (2032, 2596), and (3059, 3728). These estimates far exceed the tracer amounts buried in the pits: 1336 g for Dy_2O_3, 1337 g for Tb_4O_7, and 1331 g for Yb_2O_3. Possible explanations for these estimates being severely biased include (a) bias of the estimate of the product mass and (b) unknown laboratory bias.

An additional source of error is the use of the entire mass of the block in estimating the amounts of tracer. Although the product sample data indicated a relative homogeneous distribution of tracers in the block, these samples were taken from regions where convective mixing is expected. It is possible that areas where convective mixing would be expected to be less, such as near edges of the melt, may have a reduced concentration of tracer.

Hood

Field blank analyses, which include hood smear analyses, are given in Table 31. The pretest blank measurements are under less-than-detection limits. Blanks collected after Test 1 have some contamination of Tb and Yb, indicating a possible bias in smear results for these analytes. Table 32 gives the tracer analyses for all hood smears, with the general hood area identified. All pretest 1 tracer measurements are less-than-detection; the posttest 1 samples are detected at amounts 130 ug and greater. There is an obvious difference between pretest and posttest smear results, even when the bias indicated in the blanks is considered; this difference is evidence that material from ISV does accumulate in the hood.

Mean amounts of tracers accumulated on the top and sides of the hood during Test 1 are provided in Table 33. The table also gives the standard deviation of the data and the coefficient of variation, which is 100 times the sample means and were not significantly different between top and side for Dy, Tb, and Yb. The 90% confidence intervals for smear average amounts (ug) in

Table 31. Field blank analyses

Location	Time	Media	Tracer	Amount	Flag	Units
Test 1	Pretest	Hood Smear	DY	1.00	U	UG
Test 1	Pretest	Hood Smear	TB	1.00	U	UG
Test 1	Pretest	Hood Smear	YB	1.00	U	UG
Test 1	Posttest	Hood Smear	DY	1.00	B	UG
Test 1	Posttest	Hood Smear	TB	10.40		UG
Test 1	Posttest	Hood Smear	YB	5.00		UG
Test 2	posttest	Hood Smear	DY	0.23		UG
Test 2	Posttest	Hood Smear	TB	0.23		UG
Test 2	Posttest	Hood Smear	YB	0.26		UG

Table 32. Hood smear analyses

Location	Time	Hood Location	Area	DY	Dy Flag	TB	Tb Flag	YB	Yb Flag	Units
TEST 1	PRETEST	1	TOP	1.00	U	1.00	U	1.00	U	UG
TEST 1	PRETEST	2	TOP	1.00	U	1.00	U	1.00	U	UG
TEST 1	PRETEST	3	TOP	1.00	U	1.00	U	1.00	U	UG
TEST 1	PRETEST	4	SIDE	1.00	U	1.00	U	1.00	U	UG
TEST 1	PRETEST	5	SIDE	1.00	U	1.00	U	1.00	U	UG
TEST 1	POSTTEST	1	TOP	696.00		393.00		929.00		UG
TEST 1	POSTTEST	2	TOP	617.00		130.00		929.00		UG
TEST 1	POSTTEST	3	TOP	629.00		248.00		366.00		UG
TEST 1	POSTTEST	4	SIDE	457.00		258.00		691.00		UG
TEST 1	POSTTEST	5	SIDE	660.00		406.00		862.00		UG
TEST 1	POSTTEST	6	SIDE	1200.00		792.00		868.00		UG
TEST 2	POSTTEST	1	TOP	500.00		292.00		450.00		UG
TEST 2	POSTTEST	2	TOP	1360.00		255.00		1100.00		UG
TEST 2	POSTTEST	3	TOP	390.00		285.00		607.00		UG
TEST 2	POSTTEST	4	SIDE	23.80		10.30		26.70		UG
TEST 2	POSTTEST	5	SIDE	15.70		10.10		19.00		UG
TEST 2	POSTTEST	6	SIDE	657.00		520.00		634.00		UG

Table 33. Hood tracer analysis statistics

				TRACER								
				DY			TB			YB		
				CONCENTRATION			CONCENTRATION			CONCENTRATION		
				MEAN	STANDARD DEVIATION	COEFFICIENT OF VARIATION	MEAN	STANDARD DEVIATION	COEFFICIENT OF VARIATION	MEAN	STANDARD DEVIATION	COEFFICIENT OF VARIATION
LOCATION	MEDIA	AREA	UNITS									
TEST 1	HOOD SMEAR	SIDE	UG	772.33	384.03	49.72	485.33	275.70	56.81	807.00	100.50	12.45
		TOP	UG	647.33	42.57	6.58	257.00	131.73	51.26	741.33	325.05	43.85
TEST 2	HOOD SMEAR	SIDE	UG	232.17	367.94	158.48	180.13	294.33	163.40	226.57	352.87	155.75
		TOP	UG	750.00	531.13	70.82	277.33	19.66	7.09	719.00	339.17	47.17

the standard deviation to mean ratio.[a] A statistical test[b] confirmed that the hood after the test is (502, 919) for Dy, (182, 561) for Tb, and (595, 954) for Yb.

The surface area for the inside of the hood has been estimated at approximately 34.5 m^2 (371 ft^2). The hood smears, reported in ug, represent an approximate 0.01 m^2 area. It follows that the total estimated tracer amounts in the hood are 2.45 g for Dy, 1.28 g for Tb, and 2.67 g for Yb. The associated 90% confidence intervals for these mean amounts, assuming there is no variability in the surface area measurements, are (1.73, 3.17) for Dy, (0.63, 1.93) for Tb, and (2.05, 3.3) for Yb.

Off-gas Duct

The analytical results for smears taken inside the off-gas duct between the hood and the off-gas trailer are presented with a schematic of the sample locations (see Figure 106). Field blank data, shown in Table 31 and discussed above, apply to off-gas duct data. Pretest measurements in the duct are all less-than-detection or below the minimum reporting limit (MRL). Posttest 1 smears show tracers detected at amounts of 944 ug and greater. As in the hood, there is an obvious difference between pretest and posttest smear results; this difference is evidence that material from ISV does accumulate in the duct. Tb appears to occur at an order of magnitude greater than Dy. The data are insufficient to make inferences concerning accumulation trends and patterns.

The duct inside surface area has been estimated at 7.57 m^2 (81.5 ft^2). As for the hood, each smear represents an approximate 0.01 m^2 area. Using the duct surface area together with the means of the smears,[c] the total tracer amounts in the duct are 2.9 g Dy, 28 g Tb, and 9.3 g Yb. The following cautions are in order concerning this calculation. The calculation uses the

---

a. Also known as the relative standard deviation.

b. Student's test for the difference in two means at a significance level of 0.05 was used.

c. The means used are 3849 ug for Dy, 36876 ug for Tb, and 12304 ug for Yb.

average of the smear analyses; the average is not considered representative of the duct as a whole because of the location of the samples. The presence of bend sections of piping and reducing and expanding sections will produce flow patterns which likely result in a nonuniform and complex deposition of particulates (including any tracers present) on pipe walls. The sampling locations of the smeared samples were not chosen from the evaluation of likely flow patterns. Therefore, the estimate of deposition amounts based on the use of an overall surface area is only an order of magnitude estimate. Also, the flex pipe section had a surface of woven metal fiber; it is questionable whether a representative smear can be collected in flex pipe, which was one of the sampling locations. Smear surface area from flex pipe is expected to be different from the surface area of a smear from a standard smooth pipe. Because of the reasons stated above, the authors caution the reader concerning the accuracy of the estimate for the total tracer amount in the duct.

Off-gas Scrub Solution

Field duplicates of scrub solution samples are given in Table 34. The coefficients of variation between duplicate samples[a] range between 0.00 and 16.53 (duplicate analyses were within 0.00 and 16.53% of the mean of the duplicates) for Test 1, with one exception. Note that the coefficient of variation is inherently less than relative percent difference (RPD) typically reported by laboratories; thus, the stated range falls well within the 20% RPD limit of the analytical method. The exception, duplicate 4, was collected prior to the first start of Test 1 and was analyzed in the same batch as eight samples during Test 1. The reader should recognize that results presented below for Test 1 scrub solutions may reflect the poor precision observed in this duplicate set.

The tracer amounts given here are the sum of the amounts in the two scrub tanks in the off-gas system. To estimate the amounts in each scrub tank, solution concentrations are multiplied with tank volumes. The tank volume readings, however, are considered to be quite imprecise, and possibly biased.

---

a. No data are available for duplicate set number 3. Due to test restarts, duplicates 1, 4, and 5 are not duplicates of data represented here, but are of scrub solution media and from one of the sample analysis groups that include data presented here, and so are given.

Table 34. Field duplicate analysis statistics

				TRACER								
				DY			TB			YB		
				(AMOUNT)			(AMOUNT)			(AMOUNT)		
QC	LOCATION	MEDIA	UNITS	MEAN	STANDARD DEVIATION	COEFFICIENT OF VARIATION	MEAN	STANDARD DEVIATION	COEFFICIENT OF VARIATION	MEAN	STANDARD DEVIATION	COEFFICIENT OF VARIATION
DUPLICATE 1	TEST 1	SCRUB SOLUTION	UG/L	4.80	0.71	14.73	0.77	0.13	16.53	2.60	0.42	16.32
DUPLICATE 2	TEST 1	SOIL	MG/KG	2.10	0.14	6.73	0.37	0.03	7.64	0.93	0.08	8.41
DUPLICATE 4	TEST 1	SCRUB SOLUTION	UG/L	4.65	1.91	41.06	0.74	0.28	38.22	2.45	0.92	37.52
DUPLICATE 5	TEST 1	SCRUB SOLUTION	UG/L	1.35	0.07	5.24	0.20	0.00	0.00	0.72	0.00	0.00
DUPLICATE 6	TEST 1	SCRUB SOLUTION	UG/L	3.25	0.07	2.18	0.51	0.01	2.77	1.85	0.07	3.82
DUPLICATE 7	TEST 2	SCRUB SOLUTION	UG/L	2000.00	113.14	5.66	4225.00	304.06	7.20	4825.00	304.06	6.30
DUPLICATE 8	TEST 2	SCRUB SOLUTION	UG/L	2844.50	2977.63	104.68	10770.00	12770.35	118.57	5395.00	5395.22	100.00
DUPLICATE 9	TEST 2	SCRUB SOLUTION	UG/L	1130.00	84.85	7.51	2800.00	480.83	17.17	2820.00	56.57	2.01

This leads to noise in the results examined here, of which the reader should be aware. In addition, the analytical quality control indicates that bias is present, in differing amounts.

The results for Test 1 are plotted against hours from the start of the test in Figure 107.[a] In addition, the figure shows the depth of the melt front and tracer burial depths. The pattern shown in the plot does illustrate progressive release of the tracers with melt depths that correspond with tracer burial depths. For Dy, the release occurred at approximately the same time that the melt reached the burial depth. For Tb, the release occurred an hour or more after the melt is believed to have reached Tb burial depth. The amount of Yb in the scrub tanks increased when the melt reached the tracer burial depth, but increased further more than an hour later. The lag times observed could be a function of the melt column through which the tracer traveled to reach the off-gas system; however, the tracer burial depths are estimated (±6 in.) and could lead to as much as a three hour time window on average for release. Nonuniform releases are likely due to processing factors; penetration of cans containing tracer may have occurred at different times during processing at a particular burial depth. There also appears to be evidence that the tracer levels in the tanks dropped off after peak releases, indicating that some amount of the tracers continued past the scrub solution in the off-gas system. Note that the release amounts observed do vary with tracer type (higher with greater burial depth), despite the fact that equal amounts were buried; the reason for this is unknown.

Table 35 gives pretest and posttest tracer amounts in the scrub solution. Pretest values are actually the first measurement after the start of Test 1, and posttest 1 values are simply measurements taken prior to Test 2. Posttest 1 tracer amounts in the scrub solution provide estimates of tracer retention in the scrub tanks for the test. The estimates are 0.9 g for Dy, 1.9 g for Tb, and 2.0 g for Yb. No direct estimates of uncertainty in these numbers are available; however, field duplicate precision in other samples is approximately 5-7%. The analytical quality control statistics indicate that bias is low in scrub solution numbers.

---

a. Data points that measured LTD are plotted as the reported detection limit.

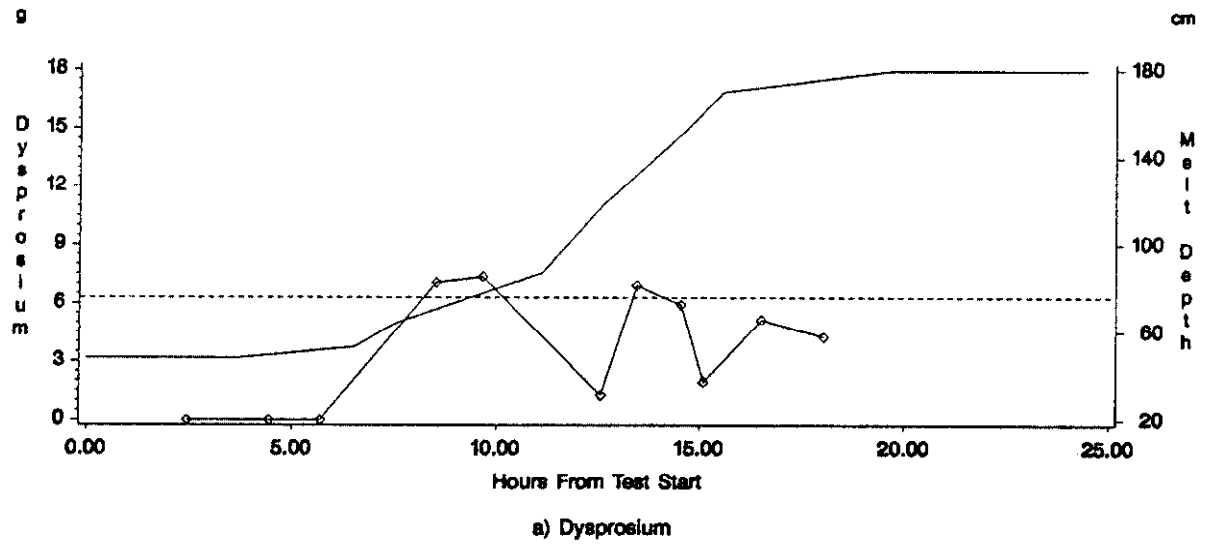

a) Dysprosium

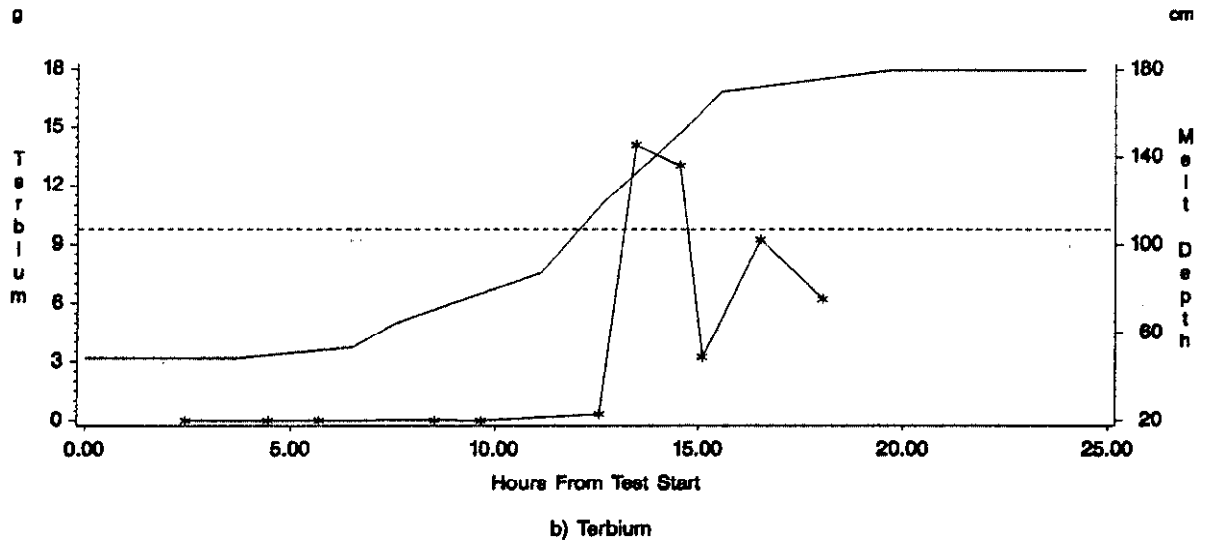

b) Terbium

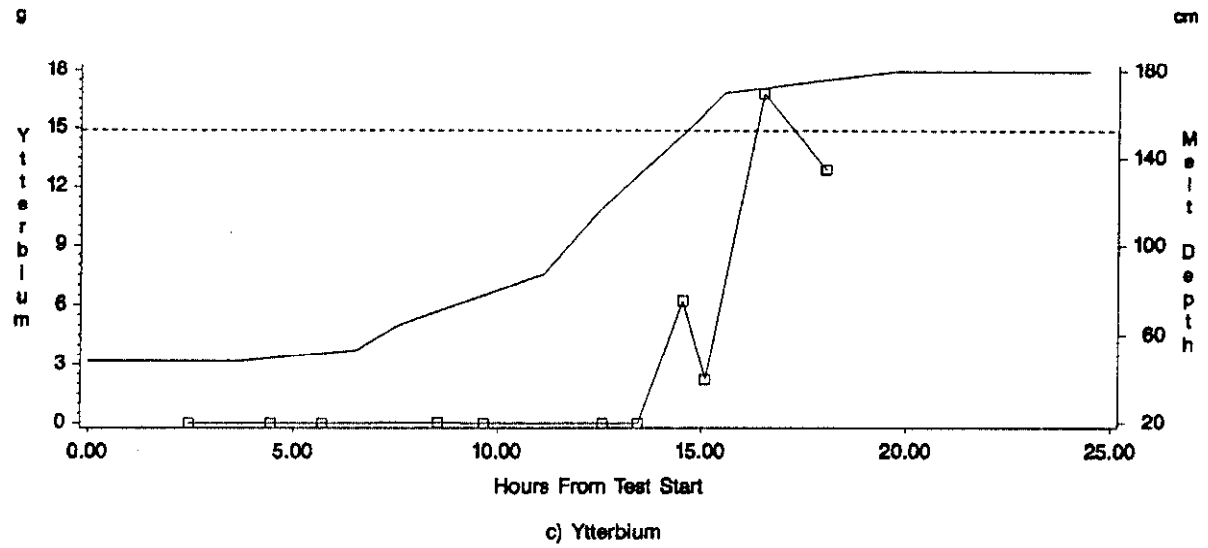

c) Ytterbium

Figure 107. Amounts of tracer in scrub solution and melt depth as a function of time during Test 1. Dashed line shows depth of burial of tracer, (a) Dysprosium, (b) Terbium, (c) Ytterbium.

Table 35. Scrub solution analysis summary

Location	Time	Media	Dy (ug)	Tb (ug)	Yb (ug)
Test 1	Posttest	Scrub Solution	898200	1936600	2043800.0
Test 1	Pretest	Scrub Solution	153	34	95.2
Test 2	Posttest	Scrub Solution	705516	1928640	1547280.0
Test 2	Pretest	Scrub Solution	898200	1936600	2043800.0

Review of the data presented in Table 35, Figure 107, and Table 36 indicate that there is the potential for significant underestimation of the scrub solution tracer amounts. At the temperature of the scrub solution it would be expected that little, if any, tracer would be able to pass further downstream. This is consistent with the data presented below which show little tracer collected on the primary HEPA filters. However, the data shown in Figure 107 indicate a trend of decreasing tracer amount for the samples collected at the end of the test. In addition, the posttest scrub samples shown in Table 35 indicate amounts much lower than the last samples shown in Figure 107. Since the posttest samples were collected several weeks after completion of the test, it is likely that settling of sediment in the tank may have resulted in a lower amount being collected in the samples. (It should be noted that the tracer materials are insoluble in water.) The possibility of material settling may also account for the lower values shown in Figure 107 for samples collected later in the test.

Table 36. Tracer concentration on primary HEPA and air inlet filters, in mg/kg.

Location	Filter Location	Analysis Group	DY	DY Flag	TB	TB Flag	YB	YB Flag
Test 1	HEPA	2	0.95	U	0.95	U	0.11	B
Test 1	HEPA	2	0.98	U	0.98	U	0.28	B
Test 1	INLET	2	134.0		0.34	B	0.19	B
Test 1	INLET	2	209.0		1.2		0.37	B
Test 1	INLET	1	263.0		1.2		0.42	B
Test 2	HEPA	2	0.47	B	0.95	B	0.98	B
Test 2	HEPA	2	0.92	B	4.3		2.2	
Test 2	HEPA	1	1.0		4.0		2.3	
Blank -		2	0.93	U	0.93	U	0.93	U

If it is assumed that, once collected in the scrub solution, tracer did not leave the scrub solution, then the maximum amounts shown in Figure 107 may represent a better estimate of the collected tracers. In this case the amounts estimated in the scrub solutions would be higher: 7.3 g for Dy, 14 g for Tb, 16.8 g for Yb.

The above considerations point out that there may be significant limitations on data collected from the scrub tanks. These tanks are in the system as operational equipment and are not designed for the purpose of sampling. The potential for nonuniform mixing and settling exists and complicates interpretation of data as shown above. Given these limitations, it may be advantageous in future testing to use isokinetic sampling schemes for off-gas sampling, and rely less on sampling of the scrub solutions.

Filters

Table 36 gives filter tracer analysis results. For Test 1, the primary HEPA filter had less-than-detection Dy and Tb, and Yb at low concentrations. The Test 1 inlet air filter, however, had comparatively high Dy. The Tb and Yb levels in the air filter were detected but were relatively low. No tracer was detected in the blank filter material.

A 90% confidence interval for Dy concentration on the test 1 air inlet filter is (92.8, 311.2) mg/kg. The interval width reflects the sample-to-sample variability observed. The analysis results indicate that the hood pressurizations were sufficient to reverse air flow direction in the area of the inlet filter and deposit tracer-bearing particulates. Although pressurizations occurred during processing of all the tracers, the data show a higher amount of Dy than the other tracers which were buried at greater depth. This is consistent with the hypothesis that materials buried at more shallow depths are more likely to be transported into the off-gas system. The greater depth of melt at later times of the test may act to reduce the amount of material released into the off-gas system from containers buried at greater depth. (Note, however, that the data for tracer in the scrub solution show larger amounts of the tracers buried at greater depths, see Figure 107.) In addition, the fact that tracer was transported to the air inlet filter suggests that entrainment may be a significant mechanism for transport. Other mechanisms such as volatization of material would not result in material being deposited on the air inlet filter. This material could only be transported to the filter during the time periods when the hood experienced positive pressure sufficient to cause air backflow down the air inlet line.

Soil

Field duplicates were collected and analyzed for pretest soil, and the results are presented in Table 34. Coefficients of variation of 6.7 to 8.4 are reported for the tracer analyses. As for scrub solution field duplicates, the stated range falls well within the 20% RPD limit of the analytical method.

Table 37 gives the tracer analysis results for all soil and sand samples. All tracers were detected in all of the samples except Posttest 1 samples, all but one of which had less-than-detection Tb measurements. One of the Posttest 1 samples had a Yb less-than-detection measurement.

To determine whether or not there is a difference between pretest and posttest tracer levels, first, pretest soils are examined to determine whether amounts differ between sampling depths, so that the data can be pooled to compare with posttest samples. A statistical test[a] indicated that there are no significant differences between depths 1 and 2 in samples from the pretest soil pile.

The pretest-posttest comparison strategy is to compare the average of pretest soils with each posttest composite split average. Averages are given in Table 38. Composite values are not combined because they represent unique conditions adjacent to the product block. The comparisons omit tracer analyses from pretest sand samples; this is considered a conservative approach because the sand appears to have higher tracer amounts than pretest soils. A series of statistical tests that controlled the testing error were performed.[b] No significant differences between pretest and individual posttest sample means were detected; however, the reader is cautioned as follows:

---

a. Student's test for the difference in two means at a significance level of 0.05 was used.

b. Student's tests were performed using a Bonferroni family confidence level of 95% for Dy for both tests and also for Yb for Test 1.

Table 37. Soil tracer analyses

Location	Time	Soil Location	Depth	Dy	Dy Flag	Tb	Tb Flag	Yb	Yb Flag	Units
TEST 1	PRETEST	1	1	1.80		0.31	B	0.76		MG/KG
TEST 1	PRETEST	2	2	2.20		0.37	B	0.92		MG/KG
TEST 1	PRETEST	3	1	2.40		0.40	B	1.00		MG/KG
TEST 1	PRETEST	3	2	2.20		0.39	B	0.98		MG/KG
TEST 1	PRETEST	3	2	2.00		0.35	B	0.87		MG/KG
TEST 1	PRETEST	4	3	1.90		0.35	B	0.85		MG/KG
TEST 1	PRETEST		.	3.20		0.56		1.30		MG/KG
TEST 1	PRETEST		.	3.50		0.62		1.40		MG/KG
TEST 1	POSTTEST	BOTTOM, 12 in.	.	2.50	B	1.00	U	2.80	B	MG/KG
TEST 1	POSTTEST	BOTTOM, 12 in.	.	2.30	B	0.99	U	1.50	B	MG/KG
TEST 1	POSTTEST	BOTTOM, 6 in.	.	2.70	B	1.00	U	1.10	B	MG/KG
TEST 1	POSTTEST	BOTTOM, 6 in.	.	2.60	B	1.00	U	1.20	B	MG/KG
TEST 1	POSTTEST	SIDE, 12 in.	.	2.40	B	0.97	U	1.20	B	MG/KG
TEST 1	POSTTEST	SIDE, 12 in.	.	2.70	B	1.00	U	6.80	B	MG/KG
TEST 1	POSTTEST	SIDE, 12 in.	.	2.40	B	1.10	B	1.00	U	MG/KG
TEST 1	POSTTEST	SIDE, 6 in.	.	2.40	B	1.00	U	1.00	B	MG/KG
TEST 1	POSTTEST	SIDE, 6 in.	.	2.50	B	0.98	U	1.10	B	MG/KG
TEST 2	POSTTEST	BOTTOM, 12 in.	.	2.60	B	.		.		MG/KG
TEST 2	POSTTEST	BOTTOM, 12 in.	.	2.50	B	.		.		MG/KG
TEST 2	POSTTEST	BOTTOM, 12 in.	.	2.70	B	.		.		MG/KG
TEST 2	POSTTEST	BOTTOM, 6 in.	.	2.60	B	.		.		MG/KG
TEST 2	POSTTEST	BOTTOM, 6 in.	.	2.30	B	.		.		MG/KG
TEST 2	POSTTEST	SIDE, 12 in.	.	2.20	B	.		.		MG/KG
TEST 2	POSTTEST	SIDE, 12 in.	.	2.20	B	.		.		MG/KG
TEST 2	POSTTEST	SIDE, 6 in.	.	2.00	B	.		.		MG/KG
TEST 2	POSTTEST	SIDE, 6 in.	.	2.00	B	.		.		MG/KG

Table 38. Soil tracer analysis means and 90% confidence limits

Location	Time	Media	Soil Location	Dy Mean	Dy Standard Error	Dy Lower Limit	Dy Upper Limit	Yb Mean	Yb Standard Error	Yb Lower Limit	Yb Upper Limit	Units
TEST 1	PRETEST	SAND		3.35000	0.15000	2.40294	4.29706	1.35000	0.05000	1.03431	1.66569	MG/KG
TEST 1	PRETEST	SOIL		2.08333	0.09098	1.90000	2.26667	0.89667	0.03639	0.82333	0.97000	MG/KG
TEST 1	POSTTEST	SOIL	BOTTOM, 12 IN.	2.40000	0.10000	1.76862	3.03138	2.15000	0.65000	-1.95394	6.25394	MG/KG
TEST 1	POSTTEST	SOIL	BOTTOM, 6 IN.	2.65000	0.05000	2.33431	2.96569	1.15000	0.05000	0.83431	1.46569	MG/KG
TEST 1	POSTTEST	SOIL	SIDE, 12 IN.	2.50000	0.10000	2.20800	2.79200	3.00000	1.90088	-2.55053	8.55053	MG/KG
TEST 1	POSTTEST	SOIL	SIDE, 6 IN.	2.45000	0.05000	2.13431	2.76569	1.05000	0.05000	0.73431	1.36569	MG/KG
TEST 2	POSTTEST	SOIL	BOTTOM, 12 IN.	2.60000	0.05774	2.43141	2.76859	.	.	.	.	MG/KG
TEST 2	POSTTEST	SOIL	BOTTOM, 6 IN.	2.45000	0.15000	1.50294	3.39706	.	.	.	.	MG/KG
TEST 2	POSTTEST	SOIL	SIDE, 12 IN.	2.20000	0.00000	2.20000	2.20000	.	.	.	.	MG/KG
TEST 2	POSTTEST	SOIL	SIDE, 6 IN.	2.00000	0.00000	2.00000	2.00000	.	.	.	.	MG/KG

- any difference is confounded by possible high bias in laboratory pretest Dy measurements

- statistical detection of a difference in means is dependent on the number of samples (few samples can only detect a large difference) and also on the error risk assumed in performing the tests

- the composite sampling method used does not provide a good estimate of the spatial variability that may be present.

Each composite represents a relatively large volume of soil and has detectable Dy and Yb. No attempt is made here to estimate the amount of tracers in the soil, which is expected to contribute to error in the mass balance calculations.

6.8 Test 1 Tracer Summary

The tracer concentration appears to be relatively evenly distributed throughout the vitreous and crystalline phases in the product. The tracer concentrations reported are 172-201 ug/g for Dy, 209-267 ug/g for Tb, and 325-396 ug/g for Yb, which correspond to respective amounts of 1538, 1968, and 3009 g in the product. The latter numbers substantially exceed the buried amounts (1164 g for Dy, 1137 g for Tb, and 1169 g for Yb). However, it should be noted that the calculation of total product amounts is based on the entire product mass. Although data from core samples show homogeneity of the product, it is likely that areas near the edges of the melt, where convective mixing is less, may contain reduced concentrations of tracers.

Tracers were found to have been deposited in the hood and no significant difference was detected between the top and bottom smear averages. The estimated total amounts are 1.73-3.17 g for Dy, 0.63-1.93 g for Tb, and 2.05-3.3 g for Yb. The tracer Dy was found on the air inlet filter, indicating that entrainment could be a significant transport mechanism. Tracers were also found to have been deposited in the off-gas duct. Order of

magnitude calculations indicate that approximately 3 g of Dy, 28 g Tb, and 9 g of Yb may have accumulated in the duct during Test 1.

Results of tracer analysis of off-gas scrub solutions show that tracers occur in the scrub solution as the melt reaches the depth of tracer burial. The fate of the tracers in the scrub solution is unclear; however, the primary HEPA filter downstream contained little or no tracer.

Based on limited posttest soil sampling, it appears that there are no significant differences between tracer pretest soil concentrations and concentrations derived from soil samples collected at specific distances from the block.

The product appears to account for most of the originally buried amounts of tracers; however, because the product analyses were performed at a different laboratory than all other analyses, this could account for some of the observed distribution. The relative amounts of the tracers (Yb > Tb > Dy) in the scrub solution is similar to relative tracer amounts in the product; this curiosity at present has no explanation.

6.9 Test 2 Tracer Results

Product

The results of tracer analysis of product samples from Test 2 are given with Test 1 data in Table 29. As expected, all Tb and Yb measurements, which were not added to Pit 2, are reported as less-than-detection (there are three exceptions, but the reported values are very low). Note that no Dy is detected in metal samples; however, because the data have questionable quality, it is not necessarily proven that this is indicative of a pattern in the partitioning of Dy in the phases of the product.

Table 30 gives 90% confidence limits for the mean of glass and crystalline samples with results that are of acceptable quality.[a] The limits for Dy are (170, 181), which is a relatively small interval. This indicates there is small variation in Dy between samples, which in turn suggests that Dy is relatively evenly distributed throughout the nonmetal phases of the product. The Dy confidence interval overlaps substantially with that for Test 1, indicating that there is no difference between nonmetal product sample means between tests. This is especially interesting since the amount of Dy added to Pit 2 was greater than that added to Pit 1.

The mass of the Test 2 product has been estimated at 17,430 kg; the amount of Dy in the product is estimated at 2,929-3,155 g, or 3,362-3,621 g Dy_2O_3. As in the calculations for Test 1, these values greatly exceed the amount originally buried (2282 g Dy_2O_3). However, as noted for Test 1, the total product amounts are based on the assumption of homogeneity throughout the entire product mass. Although the data from case samples show homogeneity of the product, it is likely that areas near the edges of the melt, where convective mixing is less, may contain reduced concentrations of tracers.

Hood

Table 31 shows that hood smear blanks for Test 2 had detectable amounts of Dy, Tb, and Yb. The amounts detected are at levels lower than the detection limit in Test 1, however. The results in Table 32 of the hood tracer analyses show detectable amounts for all three tracers, although two of the side smears are anomalously low. Table 33 gives the means and estimates of variability of the data. As for Test 1, there is not a significant difference between averages of the top and sides of the hood. A 90% confidence interval for the mean of smears in the hood in ug is (82, 900) for Dy. This range is lower than the Dy interval for Posttest 1, indicating that there is higher variability in Posttest 2 smears.

The top of the hood shows apparent decreases in smear means from Test 1 to Test 2 for Dy, Tb, and Yb, but there is not a significant difference in the

---

a. One Dy data point, of grey aphanitic material, was removed from the data set used for the calculation because it was reported as less-than-detection; this will slightly bias high the statistics given.

means. This result is unexpected because Dy was added to the Test 2 pit. There are at least two possible explanations for this. Either Dy did not accumulate in the hood during Test 2 or the movement of the hood between tests caused Dy to be removed from hood panels, and a comparable amount was added during the test. Laboratory biases are believed to be too small to account for the observed pattern.

A smear was taken of an electrode inside the hood after Test 2. The sampled electrode was one of two (A2 and B2) that showed a red-flaked coating of soft rust-colored flakes. Tracer analysis results of the electrode smear are given in Table 38. Relative to other smears collected in the hood after Test 2, this single sample appears low but similar to two of the hood side smears.

Using hood surface area calculations and the Posttest 2 hood smear data, the estimated amount of Dy in the hood after Test 2 is 0.28-3.1 grams. This amount is not appreciably different from the amount calculated for Posttest 1.

Off-gas Duct

The tracer analyses for off-gas duct smears are presented in Figure 106. The data are insufficient to determine a pattern or meaningful average. There does appear to be a difference between Posttest 1 and Posttest 2 data points; however, this difference cannot be confirmed with the available data. Note that Dy is present at the same order of magnitude as the other tracers, which was not added to the pit. This phenomenon can be seen in the Test 2 hood data also.

A sample of a large barnacle-like buildup of solids at the inlet to the venturi was collected. Tracer analysis[a] of the material is given in Table 39. The buildup indicates heavy particle loading during operations.

---

a. Analytical quality control was adequate except that laboratory control sample was not run. Matrix spike recoveries are poor, but post digestion matrix spike recoveries are acceptable.

Table 39. Miscellaneous tracer analyses

Location	Time	Smear Location	Dy	Dy Flag	Tb	Tb Flag	Yb	Yb Flag	Units
TEST 2	POSTTEST	ELECTROBE SMEAR	1.80		10.20		11.60		UG
TEST 2	POYTTEST	TRAILER PORT	2.20		149.00		123.00		MG/KG

An estimate for the amount of Dy in the off-gas duct calculated as for Test 1 with the accompanying qualifications is 0.8 grams.[a] This value is an order of magnitude less than that calculated for Test 1.

Off-gas Scrub Solution

The tracer analytical results for field duplicates are presented in Table 34. The results for duplicate set numbers 7 and 9 are acceptable (see Section 6.7), but the error in duplicate set number 8 is extremely high (duplicate analyses were 100% of the mean of the duplicates or greater).

The method for calculating the amounts in the Test 2 scrub tanks is the same as for Test 1; tank volumes are used and are believed to introduce error in the results. In addition, there was a tank overflow during Test 2, which calls into question the reliability of all of the data. Heavy particulate loading in the off-gas is believed to be responsible for scrub tank delta pressure level indicator line plugging and the difficulty in getting good flow rate through tank sample lines. Separately, the analytical quality control indicates that bias is present in differing amounts.

The available, if questionable, tracer amounts are plotted in Figure 108 with hours from the start of the test. The depth of the melt front and Dy burial depth are also shown. There is no apparent release of Dy during the test, and all three tracers exhibit a similar pattern. There is also no apparent difference[b] between pretest and posttest (actually last available data point) values, which are shown in Table 35. The magnitudes of the amounts in the scrub tanks during the test are all much less than peak values for Test 1. The data appear to represent residual tracer amounts from Test 1. Note that the three tracers show the same general pattern. Since terbium oxide and ytterbium oxide were not added to Test Pit 2, their total amounts in the scrub solution would be expected to be relatively constant. The fact that

---

a. The mean value used is 1061 ug.

b. No direct estimates of uncertainty are available to test this hypothesis.

all three tracers show the same pattern may reflect an inaccurate level indication. During processing, the tank level fluctuates based on relative amounts of evaporation and condensation in the scrub system. Inaccurate level measurements would equally affect the calculated amounts of any elements not being added or subtracted from the system. This is possibly the case for the data shown in Figure 108.

Despite the above considerations regarding the tank level measurement, the data for dysprosium in Figure 108 suggest that a significant amount of Dy did not enter the off-gas system during Test 2.

Filters

The primary HEPA filter tracer analysis for Test 2 is given in Table 36. All of the tracers were detected, even those added to Test Pit 1 and not Test Pit 2. The tracer added to Test Pit 2 (Dy) was present at levels comparable to those added to Test Pit 1 and not Test Pit 2, indicating that Test 2 may not have contributed to HEPA filter tracer amounts. The upper 90% confidence limit for Dy, 1.28 mg/kg, implies that only about 4.3 mg Dy was retained on the 3.36 kg filter.

Soil

Table 36 shows that Dy was detected in posttest 2 composite soil samples. As in the posttest 1 soils, there are no differences between the mean Dy concentration in pretest soils and the mean of composite splits for each compositing situation (means the given in Table 37). The comments concerning the meaning of the "no differences" statement that are discussed in the soil section for Test 1 apply here. That is, differences may be present and simply not detected with the sampling strategy used and potential for laboratory bias in sample results.

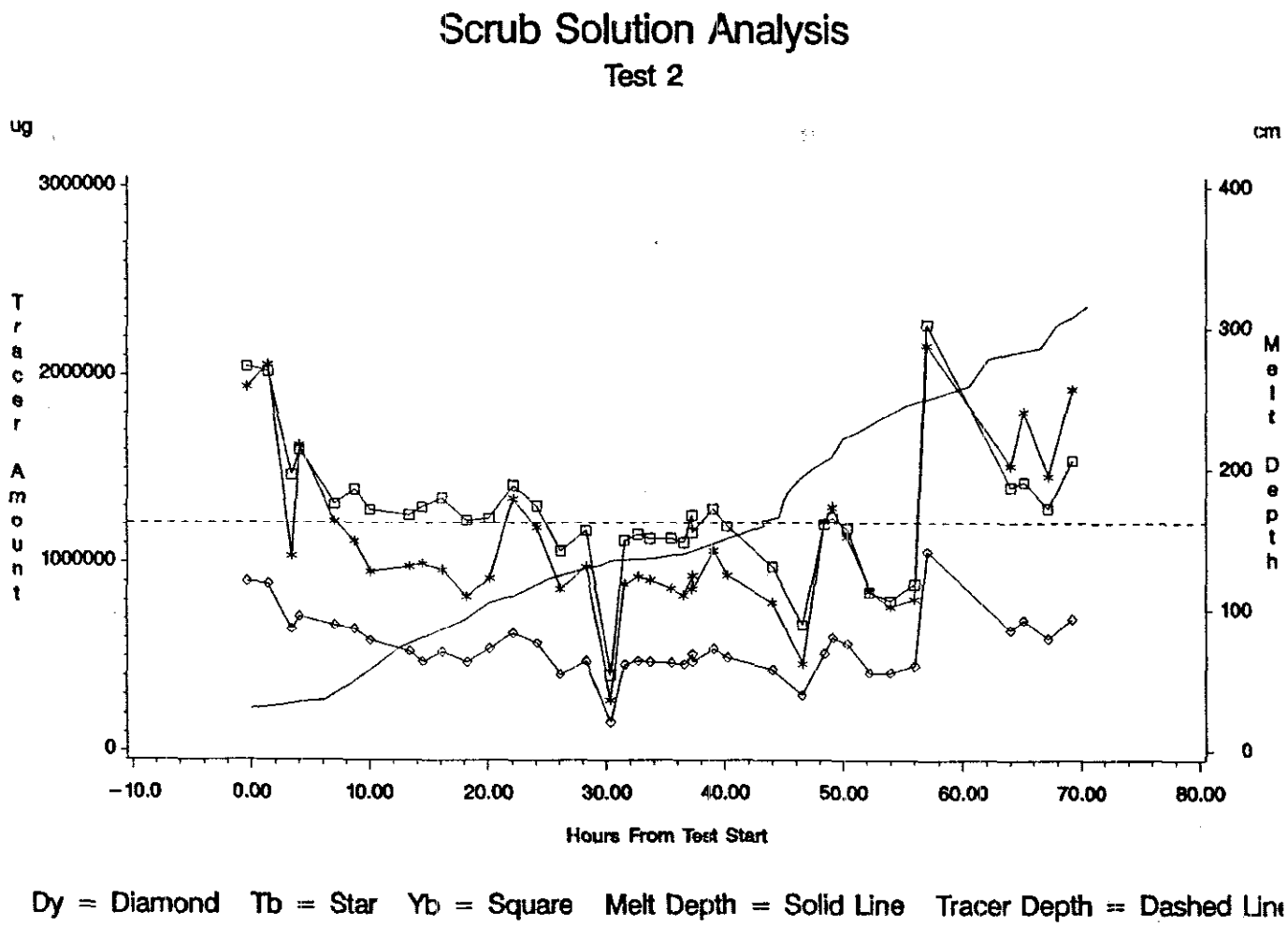

Figure 108. Amounts of tracers Dy, Tb, and Yb in scrub solution and melt depth during Test 2. Dashed line shows depth of burial of Dy.

6.10 Test 2 Tracer Summary

As in Test 1, the Dy concentration of the nonmetal phases of product appears to be relatively evenly distributed in the product. The Dy concentrations reported are 170-181 ug/g, which corresponds to 2929-3155 total grams of Dy in the Test 2 product. Also as in Test 1, the latter number is considered to be in error, considering that it substantially exceeds the buried amounts. The observed concentrations do not appear to be different from those observed in Test 1.

Hood and duct smear data and HEPA filter data indicate that Dy may not have entered the off-gas system. This may also be supported by scrub tank data, but quality control problems complicate this assessment.

Based on limited posttest soil sampling (the same as in Test 1), it appears that there are no significant differences between tracer pretest soil concentrations and concentrations derived from soil samples collected at specific distances from the block.

6.11 General Summary of Test Tracer Results

The tracer study results were reviewed to determine if differences in tracer behavior during ISV processing could be concluded to result from the differences in pit configuration between the two tests or operational differences during ISV processing of the two pits. Significant differences between the configuration of the two pits that may likely influence release characteristics include the additional 0.6 m (2 ft) of overburden in Pit 2, and the stacked layered waste in Pit 2 as compared to the randomly-dumped Pit 1 waste. Significant operational differences between the two tests include the more rapid processing of Pit 1 as compared to Pit 2. Test 2 operations were intended to minimize the pressurizations observed in Test 1. In Test 2, the stacked can region was observed to have heated up in a relatively uniform manner with few transient spikes as compared to Test 1.

The differences in pit configuration and test operations could well have influenced released tracer amounts. However comparison between tests is confounded by the use of three different tracers in Test 1 as compared to one tracer in Test 2. Also, the one common tracer between the two tests (Dy_2O_3) was buried at different depths in the two tests. Additionally, several aspects of the sampling for Test 2 restrict interpretation. The use of the posttest smear data from Test 1 as pretest smear data for Test 2 is suspect. It is possible that material may have been lost during movement of the hood (after posttest 1 smearing) and the data suggest this possibility and reduces the confidence in the hood smear data for Test 2. The scrub data results from Test 2 are also called into question by the problems experienced with the tank level transducer.

Despite the sampling concerns, the data suggest that tracer release for Test 2 is lower than Test 1. This is possible due to the test difference noted above which may act to promote retention of elements in the glass. A less quiescent melt with more active gas releases, such as in Test 1, may promote more entrainment and release of elements into the off-gas system.

Previous data from ISV tests at PNL (see Reference 2) have suggested that elements at greater depth are retained preferentially in the melt. This is consistent with the apparent reduced release of tracer in Test 2 compared to Test 1. However as indicated above, there are too many differences between tests to allow for conclusions regarding effect of depth on released amounts for these tests. Also it is noteworthy that the data from Test 1 show that the tracers at greater depth were released into the off-gas system in greater amounts. Since the three Test 1 tracers were different chemical elements, the different released amounts may possibly be entirely due to chemical transport in the tracers. It appears that further testing is warranted to establish the relationship, if any, between element release and initial depth below ground surface.

A direct extrapolation of these test results to plutonium behavior is not possible. Empirical data do not exist from which quantitative predictions of Pu behavior could be drawn from data involving rare-earth tracers. Nevertheless the data presented indicate that the vast majority of the tracer

elements are retained in the melt; this is consistent with previous data reported by PNL (see Reference 2) for Pu and other elements. Order-of-magnitude estimates for amounts of tracer materials released into the off-gas system for Test 1 were several grams to several tens of grams. This corresponds to up to several percent of the amounts initially added to the pit.

Further experimental work will be necessary if it is desired to make quantitative estimates of Pu release during buried waste ISV processing.

7. ANALYTICAL MODELING OF HOOD TRANSIENTS

Hood pressure and temperature spikes were observed in both Test 1 and Test 2 (see Figures 22 and 70). In several instances the pressure spikes were of sufficient magnitude to result in positive pressure within the hood plenum.

The occurrence of pressure and temperature spikes during processing of buried waste was a key observation from these tests. There has been some previous data for ISV of combustible materials (see Reference 2) but the data did not show the sharp spikes observed in these tests. The occurrence of pressure and temperature spikes within the hood plenum is of concern because of the potential to exceed the design limits of the hood. Additionally, the occurrence of positive pressure in the hood provides a driving force for gas release from the hood that bypasses the off-gas treatment system. Such gas release has the potential to release hazardous materials to the environment.

The current tests, being designed to simulate representative SDA buried waste conditions, were not specifically designed to collect data for determining the mechanisms which resulted in the hood plenum transients. Nevertheless, an attempt has been made to model the transients analytically in order to understand the contributing factors for the spikes.

7.1 Energy Flows in the Hood

Figure 109 shows a model of the energy inflows and outflows to the hood plenum. The energy flows are described as follows:

1. Energy convection due to inlet airflow. This energy flow into the hood plenum can be estimated based on knowledge of ambient temperature and inlet airflow rate. However, no direct measurement of inlet airflow is available. Measurements of flow were taken at the stack outlet. However, note the following equation:

$$\dot{m}_{stack} = \dot{m}_{inlet} + \dot{m}_{melt}$$

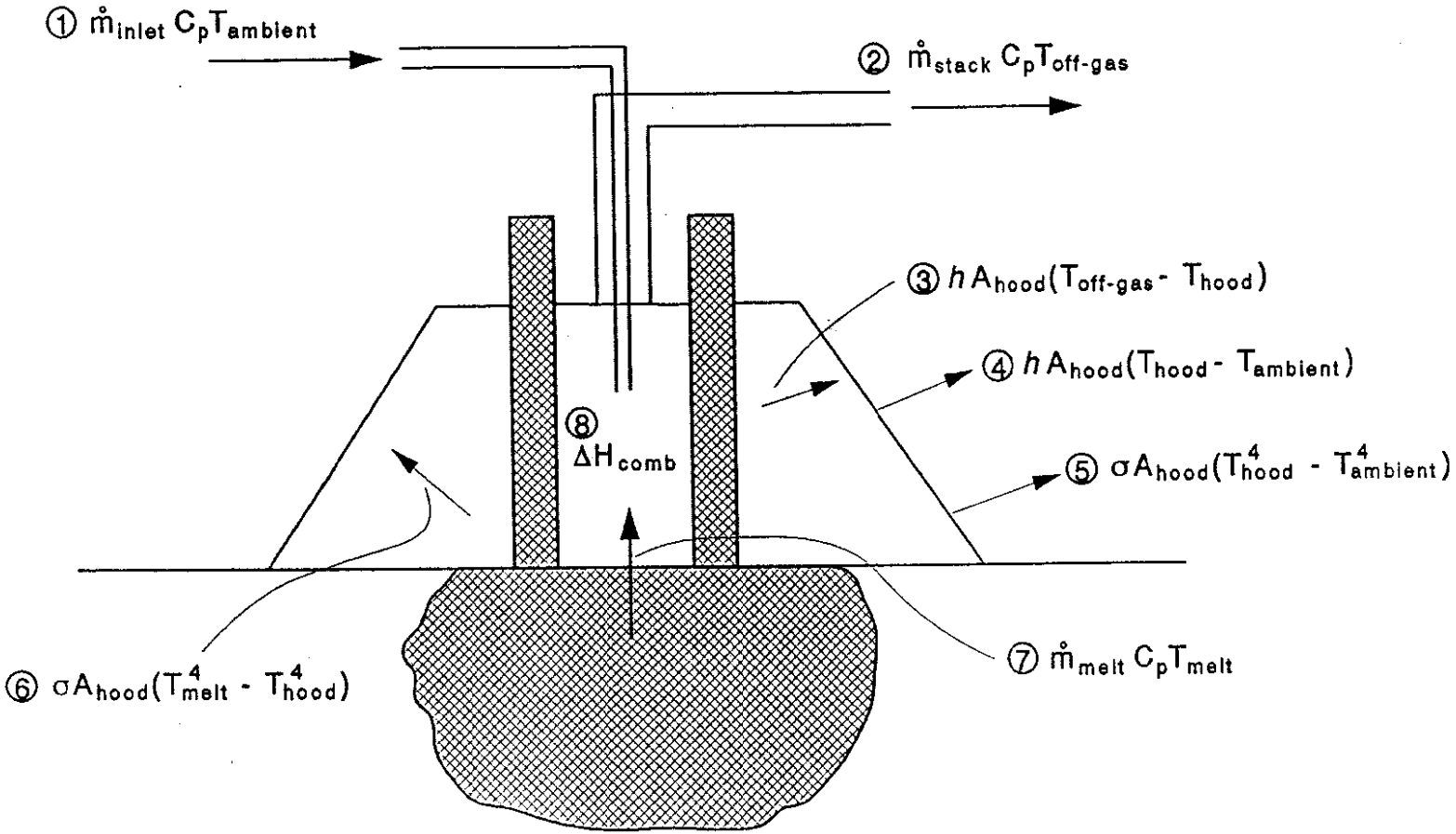

Figure 109. Schematic of energy flows in the hood plenum.

The relative contributions to the total flow of $\dot{m}_{inlet}$ and $\dot{m}_{melt}$ are not known. Additionally, the inlet flow itself is a combination of flow through the inlet air line and leakage flow through the hood panels or through the soil. In order to obtain an accurate measurement of $\dot{m}_{inlet}$, it would be necessary to measure flow in the inlet air line and eliminate (minimize) leakage flow through the hood and soil. The total amount of $\dot{m}_{melt}$ is a result of gases released directly from the melt as well as gases released along the sides of the melt; the temperatures of these two streams will be different. (It is assumed that direct measurement of $\dot{m}_{melt}$ is not feasible; it could be calculated if accurate measurements of $\dot{m}_{stack}$ and $\dot{m}_{inlet}$ were available.)

2. Energy convection due to air outflow. This energy flow is available because stack flowrate and temperature were recorded and off-gas temperature was recorded. It would be preferable (in future tests) to measure both temperature and flowrate in the off-gas pipe, as opposed to using the stack flowrate measurement.

3. Convection of heat from the off-gas air in the plenum to the hood surface. The driving force for this mode of heat transfer is the temperature difference between the plenum internal air and the hood surface. The air flow within the hood will result in forced convection; however the overall contribution of this heat transfer mode is probably lower than the other contributors.

4. Convection of heat from the hood surface to ambient air. The driving force for this mode of heat transfer is the temperature difference between the hood surface and the external ambient air. The overall contribution of this heat transfer mode is probably small relative to other contributors.

5. Radiation from the hood surface to the environment. This energy term can be calculated based on knowledge of the hood external surface temperature and ambient temperature.

6. Radiation from the melt surface to the hood and (particulate-laden) air. This term cannot be directly quantified from the available data; however it may be a significant contributor to plenum heatup, particularly when the melt cold cap is disrupted. Data from the processing of the instrumental can in Test 2 (see Section 4.4.1) suggest that steam release and associated cold cap disruption and subsequent radiation may have resulted in the observed hood plenum heatup. This hypothesis is also supported by data from an underground tank ISV test in which plenum heatup was observed in the absence of combustible materials.[33]

7. Superheat of gases released from the melt. This term cannot be directly quantified because no value for $\dot{m}_{melt}$ is available (see above). Were a value for $\dot{m}_{melt}$ available, an estimate of the gas temperature could be used in order to approximate the energy contribution of the hot gases being introduced into the plenum. It is possible this term may be a significant source of energy during transient surge releases of gases from the melt. Particularly in the case of steam release from the melt (where no heat of combustion contributes), the relative amount of superheat energy may be large. As indicated above, steam release likely contributed to some transient hood heatup observed in these tests.

8. Heat of combustion of pyrolysis gases being oxidized at the melt surface. The energy resulting from combustion of pyrolysis gases in the presence of oxygen introduced by the air inlet line is a major contributor to hood temperature and pressure spikes.

7.2 Modeling Uncertainties

Attempts to analytically model the transient spikes within the hood were hampered by the inability to validate key assumptions in the models used. Several areas of notable uncertainty were as follows:

- Inability to differentiate between radiative heating and combustion. Initial thoughts were that radiation was negligible as a mechanism of gas and hood heatup and resultant pressurization. However, this assumption has been called into question. Preliminary evaluation of a pilot-scale ISV test conducted at Hanford (see Reference 33) indicated that radiation may be signififcant as a heatup mechanism. It is postulated that gas release from the melt may disrupt the cold cap and increase the amount of radiative flux. Although clean air would be largely transparent to the radiation, the presence of large amounts of particulate in the air may result in absorption of the radiation and rapid heatup.

- Inability to quantify gas release rates from the melt. Original analytical efforts focussed on determining gas release rates from the melt that would result in the observed hood response. These attempts assumed complete combustion as one mechanism for energy input. Other mechanisms were heat capacitance of the gas released from the melt, and convective flows of inlet and outlet air. The assumption of complete combustion is not valid; the data showing off-gas spikes of CO, CO_2 and O_2 indicate that combustion is not complete. Thus, it was not possible to determine gas release rates from the melt by inference from pressure/temperature spikes. Note that it is not possible to directly calculate gas release rates from the melt because the rate of air inflow was not monitored; only the stack flowrate was measured. Air inflow is not a straightforward measurement due to the large magnitude of leakage through hood joints and through the soil around the base of the hood. In addition, the gas released from the melt may either be released by bubbling up through the melt itself, or by flowing through the porous dry soil zone at the periphery of the melt and being released at the edges of the melt surface. The temperature of released gas will be different depending upon its release path.

The above discussion indicates that the attempt to analytically model the temperature and pressure transients within the hood and obtain a quantitative match with the data was not fruitful. This is not particularly surprising since the tests were not designed to obtain separate effects data on transients. These tests were the first field tests conducted on buried waste and, as such, provided the first data indicating that pyrolysis gas release and subsequent combustion of buried combustible waste may result in significant spikes of pressure and temperature in the hood. Further tests will be necessary to delineate the physical mechanisms of gas release from the melt and combustion. Understanding these mechanisms is necessary in order to have the necessary degree of understanding and predicive capability to support ISV processing on contaminated buried waste.

7.3 Discussion of Differences Between Tests

Several qualitative differences between the transient pressure and temperature spikes in Test 1 and Test 2 should be noted. In general, the spikes observed in Test 1 were more numerous and more severe. This may be due to the faster melt rate, less overburden, and absence of uniform heatup of the waste region for Test 1 as compared to Test 2. Additional testing and/or analytical modeling will be required to establish the differences in off-gas transients under different operational and waste pit configurations.

An additional noteworthy observation is that spiking appeared to be less severe at later times during the test. This would support hypothesis that greater overburden may result in lessening of transient spikes. During later parts of a test, the amount of melted glass is larger. This may offer some buffering of gas release rates from the melt and thus act to reduce the severity of spikes. Again, further testing and modeling is needed to confirm this hypothesis and establish the significant physical mechanisms.

7.4 Recommendations for Future ISV Off-Gas Tests

Based on the results of analytical efforts for these tests, some recommendations can be made for test design and data collection for future test efforts. These are as follows:

- Quantify completeness of combustion within the hood by more accurate measurement of off-gas composition. The composition should be measured in the off-gas line upstream of the scrub system.

- Obtain accurate measurements of air inflow. This may require careful attention to prevention of leakage through the soil at the base of the hood. A flow measurement device should be placed in the air inlet line.

- Determine/estimate the magnitude of the transient heatup contribution due to radiation from the melt to the hood and plenum gases. As indicated above, there is evidence that radiation may provide a significant contribution to hood transients.

- Determine the magnitude of plenum heatup resulting from release of superheated steam (or other gas) from the melt (or from sides of the melt) into the hood plenum. The heatup from the gases must be decoupled from the increase of radiation energy which may result from melt bubbling disrupting the melt surface.

- Consideration should be given to design of techniques to measure rates of gas release through the melt or around the sides of the melt.

It is anticipated that future testing and analytical studies will provide insight required to understand the mechanisms resulting in hood plenum heatup and pressurizations. Based on this understanding designs may incorporate features to reduce or prevent transient positive pressure spikes within the hood.

8. CONCLUSIONS

Based on analyses of test data, the following conclusions are made relative to the application of ISV to buried waste.

General

- In situ vitrification is a feasible technology for application to buried wastes. The process incorporated and dissolved simulated waste containers into the melt to produce a durable glass and crystalline product. The electrode feed technology was successful in processing the high metal content waste.

- Refinements in equipment design are needed for production scale processing equipment.

ISV Processing

- The small volume of glass in Test 1 due to extensive subsidence (densification) resulted in electrical instabilities for the intermediate-scale transformer during periods of gas releases and encounters with waste containers in the melt. A large volume of glass associated with a large-scale application combined with independent two-phase control of the transformer, and uncoated electrodes will likely result in electrically balanced transformer operations.

- Because the coated graphite electrodes in Test 1 stuck to the frozen layer of glass covering the melt, uncoated graphite electrodes appear to be preferable to silica-based coated graphite electrodes. This sticking created unacceptable electrical conditions with the inability to adjust electrode positions. The extent (rate) of graphite oxidation of uncoated electrodes appears to be acceptable.

- Consistent with the rapid rate of downward melt growth experienced in the two tests, the volume of water vapor condensed in the process off-gas treatment system nearly exceeded the evaporative capability of the intermediate-scale system. Large-scale machine designs for buried wastes will require an increased evaporative capability relative to current designs to prevent the accumulation of secondary liquid wastes.

- Evidence does not support the likelihood of underground fires, unless there is a sufficent oxygen source from outside of the melt boundaries. Even with oxygen present, the consequences of underground fires in buried waste are expected to be minor due to their localized nature.

- Subsidence of the vitrified area was significant relative to previous ISV applications. This densification resulted in the uncovering of adjacent waste material along the perimeter of the vitrified zone. It is desirable to incorporate into the equipment design the ability to add glass-forming materials (soil) during processing to prevent adjacent waste from being uncovered. The hazards of posttest activities would be increased if uncovered wastes exists.

- Incomplete processing of the waste may occur at the edges of the vitrified zone. For a production-scale application of ISV to buried wastes, sequential overlapping processing locations would result in multiple blocks being fused together into a single large monolith.

- Increased levels of particulate generation in the off-gas were apparent relative to previous ISV applications at contaminated soil sites. Consequently, the design of a large-scale system should address the particulate buildup that was observed in the small diameter piping, tanks, and scrubber spray nozzles.

- Stacked metal waste layers or large metal objects offer the potential to promote lateral and vertical heat transfer. Soil

provides a high resistance to heat transfer, which results in steep thermal gradients near the melt front boundary. In stacked waste layers or high metal regions, thermal energy may be more readily transferred away from the immediate melt front boundary. In Test 2, the downward melt growth, as evidenced by electrode depth, was slowed while the stacked can region was heating up. It appeared that the downward melt growth was hindered until the stacked can region had sufficiently heated to vaporize water present in the region, then the downward progression of the melt resumed. A positive aspect of this phenomenon is that the stacked can layer in Test 2 gradually heated and released pressurized gases to the surrounding soil well ahead of the advancing melt front. This apparently resulted in a decrease in the severity of the temperature and pressure spikes compared to those observed in Test 1.

Hood Pressure and Temperature Spikes

- A robust off-gas processing system will be required to effectively contain the off-gases inside the hood. The hood must be designed to accommodate the relatively slow developing pressure spikes created by gas releases from containers, combustion, and thermal expansion of gas. The pressure spikes experienced in Tests 1 and 2 were not characteristic of detonations that produce rapid pressure spikes. The hood must be capable of withstanding contact from splatter of molten glass and must be capable of accommodating short duration gas temperatures in excess of 700°C.

- Test 1 results indicated that waste buried at greater depths had less impact on the transient temperature and pressure spikes than waste buried near the surface. Consequently, it is desirable to incorporate a means into the equipment design to add glass-forming materials during processing. In addition, an adequate amount of cover soil over the buried waste is essential to ensure adequate glass volume exists as glass flows into voids. Sufficient glass volume will buffer the effects of the transient temperature and pressure spikes and act to limit electrical instabilities.

- Further testing and analyses will be necessary to delineate the physical mechanisms of gas release from the melt and combustion. Understanding these mechanisms is necessary in order to have the necessary degree of understanding and predictive capability to support ISV processing on contaminated buried waste. Future test and data collection design should provide for measurement of heat transfer effects from combustion, radiation, and superheat of melt gases. Hood inlet and outlet flows and composition require accurate measurement.

ISV Product

- Based on MCC-1 leach testing data, the durability of the IFT waste form is comparable to obsidian and granite, and 4 to 10 times more durable (based on MCC-1 testing) than typical high-level nuclear waste glasses.

- Preliminary results from intrinsic rate constant measurements using pH stat/ISE and soxhlet extraction methods showed that the intrinsic dissolution rates of the ISV samples range from 0.01 to 0.06 $g/(m^2 \cdot d)$ at 90°C and pH 7. These intrinsic dissolution rate values are 10 to 100 times smaller than measured for a typical borosilicate nuclear waste glass.

- During cooling, devitrification occurred within the glass monolith producing a feather-like crystalline phase called augite. The mineral augite, a variety of clinopyroxene, is a calcium-magnesium-iron rich silicate. Augite is a common, naturally occurring pyroxene found in volcanic rocks, such as the basaltic rocks found at the INEL, which have compositions and cooling histories similar to the vitrified material in the Intermediate Field Tests reported here.

- Differences in durability corresponded to the degree of crystallinity in the samples. Samples that appeared to the eye to be completely devitrified (approximately 50% volume) show consistently lower releases for Ca, Mg, Al, and Si compared with

samples that analyzed x-ray amorphous. The releases of Ca and Mg are as much as two to three times smaller for the other devitrified samples. This difference may be due to smaller dissolution rates for the glass matrix, the crystalline phase(s), or both. Smaller dissolution rate constants appear to be the most likely cause for the smaller releases observed with the devitrified IFT samples. Because most of the ISV monolith is devitrified and no waste component segregation was observed, the lower release rates for the devitrified phase of the ISV waste form will result in a lower (than all glassly phase) overall release source term for heath-based risk assessments.

- Solids characterization of the ISV products showed that the ISV melts are reducing waste, resulting in Fe^{2+}/Fe ratios >90%. Under equivalent closed-system conditions, as might occur during the slow migration of water through cracks in the solid mass, the reaction of the ISV glass with water reduces the redox potential to the lower stability limit of water. Under these conditions, several redox sensitive elements, such as Se and Pu, are expected to be sequestered in an alteration layer on the glass surface resulting in a smaller predicted release rate than calculated from the matrix dissolution rate alone.

- TCLP testing was conducted to document that the ISV waste form could be disposed of in a landfill. The IFT waste forms do not exhibit hazardous characteristics of TCLP toxicity. In most cases, the TCLP results are below detection limits or 10 to 100 times lower than the maximum acceptable concentrations. Two metal samples (taken from the bottom of pit 2) have TCLP leachate concentrations 10% to 20% of the maximum acceptable concentration for chromium. This is thought to be due to the stainless steel in the samples.

Tracer Study

- Order-of-magnitude estimates for amounts of tracer materials released into the off-gas system for Test 1 were several grams to several tens of grams. This corresponds to up to several percent of the amounts initially added to the pit. The data suggest that during buried waste ISV processing, the release of rare-earth tracers in the melt is greater than values previously reported for plutonium release during processing of contaminated soil. These tests are inconclusive regarding the amount of expected Pu release associated with ISV processing of buried waste. Additional efforts are required to assess the adequacy of these tracers to simulate Pu compounds found in buried waste. Similarly, additional theoretical insight is needed in understanding the mechanisms of contaminant release from the melt.

9. REFERENCES

1. D. A. Arrenholz and J. L. Knight, A Brief Analysis and Description of Transuranic Wastes in the Subsurface Disposal Area of the Radioactive Waste Management Complex at INEL, EGG-WTD-9438, February 1991.

2. J. L. Buelt et al., In Situ Vitrification of Transuranic Wastes: Systems Evaluation and Applications Assessment, Battelle Pacific Northwest Laboratory, PNL-4800, Supplement 1, 1987.

3. K. H. Oma et al., In Situ Vitrification of Transuranic Wastes: Systems Evaluation and Applications Assessment, Battelle Pacific Northwest Laboratory, PNL-4800, 1983.

4. J. O. Low, Annual Technology Assessment and Progress Report for the Buried Transuranic Waste Program at the Idaho National Engineering Laboratory, EGG-2429, December 1989.

5. T. L. Clements, Jr., Content Code Assessments for INEL Contact-Handled Stored Transuranic Wastes, WM-F1-82-021, October 1982.

6. J. R. Bishoff and R. J. Hudson, Early Waste Retrieval Final Report, EG&G Idaho, Inc., TREE-1321, August 1979.

7. K. B. McKinley and J. D. McKinney, Initial Drum Retrieval Final Report, EG&G Idaho, Inc., TREE-1286, August 1978.

8. S. S. Koegler, Disposal of Hazardous Wastes by In Situ Vitrification, Battelle Pacific Northwest Laboratory, PNL-6281, 1987.

9. S. O. Bates, In Situ Vitrification Waste Form Product Evaluation Strategy, EGG-WTD-9148, August 1990.

10. U.S. Environmental Protection Agency, "Toxicity Characteristic Leaching Procedure (TLCP)." 40-CFR-268, Appendix I, U.S. Federal Register. Washington, D.C., 1988, Pg. 724-738.

11. U.S. Federal Register, Vol 55 #61, March 29, 1990, pp. 11798-11877.

12. B. P. McGrail, S. O. Bates, "An Evaluation of In-Situ Vitrification for Remediation of a Buried Waste Site," Seventh International Conference on the Physics of Non-Crystalline Solids, Cambridge, England, August 1991.

13. Materials Characterization Center, "MCC-1P Static Leach Test Method." In Nuclear Waste Materials Handbook. Test Methods. DOE/TIC-11400, Rev. 7, Technical Information Center, Springfield, Virginia, 1986.

14. Materials Characterization Center, "MCC-3S Agitated Powder Leach Test Method." In Nuclear Waste Materials Handbook. Test methods. DOE/TIC-11400, Rev. 7, Technical Information Center, Springfield, Virginia, 1986.

15. C. M. Jantzen, and N. E. Bibler, Product Consistency Test (PCT) for DWPF Glass: Part 1. Test Development and Protocol, DPST-87-575, Savannah River Laboratory, Aiken, South Carolina, 1987.

16. J. L. Dussossoy, "R7T7 Glass initial Dissolution Rate Measurements Using a High-Temperature Soxhlet Device." In Scientific Basis for Nuclear Waste Management XIV, Materials Research Society, Pittsburgh, Pennsylvania, 1991.

17. C. H. Kindle, and M. R. Kreiter, Comprehensive Data Base of High-Level Nuclear Waste Glasses-September 1987 Status Report. Volume 1 - Discussion and Glass Durability Data. PNL-6353, Vol 1. Pacific Northwest Laboratory, Richland, Washington, 1987.

18. B. Grambow, "A General Rate Equation for Nuclear Waste Glass Corrosion." In Scientific Basis for Nuclear Waste Management XIV, Materials Research Society, Pittsburgh, Pennsylvania, 1985.

19. B. P. Mcgrail, A conjoint Geochemical-Mass Transport Model for Near-Field Radionuclide Release Calculations, PNL-6174, Pacific Northwest Laboratory, Richland, Washington, 1987.

20. J. G. Carter, S. O. Bates, and G. D. Maupin, In Situ Vitrification of Oak Ridge National Laboratory Soil and Limestone, PNL-6174, Pacific Northwest Laboratory, Richland, Washington, 1987.

21. B. C. Bunker, G. W. Arnold, E. K. Beauchamp, and D. E. Day, "Mechanisms for Alkali Leaching In Mixed Na-K Silicate Glasses." J. Non.-Cryst. Solids, 58:295-322, 1983.

22. N. Kawanishi, H. Igarashi, H. Nagaki, and N. Tsunoda, Leaching Test on Chemical Durability of Glasses Containing Simulated High Level Wastes, PNCT N831-80-01, Power Reactor and Nuclear Fuels Corporation, Japan, 1980.

23. K. Ishiguro, F. Kamei, N. Sasaki, and H. Nagaki, Long-Term Soxhlet Leach Tests of Simulated Waste Glasses (I). PNCT N831-83-01, Power Reactor and Nuclear Fuels Corporation, Japan, 1983.

24. F. Delage, F. and J. L. Dussossoy, "R7T7 Glass Initial Dissolution Rate Measurements Using a High-Temperature Soxhlet Device." In Scientific Basis for Nuclear Waste Management XIV, Materials Research Society, Pittsburgh, Pennsylvania, 1991.

25. B. C. Bunker, G. W. Arnold, E. K. Beauchamp, and D. E. Day, "Mechanisms for Alkali Leaching in Mixed Na-K Silicate Glasses." J. Non-Cryst. Solids, 58:295-322, 1983.

26. J. Schott, R. A. Berner, and E. L. Sjoberg, "Mechanism of Pyroxene and Amphibole Weathering - I. Experimental Studies on Iron-Free Minerals." *Geochim. Cosmochim, Acta* 45:2123-2135, 1981.

27. C. M. Eggleston, M. F. Hochella, and G. A. Parks, "Sample Preparation and Aging Effects on the Dissolution Rate and Surface Composition of Diopside." *Geochim. Cosmochim. Acta* 53:797-804, 1989.

28. T. J. Wolery, EQ3NR - A computer Program for Geochemical Aqueous Speciation-Solubility Calculations: User's Guide and Documentation. UCRL-53414, Lawrence Livermore Laboratory, Livermore, California, 1983.

29. P. R. Stoots and C. E. Edinborough, In Situ Vitrification Intermediate-Scale Sampling and Analysis Plan, Rev 4, EGG-WM-8661, November 1990.

30. R. L. Hooker, Incinerator Carryover Tests with Dysprosium as a Stand-In for Plutonium, DPST-81-603, 1981.

31. P. G. Shaw and G. G. Loomis, Plutonium Contamination Control Studies During a Glove-Box Scale Simulated Excavation of TRU Buried Waste, EGG-WM-8289, October 1989.

32. J. E. Flynn, et al., Annual Report on TRU Waste Form Studies with Special Reference to Iron-Enriched Basalt, EGG-FM-5366, June 1981.

33. L. E. Thompson, "Underground Storage Tank Remediation by use of In-Situ Vitrification," Proceeding of Waste Management '91, Tucson, Arizona, March 1991.

APPENDIX A
TRACER DATA

SAMPLE	LOCATION	TIME	DATE	HOUR	MEDIA	LOCATION IN MEDIA	TANK VOLUME	FIELD QC	Dy	Dy FLAG	Tb	Tb FLAG	Yb	Yb FLAG	UNITS
IJ010A901D	TEST 1	PRETEST	31MAY1990	.	DUCT SMEAR	1	.		2.20	B	1.00	U	1.00	U	UG
IJ009A901D	TEST 1	PRETEST	31MAY1990	.	DUCT SMEAR	2	.		1.00	U	1.00	U	1.00	U	UG
IJ008A901D	TEST 1	PRETEST	31MAY1990	.	DUCT SMEAR	3	.		1.00	U	1.00	U	1.00	U	UG
IJ011A901D	TEST 1	PRETEST	31MAY1990	.	DUCT SMEAR	4	.		1.00	U	1.00	U	1.00	U	UG
IJ007A901D	TEST 1	PRETEST	31MAY1990	.	DUCT SMEAR	5	.		1.00	U	1.00	U	1.00	U	UG
IJ006A901H	TEST 1	PRETEST	31MAY1990	.	HOOD SMEAR		.	blank	1.00	U	1.00	U	1.00	U	UG
IJ001A901H	TEST 1	PRETEST	31MAY1990	.	HOOD SMEAR	1	.		1.00	U	1.00	U	1.00	U	UG
IJ002A901H	TEST 1	PRETEST	31MAY1990	.	HOOD SMEAR	2	.		1.00	U	1.00	U	1.00	U	UG
IJ003A901H	TEST 1	PRETEST	31MAY1990	.	HOOD SMEAR	3	.		1.00	U	1.00	U	1.00	U	UG
IJ004A901H	TEST 1	PRETEST	31MAY1990	.	HOOD SMEAR	4	.		1.00	U	1.00	U	1.00	U	UG
IJ005A901H	TEST 1	PRETEST	31MAY1990	.	HOOD SMEAR	5	.		1.00	U	1.00	U	1.00	U	UG
IA001A90	TEST 1	PRETEST	07JUN1990	.	SOIL	1	.		1.80		0.31	B	0.76		MG/KG
IA002A90	TEST 1	PRETEST	07JUN1990	.	SOIL	2	.		2.20		0.37	B	0.92		MG/KG
IA003A90	TEST 1	PRETEST	07JUN1990	.	SOIL	3	.		2.40		0.40	B	1.00		MG/KG
IA004A90	TEST 1	PRETEST	07JUN1990	.	SOIL	3	.	dup2	2.20		0.39	B	0.98		MG/KG
IA004B90	TEST 1	PRETEST	07JUN1990	.	SOIL	3	.	dup2	2.00		0.35	B	0.87		MG/KG
IA005A90	TEST 1	PRETEST	07JUN1990	.	SOIL	4	.		1.90		0.35	B	0.85		MG/KG
ID001A901A0	TEST 1	PRETEST	12JUN1990	1800	SCRUB SOLUTION	TANK 1	110	dup4	6.00		0.94	B	3.10		UG/L
ID003A901A0	TEST 1	PRETEST	12JUN1990	1800	SCRUB SOLUTION	TANK 1	110	dup4	3.30		0.54	B	1.80	B	UG/L
ID002A901B0	TEST 1	PRETEST	12JUN1990	1800	SCRUB SOLUTION	TANK 2	120	dup5	1.30	B	0.20	B	0.72	B	UG/L
ID004A901B0	TEST 1	PRETEST	12JUN1990	1800	SCRUB SOLUTION	TANK 2	120	dup5	1.40	B	0.20	B	0.72	B	UG/L
ID005A901A1	TEST 1		12JUN1990	2100	SCRUB SOLUTION	TANK 1	122	dup1	5.30		0.86	B	2.90		UG/L
ID005B90IA1	TEST 1		12JUN1990	2100	SCRUB SOLUTION	TANK 1	122	dup1	4.30		0.68	B	2.30		UG/L
IA006A90	TEST 1	PRETEST	14JUN1990	.	SAND		.		3.20		0.56		1.30		MG/KG
IA007A90	TEST 1	PRETEST	14JUN1990	.	SAND		.		3.50		0.62		1.40		MG/KG
ID001A901A1	TEST 1	PRETEST	14JUN1990	1600	SCRUB SOLUTION	TANK 1	165	dup3	.		.		.		
ID003A901A1	TEST 1	PRETEST	14JUN1990	1600	SCRUB SOLUTION	TANK 1	165	dup3	.		.		.		
ID033A901A1	TEST 1	PRETEST	14JUN1990	1800	SCRUB SOLUTION	TANK 1	160	dup6	3.20		0.50	B	1.80	B	UG/L
ID033B9C1A1	TEST 1	PRETEST	14JUN1990	1800	SCRUB SOLUTION	TANK 1	160	dup6	3.30		0.52	B	1.90	B	UG/L
ID034A901B1	TEST 1	PRETEST	14JUN1990	1800	SCRUB SOLUTION	TANK 2	170		0.90	B	0.20	U	0.56	B	UG/L
ID035A901A1	TEST 1		14JUN1990	2000	SCRUB SOLUTION	TANK 1	130		3.60		0.56	B	2.10		UG/L
ID036A901B1	TEST 1		14JUN1990	2000	SCRUB SOLUTION	TANK 2	160		1.30	B	0.20	U	0.70	B	UG/L
ID037A901A1	TEST 1		14JUN1990	2155	SCRUB SOLUTION	TANK 1	143		3.20		0.48	B	1.80	B	UG/L
ID038A901B1	TEST 1		14JUN1990	2155	SCRUB SOLUTION	TANK 2	119		0.68	B	0.20	U	0.42	B	UG/L
ID039A901A1	TEST 1		15JUN1990	5	SCRUB SOLUTION	TANK 1	150		45500.00		200.00	B	197.00	B	UG/L
ID040A901B1	TEST 1		15JUN1990	5	SCRUB SOLUTION	TANK 2	165		1470.00		10.00	U	10.00	U	UG/L
ID041A901A1	TEST 1		15JUN1990	153	SCRUB SOLUTION	TANK 1	166		42200.00		10.00	U	10.00	U	UG/L
ID042A901B1	TEST 1		15JUN1990	153	SCRUB SOLUTION	TANK 2	193		1800.00		10.00	U	10.00	U	UG/L
ID043A901A1	TEST 1		15JUN1990	407	SCRUB SOLUTION	TANK 1	155		5570.00		939.00		10.00	U	UG/L
ID044A901B1	TEST 1		15JUN1990	407	SCRUB SOLUTION	TANK 2	250		1630.00		757.00		10.00	U	UG/L

SAMPLE	LOCATION	TIME	DATE	HOUR	MEDIA	LOCATION IN MEDIA	TANK VOLUME	FIELD QC	Dy	Dy FLAG	Tb	Tb FLAG	Yb	Yb FLAG	UNITS
ID045A90IA1	TEST 1		15JUN1990	500	SCRUB SOLUTION	TANK 1	200		33200.00		69700.00		15.00	B	UG/L
ID046A90IB1	TEST 1		15JUN1990	500	SCRUB SOLUTION	TANK 2	200		1440.00		750.00	U	10.00	U	UG/L
ID047A90IA1	TEST 1		15JUN1990	605	SCRUB SOLUTION	TANK 1	184		30500.00		69800.00		33100.00		UG/L
ID048A90IB1	TEST 1		15JUN1990	605	SCRUB SOLUTION	TANK 2	235		1390.00		825.00		530.00		UG/L
ID049A90IA1	TEST 1		15JUN1990	718	SCRUB SOLUTION	TANK 1	215		7420.00		13800.00		8050.00		UG/L
ID050A90IB1	TEST 1		15JUN1990	718	SCRUB SOLUTION	TANK 2	230		1550.00		1110.00		2170.00		UG/L
ID051A90IA1	TEST 1		15JUN1990	803	SCRUB SOLUTION	TANK 1	202		23900.00		44300.00		80100.00		UG/L
ID052A90IB1	TEST 1		15JUN1990	803	SCRUB SOLUTION	TANK 2	239		1400.00		1260.00		2500.00		UG/L
ID053A90IA1	TEST 1		15JUN1990	1015	SCRUB SOLUTION	TANK 1	185		21200.00		31900.00		64900.00		UG/L
ID054A90IB1	TEST 1		15JUN1990	1015	SCRUB SOLUTION	TANK 2	280		1260.00		1190.00		3160.00		UG/L
IJ022A90ID	TEST 1	POST TEST	25JUN1990	.	DUCT SMEAR	1	.		5860.00		79400.00		24500.00		UG
IJ021A90ID	TEST 1	POST TEST	25JUN1990	.	DUCT SMEAR	2	.		2370.00		35900.00		11300.00		UG
IJ020A90ID	TEST 1	POST TEST	25JUN1990	.	DUCT SMEAR	3	.		6930.00		23200.00		7380.00		UG
IJ023A90ID	TEST 1	POST TEST	25JUN1990	.	DUCT SMEAR	4	.		3140.00		40700.00		16400.00		UG
IJ019A90ID	TEST 1	POST TEST	25JUN1990	.	DUCT SMEAR	5	.		944.00		5180.00		1940.00		UG
IJ012A90IH	TEST 1	POST TEST	25JUN1990	.	HOOD SMEAR		.	blank	1.00	B	10.40		5.00		UG
IJ013A90IH	TEST 1	POST TEST	25JUN1990	.	HOOD SMEAR	1	.		696.00		393.00		929.00		UG
IJ014A90IH	TEST 1	POST TEST	25JUN1990	.	HOOD SMEAR	2	.		617.00		130.00		929.00		UG
IJ015A90IH	TEST 1	POST TEST	25JUN1990	.	HOOD SMEAR	3	.		629.00		248.00		366.00		UG
IJ016A90IH	TEST 1	POST TEST	25JUN1990	.	HOOD SMEAR	4	.		457.00		258.00		691.00		UG
IJ017A90IH	TEST 1	POST TEST	25JUN1990	.	HOOD SMEAR	5	.		660.00		406.00		862.00		UG
IJ018A90IH	TEST 1	POST TEST	25JUN1990	.	HOOD SMEAR	6	.		1200.00		792.00		868.00		UG
7808229001	TEST 1	POST TEST	20AUG1990	.	FILTER		.	SPLIT1	0.95	U	0.95	U	0.11	B	MG/KG
7808229001	TEST 1	POST TEST	20AUG1990	.	FILTER		.	SPLIT1	0.98	U	0.98	U	0.28	B	MG/KG
7808229002	TEST 1	POST TEST	20AUG1990	.	FILTER		.	SPLIT2	134.00		0.34	B	0.19	B	MG/KG
7808229002	TEST 1	POST TEST	20AUG1990	.	FILTER		.	SPLIT2	209.00		1.20		0.37	B	MG/KG
7808229002	TEST 1	POST TEST	20AUG1990	.	FILTER		.	SPLIT2	263.00		1.20		0.42	B	MG/KG
HEPA BLANK	TEST 1	POST TEST	20AUG1990	.	FILTER		.	BLANK	0.93	U	0.93	U	0.93	U	MG/KG
IB010A90I	TEST 1	POST TEST	02OCT1990	.	SOIL	BOTTOM, 12 IN.	.		2.50	B	1.00	U	2.80	B	MG/KG
IB010B90I	TEST 1	POST TEST	02OCT1990	.	SOIL	BOTTOM, 12 IN.	.		2.30	B	0.99	U	1.50	B	MG/KG
IB011A90I	TEST 1	POST TEST	02OCT1990	.	SOIL	BOTTOM, 6 IN.	.		2.70	B	1.00	U	1.10	B	MG/KG
IB011B90I	TEST 1	POST TEST	02OCT1990	.	SOIL	BOTTOM, 6 IN.	.		2.60	B	1.00	U	1.20	B	MG/KG
IB008A90I	TEST 1	POST TEST	02OCT1990	.	SOIL	SIDE, 12 IN.	.		2.40	B	0.97	U	1.20	B	MG/KG
IB008B90I	TEST 1	POST TEST	02OCT1990	.	SOIL	SIDE, 12 IN.	.		2.70	B	1.00	U	6.80	B	MG/KG
IB008C90I	TEST 1	POST TEST	02OCT1990	.	SOIL	SIDE, 12 IN.	.		2.40	B	1.10	B	1.00	U	MG/KG
IB009A90I	TEST 1	POST TEST	02OCT1990	.	SOIL	SIDE, 6 IN.	.		2.40	B	1.00	U	1.00	B	MG/KG
IB009B90I	TEST 1	POST TEST	02OCT1990	.	SOIL	SIDE, 6 IN.	.		2.50	B	0.98	U	1.10	B	MG/KG
IC013C90IW	TEST 1	POST TEST	.	.	PRODUCT	1	.		58.00		42.00	U	5.00	U	UG/G
IC044B90IW	TEST 1	POST TEST	.	.	PRODUCT	2	.		169.00		199.00		320.00		UG/G
IC044D90IW	TEST 1	POST TEST	.	.	PRODUCT	3	.		187.00		227.00		359.00		UG/G

SAMPLE	LOCATION	TIME	DATE	HOUR	MEDIA	LOCATION IN MEDIA	TANK VOLUME	FIELD QC	Dy Dy	Dy FLAG	Tb Tb	Tb FLAG	Yb Yb	Yb FLAG	UNITS
IC044H901W	TEST 1	POST TEST	.	.	PRODUCT	4	.		224.00		284.00		362.00		UG/G
IC048D901W	TEST 1	POST TEST	.	.	PRODUCT	5	.		192.00		240.00		390.00		UG/G
IC048F901W	TEST 1	POST TEST	.	.	PRODUCT	6	.		197.00		241.00		374.00		UG/G
IC048H901W	TEST 1	POST TEST	.	.	PRODUCT	7	.		188.00		233.00		378.00		UG/G
IH061D901W	TEST 1	POST TEST	.	.	PRODUCT	8	.		6.00	U	42.00	U	5.00	U	UG/G
ID001A901A02	TEST 2	PRETEST	11JUL1990	1515	SCRUB SOLUTION	TANK 1	110		5200.00		13100.00		11300.00		UG/L
ID002A901B02	TEST 2	PRETEST	11JUL1990	1515	SCRUB SOLUTION	TANK 2	140		2330.00		3540.00		5720.00		UG/L
ID003A901A02	TEST 2		11JUL1990	1621	SCRUB SOLUTION	TANK 1	126		4840.00		13500.00		10700.00		UG/L
ID004A901B02	TEST 2		11JUL1990	1621	SCRUB SOLUTION	TANK 2	130		2150.00		2720.00		5180.00		UG/L
ID005A901A12	TEST 2		11JUL1990	1821	SCRUB SOLUTION	TANK 1	112		3850.00		7190.00		8650.00		UG/L
ID006A901B12	TEST 2		11JUL1990	1821	SCRUB SOLUTION	TANK 2	130		1660.00		1760.00		3830.00		UG/L
ID007A901A12	TEST 2		11JUL1990	1900	SCRUB SOLUTION	TANK 1	140		3620.00		10100.00		8040.00		UG/L
ID008A901B12	TEST 2		11JUL1990	1900	SCRUB SOLUTION	TANK 2	131		1590.00		1600.00		3640.00		UG/L
ID009A901A12	TEST 2		11JUL1990	2200	SCRUB SOLUTION	TANK 1	122		3970.00		8560.00		7550.00		UG/L
ID010A901B12	TEST 2		11JUL1990	2200	SCRUB SOLUTION	TANK 2	127		1430.00		1370.00		3070.00		UG/L
ID011A901A12	TEST 2		11JUL1990	2339	SCRUB SOLUTION	TANK 1	138		3730.00		7080.00		8020.00		UG/L
ID012A901B12	TEST 2		11JUL1990	2339	SCRUB SOLUTION	TANK 2	120		1120.00		1120.00		2370.00		UG/L
ID013A901A12	TEST 2		12JUL1990	140	SCRUB SOLUTION	TANK 1	151		3140.00		5530.00		6930.00		UG/L
ID014A901B12	TEST 2		12JUL1990	140	SCRUB SOLUTION	TANK 2	125		886.00		929.00		1880.00		UG/L
ID015A901A12	TEST 2		12JUL1990	420	SCRUB SOLUTION	TANK 1	104		4070.00		8420.00		9890.00		UG/L
ID016A901B12	TEST 2		12JUL1990	420	SCRUB SOLUTION	TANK 2	142		743.00		723.00		1580.00		UG/L
ID017A901A12	TEST 2		12JUL1990	525	SCRUB SOLUTION	TANK 1	120		3170.00		7310.00		8840.00		UG/L
ID018A901B12	TEST 2		12JUL1990	525	SCRUB SOLUTION	TANK 2	130		710.00		884.00		1800.00		UG/L
ID029A901A22	TEST 2		12JUL1990	744	SCRUB SOLUTION	TANK 1	128		3430.00		6680.00		8780.00		UG/L
ID030A901B22	TEST 2		12JUL1990	744	SCRUB SOLUTION	TANK 2	133		654.00		798.00		1660.00		UG/L
ID031A901A22	TEST 2		12JUL1990	951	SCRUB SOLUTION	TANK 1	78		4320.00		8140.00		10800.00		UG/L
ID032A901B22	TEST 2		12JUL1990	951	SCRUB SOLUTION	TANK 2	183		740.00		1010.00		2080.00		UG/L
ID019A901A12	TEST 2		12JUL1990	1145	SCRUB SOLUTION	TANK 1	75		4830.00		8690.00		10500.00		UG/L
ID020A901B12	TEST 2		12JUL1990	1145	SCRUB SOLUTION	TANK 2	180		1010.00		1470.00		2490.00		UG/L
ID021A901A12	TEST 2		12JUL1990	1345	SCRUB SOLUTION	TANK 1	113		3510.00		8870.00		7710.00		UG/L
ID022A901B12	TEST 2		12JUL1990	1345	SCRUB SOLUTION	TANK 2	232		985.00		1460.00		2330.00		UG/L
ID023A901A12	TEST 2		12JUL1990	1545	SCRUB SOLUTION	TANK 1	126		3320.00		7620.00		7440.00		UG/L
ID024A901B12	TEST 2		12JUL1990	1545	SCRUB SOLUTION	TANK 2	180		853.00		1240.00		2030.00		UG/L
ID025A901A12	TEST 2		12JUL1990	1745	SCRUB SOLUTION	TANK 1	148		2040.00		4740.00		5240.00		UG/L
ID026A901B12	TEST 2		12JUL1990	1745	SCRUB SOLUTION	TANK 2	160		658.00		991.00		1770.00		UG/L
ID027A901A12	TEST 2		12JUL1990	1955	SCRUB SOLUTION	TANK 1	150		2380.00		5220.00		5710.00		UG/L
ID028A901B12	TEST 2		12JUL1990	1955	SCRUB SOLUTION	TANK 2	132		902.00		1460.00		2350.00		UG/L
ID033A901A12	TEST 2		12JUL1990	2118	SCRUB SOLUTION	TANK 1	153	dup7	2080.00		4440.00		5040.00		UG/L
ID033B901A12	TEST 2		12JUL1990	2118	SCRUB SOLUTION	TANK 1	153	dup7	1920.00		4010.00		4610.00		UG/L
ID034A901B12	TEST 2		12JUL1990	2118	SCRUB SOLUTION	TANK 2	134		1170.00		2030.00		3010.00		UG/L

SAMPLE	LOCATION	TIME	DATE	HOUR	MEDIA	LOCATION IN MEDIA	TANK VOLUME	FIELD QC	Dy	Dy FLAG	Tb	Tb FLAG	Yb	Yb FLAG	UNITS
ID035A901A12	TEST 2		12JUL1990	2228	SCRUB SOLUTION	TANK 1	144		1940.00		3940.00		4630.00		UG/L
ID036A901B12	TEST 2		12JUL1990	2228	SCRUB SOLUTION	TANK 2	137		1310.00		2320.00		3280.00		UG/L
ID037A901A12	TEST 2		12JUL1990	2336	SCRUB SOLUTION	TANK 1	154		2050.00		4150.00		4840.00		UG/L
ID038A901B12	TEST 2		12JUL1990	2336	SCRUB SOLUTION	TANK 2	123		1310.00		2310.00		3280.00		UG/L
ID039A901A12	TEST 2		13JUL1990	37	SCRUB SOLUTION	TANK 1	162		1930.00		3830.00		4530.00		UG/L
ID040A901B12	TEST 2		13JUL1990	37	SCRUB SOLUTION	TANK 2	114		1400.00		2490.00		3440.00		UG/L
ID041A901A12	TEST 2		13JUL1990	225	SCRUB SOLUTION	TANK 1	157		1890.00		3650.00		4450.00		UG/L
ID042A901B12	TEST 2		13JUL1990	225	SCRUB SOLUTION	TANK 2	112		1500.00		2570.00		3800.00		UG/L
ID043A901A12	TEST 2		13JUL1990	330	SCRUB SOLUTION	TANK 1	136		1890.00		3520.00		4550.00		UG/L
ID044A901B12	TEST 2		13JUL1990	330	SCRUB SOLUTION	TANK 2	128		1590.00		2720.00		3800.00		UG/L
ID045A901A12	TEST 2		13JUL1990	412	SCRUB SOLUTION	TANK 1	144		2090.00		3940.00		5100.00		UG/L
ID046A901B12	TEST 2		13JUL1990	412	SCRUB SOLUTION	TANK 2	119		1780.00		3050.00		4360.00		UG/L
ID047A901A12	TEST 2		13JUL1990	452	SCRUB SOLUTION	TANK 1	153		1970.00		3680.00		4800.00		UG/L
ID048A901B12	TEST 2		13JUL1990	452	SCRUB SOLUTION	TANK 2	110		1560.00		2690.00		3840.00		UG/L
ID049A901A12	TEST 2		13JUL1990	600	SCRUB SOLUTION	TANK 1	272		861.00		1900.00		2040.00		UG/L
ID050A901B12	TEST 2		13JUL1990	600	SCRUB SOLUTION	TANK 2	196		1560.00		2780.00		3740.00		UG/L
ID051A901A12	TEST 2		13JUL1990	750	SCRUB SOLUTION	TANK 1	242		862.00		1820.00		2050.00		UG/L
ID052A901B12	TEST 2		13JUL1990	750	SCRUB SOLUTION	TANK 2	199		1440.00		2470.00		3500.00		UG/L
ID053A901A12	TEST 2		13JUL1990	1100	SCRUB SOLUTION	TANK 1	162		1190.00		2550.00		2740.00		UG/L
ID054A901B12	TEST 2		13JUL1990	1100	SCRUB SOLUTION	TANK 2	191		1250.00		1980.00		2800.00		UG/L
ID061A901A12	TEST 2		13JUL1990	1330	SCRUB SOLUTION	TANK 1	129	dup9	1190.00		3140.00		2780.00		UG/L
ID061B901A12	TEST 2		13JUL1990	1330	SCRUB SOLUTION	TANK 1	129	dup9	1070.00		2460.00		2860.00		UG/L
ID062A901B12	TEST 2		13JUL1990	1330	SCRUB SOLUTION	TANK 2	210		1410.00		2200.00		3190.00		UG/L
ID063A901A12	TEST 2		13JUL1990	1521	SCRUB SOLUTION	TANK 1	204		1600.00		4440.00		3780.00		UG/L
ID064A901B12	TEST 2		13JUL1990	1521	SCRUB SOLUTION	TANK 2	160		1190.00		1930.00		2710.00		UG/L
ID065A901A12	TEST 2		13JUL1990	1645	SCRUB SOLUTION	TANK 1	244		1770.00		4200.00		3570.00		UG/L
ID066A901B12	TEST 2		13JUL1990	1645	SCRUB SOLUTION	TANK 2	207		819.00		1330.00		1780.00		UG/L
ID067A901A12	TEST 2		13JUL1990	1758	SCRUB SOLUTION	TANK 1	308		1350.00		2880.00		2770.00		UG/L
ID068A901B12	TEST 2		13JUL1990	1758	SCRUB SOLUTION	TANK 2	215		723.00		1160.00		1530.00		UG/L
ID069A901A12	TEST 2		13JUL1990	1914	SCRUB SOLUTION	TANK 1	264		1180.00		2580.00		2410.00		UG/L
ID070A901B12	TEST 2		13JUL1990	1914	SCRUB SOLUTION	TANK 2	151		700.00		1120.00		1380.00		UG/L
ID071A901A12	TEST 2		13JUL1990	2100	SCRUB SOLUTION	TANK 1	150		1520.00		3180.00		2850.00		UG/L
ID072A901B12	TEST 2		13JUL1990	2100	SCRUB SOLUTION	TANK 2	320		590.00		909.00		1160.00		UG/L
ID073A901A12	TEST 2		13JUL1990	2300	SCRUB SOLUTION	TANK 1	140		1740.00		3550.00		3350.00		UG/L
ID074A901B12	TEST 2		13JUL1990	2300	SCRUB SOLUTION	TANK 2	320		648.00		965.00		1300.00		UG/L
ID075A901A12	TEST 2		13JUL1990	2400	SCRUB SOLUTION	TANK 1	335		1970.00		3910.00		3870.00		UG/L
ID076A901B12	TEST 2		13JUL1990	2400	SCRUB SOLUTION	TANK 2	177		2250.00		4810.00		5500.00		UG/L
ID077A901A12	TEST 2		14JUL1990	205	SCRUB SOLUTION	TANK 1	200		3480.00		9380.00		7560.00		UG/L
ID079A901A12	TEST 2		14JUL1990	500	SCRUB SOLUTION	TANK 1	200		1440.00		3830.00		2940.00		UG/L
ID081A901A12	TEST 2		14JUL1990	700	SCRUB SOLUTION	TANK 1	155		1940.00		5580.00		3950.00		UG/L

SAMPLE	LOCATION	TIME	DATE	HOUR	MEDIA	LOCATION IN MEDIA	TANK VOLUME	FIELD QC	Dy	Dy FLAG	Tb	Tb FLAG	Yb	Yb FLAG	UNITS
ID082A901B12	TEST 2		14JUL1990	700	SCRUB SOLUTION	TANK 2	360		950.00		1820.00		2200.00		UG/L
ID083A901A12	TEST 2		14JUL1990	847	SCRUB SOLUTION	TANK 1	186		1680.00		5450.00		3120.00		UG/L
ID084A901B12	TEST 2		14JUL1990	847	SCRUB SOLUTION	TANK 2	391		987.00		2040.00		2180.00		UG/L
ID085A901A22	TEST 2		14JUL1990	1050	SCRUB SOLUTION	TANK 1	163		1330.00		4300.00		2750.00		UG/L
ID086A901B22	TEST 2		14JUL1990	1050	SCRUB SOLUTION	TANK 2	456		834.00		1670.00		1850.00		UG/L
ID087A901A22	TEST 2	POST TEST	14JUL1990	1252	SCRUB SOLUTION	TANK 1	161		2220.00		7700.00		4720.00		UG/L
ID088A901B22	TEST 2	POST TEST	14JUL1990	1252	SCRUB SOLUTION	TANK 2	518		672.00		1330.00		1520.00		UG/L
ID089A901A12	TEST 2	POST TEST	14JUL1990	1532	SCRUB SOLUTION	TANK 1	178	dup8	4950.00		19800.00		9210.00		UG/L
ID089B901A12	TEST 2	POST TEST	14JUL1990	1532	SCRUB SOLUTION	TANK 1	178	dup8	739.00		1740.00		1580.00		UG/L
IJ034A901D	TEST 2	POST TEST	23JUL1990	.	DUCT SMEAR	1	.		2260.00		7450.00		2090.00		UG
IJ033A901D	TEST 2	POST TEST	23JUL1990	.	DUCT SMEAR	2	.		1650.00		5340.00		2030.00		UG
IJ032A901D	TEST 2	POST TEST	23JUL1990	.	DUCT SMEAR	3	.		394.00		438.00		274.00		UG
IJ035A901D	TEST 2	POST TEST	23JUL1990	.	DUCT SMEAR	4	.		658.00		1250.00		1460.00		UG
IJ031A901D	TEST 2	POST TEST	23JUL1990	.	DUCT SMEAR	5	.		343.00		921.00		418.00		UG
IJ037A9011	TEST 2	POST TEST	23JUL1990	.	ELECTRODE SMEAR		.		6.00		10.20		11.60		UG
IJ024A901H	TEST 2	POST TEST	23JUL1990	.	HOOD SMEAR		.	blank	0.23		0.23		0.26		UG
IJ025A901H	TEST 2	POST TEST	23JUL1990	.	HOOD SMEAR	1	.		500.00		292.00		450.00		UG
IJ026A901H	TEST 2	POST TEST	23JUL1990	.	HOOD SMEAR	2	.		1360.00		255.00		1100.00		UG
IJ027A901H	TEST 2	POST TEST	23JUL1990	.	HOOD SMEAR	3	.		390.00		285.00		607.00		UG
IJ028A901H	TEST 2	POST TEST	23JUL1990	.	HOOD SMEAR	4	.		23.80		10.30		26.70		UG
IJ029A901H	TEST 2	POST TEST	23JUL1990	.	HOOD SMEAR	5	.		15.70		10.10		19.00		UG
IJ030A901H	TEST 2	POST TEST	23JUL1990	.	HOOD SMEAR	6	.		657.00		520.00		634.00		UG
IJ036A9011	TEST 2	POST TEST	23JUL1990	.	TRAILER PORT		.		56.90		149.00		123.00		MG/KG
7808229003	TEST 2	POST TEST	20AUG1990	.	FILTER		.	SPLIT3	0.47	B	0.95	B	0.98	B	MG/KG
7808229003	TEST 2	POST TEST	20AUG1990	.	FILTER		.	SPLIT3	0.92	B	4.30		2.20		MG/KG
7808229003	TEST 2	POST TEST	20AUG1990	.	FILTER		.	SPLIT3	1.00		4.00		2.30		MG/KG
IB004A9012	TEST 2	POST TEST	04OCT1990	.	SOIL	BOTTOM, 12 IN.	.		2.60	B	.		.		MG/KG
IB004B9012	TEST 2	POST TEST	04OCT1990	.	SOIL	BOTTOM, 12 IN.	.		2.50	B	.		.		MG/KG
IB004C9012	TEST 2	POST TEST	04OCT1990	.	SOIL	BOTTOM, 12 IN.	.		2.70	B	.		.		MG/KG
IB003A9012	TEST 2	POST TEST	04OCT1990	.	SOIL	BOTTOM, 6 IN.	.		2.60	B	.		.		MG/KG
IB003B9012	TEST 2	POST TEST	04OCT1990	.	SOIL	BOTTOM, 6 IN.	.		2.30	B	.		.		MG/KG
IB001A9012	TEST 2	POST TEST	04OCT1990	.	SOIL	SIDE, 12 IN.	.		2.20	B	.		.		MG/KG
IB001B9012	TEST 2	POST TEST	04OCT1990	.	SOIL	SIDE, 12 IN.	.		2.20	B	.		.		MG/KG
IB002A9012	TEST 2	POST TEST	04OCT1990	.	SOIL	SIDE, 6 IN.	.		2.00	B	.		.		MG/KG
IB002B9012	TEST 2	POST TEST	04OCT1990	.	SOIL	SIDE, 6 IN.	.		2.00	B	.		.		MG/KG
IC086C901E	TEST 2	POST TEST	.	.	PRODUCT	.	.		195.00		42.00	U	6.00		UG/G
IC006C901E	TEST 2	POST TEST	.	.	PRODUCT	1	.		6.00	U	42.00	U	6.00		UG/G
IC007D901E	TEST 2	POST TEST	.	.	PRODUCT	2	.		84.00		42.00	U	5.00	U	UG/G
IC026D901E	TEST 2	POST TEST	.	.	PRODUCT	3	.		186.00		42.00	U	5.00	U	UG/G
IC026F901E	TEST 2	POST TEST	.	.	PRODUCT	4	.		183.00		42.00	U	5.00	U	UG/G

SAMPLE	LOCATION	TIME	DATE	HOUR	MEDIA	LOCATION IN MEDIA	TANK VOLUME	FIELD QC	Dy	Dy FLAG	Tb	Tb FLAG	Yb	Yb FLAG	UNITS
IC026I90IE	TEST 2	POST TEST	.	.	PRODUCT	5	.		182.00		42.00	U	5.00	U	UG/G
IC026M90IE	TEST 2	POST TEST	.	.	PRODUCT	6	.		177.00		42.00	U	5.00	U	UG/G
IC027D90IE	TEST 2	POST TEST	.	.	PRODUCT	7	.		172.00		42.00	U	5.00	U	UG/G
IC037D90IE	TEST 2	POST TEST	.	.	PRODUCT	9	.		181.00		42.00	U	5.00	U	UG/G
IC037F90IE	TEST 2	POST TEST	.	.	PRODUCT	10	.		171.00		42.00	U	5.00	U	UG/G
IH037J90IE	TEST 2	POST TEST	.	.	PRODUCT	11	.		6.00	U	42.00	U	5.00	U	UG/G
IC043D90IE	TEST 2	POST TEST	.	.	PRODUCT	15	.		173.00		42.00	U	5.00	U	UG/G
IC043F90IE	TEST 2	POST TEST	.	.	PRODUCT	16	.		155.00		42.00	U	5.00	U	UG/G
IC043J90IE	TEST 2	POST TEST	.	.	PRODUCT	17	.		6.00	U	42.00	U	8.00		UG/G
IH074D90IE	TEST 2	POST TEST	.	.	PRODUCT	18	.		6.00	U	42.00	U	5.00	U	UG/G